UNIVERSITY OF PALERMO
PHD JOINT PROGRAM:
UNIVERSITY OF CATANIA - UNIVERSITY OF MESSINA
XXXV CYCLE

DOCTORAL THESIS

From classical to operatorial models

Author:
Guglielmo Inferrera

Supervisor:
Prof. Francesco Oliveri

Co-Supervisor:
Prof. Patrizia Rogolino

A thesis submitted in fulfillment of the requirements for the degree of Doctor of Philosophy

in

Mathematics and Computational Sciences

January 30, 2023

Declaration of Authorship

I, Guglielmo Inferrera, declare that this thesis titled "From classical to operatorial models" and the work presented in it are my own. I confirm that:

- This work was done wholly or mainly while in candidature for a research degree at this University.
- Where any part of this thesis has previously been submitted for a degree or any other qualification at this University or any other institution, this has been clearly stated.
- Where I have consulted the published work of others, this is always clearly attributed.
- Where I have quoted from the work of others, the source is always given. With the exception of such quotations, this thesis is entirely my own work.
- I have acknowledged all main sources of help.
- Where the thesis is based on work done by myself jointly with others, I have made clear exactly what was done by others and what I have contributed myself.

Signed: 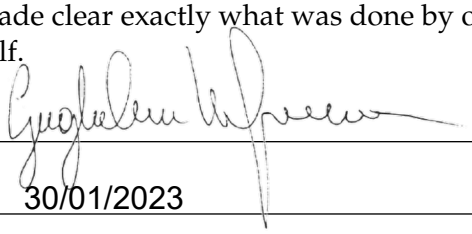

Date: 30/01/2023

"*Always feeling, always thinking, always learning, this is how we truly live. He who aspires to nothing, who learns nothing, is not worthy to live.*"

Arthur Helps

UNIVERSITY OF PALERMO

Abstract

Department of Mathematics and Computer Science

Doctor of Philosophy

From classical to operatorial models

by GUGLIELMO INFERRERA

Mathematical models for the collective dynamics of interacting and spatially distributed populations find applications in several contexts (biology, ecology, social sciences). Their formulation depends primarily on the (continuous or discrete) description of the space. Reaction-diffusion equations have been widely used in bio-ecology (morphogenesis, migration of biological species, tumor growth, neuro-degenerative diseases) and in the social sciences (diffusion of opinions or decision-making processes), and exhibit complex behaviors (propagation of oscillatory phenomena, pattern formation caused by instability). A reaction–diffusion system exhibits diffusion-driven instability, sometimes called Turing instability, if the homogeneous steady state is stable to small perturbations in the absence of diffusion but unstable to small spatial perturbations when diffusion is present. In this thesis, we move from this classical approach, considering a so called *crimo-taxis* model (Epstein, 1997), and proposing two variants (Inferrera et al., 2022) enabling us to study the formation of some patterns due to instability driven by self- and cross-diffusion terms, to operatorial models built by means of some techniques typical of quantum mechanics (see Bagarello, 2012; Bagarello, 2019). The leading idea in this approach relies on the evidence, shown in the last fifteen years in several applications, that the operatorial framework provides useful tools for describing the interactions occurring within macroscopic systems. Therefore, three applications of the operatorial formalism are discussed:

1. an operatorial version of *crimo-taxis model*;
2. a model where two populations spatially distributed in a one–dimensional domain compete both locally and nonlocally and are able to migrate (Inferrera and Oliveri, 2022);
3. a model of a finite number of agents subjected both to cooperative and competitive interactions (Gorgone, Inferrera, and Oliveri, 2022).

Acknowledgements

In this journey I was lucky enough to have met wonderful people who, besides being work colleagues, have also become friends. So it seems right to me to make some thanks.
The first person I want to thank is the one who has been close to me since the master's thesis, that is my supervisor Prof. Francesco Oliveri. I must say that he was an excellent teacher and sometimes even a father making himself available in the misfortunes that have happened to me. He taught me that to actually understand something you have to hit your head on your own (although I needed that advice from time to time to move on). I hope that we will continue to talk and maybe one day to find ourselves together again. Thanks for everything; I will always love you.
I also thank my co-supervisor Prof. Patrizia Rogolino for the advice given on research. Her presence made always the office a pleasant place.
I also want to thank Dr. Matteo Gorgone for all the advice he gave me in these three years. I hope to work with you again in the future.
I thank Prof. MariaCarmela Lombardo (coordinator of the PhD) for her availability over the past three years, especially in times of difficulty.
I also thank Prof. Elvira Barbera for being always available with us PhD students.
During my PhD I was lucky because colleagues who I prefer to call friends now are part of my life. So I want to thank them all for the time spent together in the last two years.
Thanks Antonella Pollino for your advices as a big sister even though most of the time you needed mine to avoid losing money. Anyway, we have enjoyed these two years, alternating moments of depression with moments of joy.
I want to especially thank my friend and colleague Antonino Ficarra. Thank you for putting up with me and supporting me in all the misfortunes that have happened to me in the last two years. You are a true friend. We have combined some bullshit ahaha. However, we also managed to make a mission together and apart from obviously the seminars and research, we had really good days together. I hope in the future I can still share the office with you.
During the three year of my PhD, six other people joined the office with whom I also shared experiences outside the university. So, I thank Aldo Ruta, Davide Giacobello, Alessandra Rizzo, Emanuele Sgroi, Carmelo Cisto and Fortunato Maesano; thank you very much for everything. With your entry I think our office has become one of the craziest office in Italy.
Special thanks to Carmelo Munafò. From the beginning we had a great time sharing a lot of things. We also worked together to complete a paper; I hope there will be others in the future. I was really lucky to have met you but not only for the work but also for the friendship that has been created between us. You are a true friend. Maybe one day we will be back in the same office.
I also thank my mom for everything she gives me every day and for being always close to me, never making me miss anything. I've been a bit unlucky in the last period but I'll come back stronger than before so you don't worry anymore. Thanks for being always there.
I also want to thank my sister Serena for the good she shows me and for being always there in times of need. Sometimes you are really heavy but I love you all the same.
I also thank my brother Giovanni for his love and for helping me in my time of need. I love you Esterina (my little sister).
Last but not least, I want to thank my girlfriend Agata Mallimaci. Thank you for

being always with me in both happy and sad moments. Thank you for the love you show me every day. Now, it is very close the time to start our life together.
I also thank my girlfriend's family for the love they show me every day.
Thank you for finishing all my childhood friends for being always close to me especially in times of difficulty. Thank you dad for the memories you left me. You passed away 18 years ago, I always miss you but I feel you protect me and you are always close to me.

Contents

Abstract v

Acknowledgements vii

0 Introduction 1

1 Reaction-diffusion systems 5
1.1 Introduction . . . 5
1.2 Reaction–diffusion equations . . . 6
1.2.1 General conditions for diffusion–driven instability . . . 7
1.3 The crimo–taxis model in a street . . . 7
1.4 Modified models . . . 10
1.5 Linear stability analysis . . . 11
1.6 Analysis of the complete system: Turing instability . . . 12
1.6.1 First variant . . . 13
1.6.2 Second variant . . . 15
1.7 Numerical results . . . 17
1.7.1 First variant . . . 17
1.7.2 Second variant . . . 20
1.8 Conclusions . . . 26

2 The quantum framework 31
2.1 Background and preliminaries . . . 31
2.2 Canonical relations and number representation . . . 32
2.3 Heisenberg representation . . . 35
2.4 Operatorial models of macroscopic systems . . . 35
2.4.1 Systems modeled by quadratic Hamiltonians . . . 35
2.5 Spatial models . . . 37
2.6 $(\mathcal{H},\rho)$–induced dynamics . . . 38
2.6.1 The rule ρ as a map in the space of the parameters of $\mathcal{H}$ . . . 38
2.7 Similitudes between a reaction-diffusion system and an operatorial model . . . 39

3 Operatorial Model of crimo-taxis in a street 41
3.1 The model . . . 41
3.2 Numerical results . . . 46
3.2.1 Simplified model in one cell . . . 46
3.2.2 Spatial model . . . 46

4 Spatially distributed competing populations 55
4.1 The operatorial model: Heisenberg dynamics and $(\mathcal{H},\rho)$–induced dynamics . . . 55
4.1.1 $(\mathcal{H},\rho)$–induced dynamics . . . 59

4.2 Numerical simulations 60
4.2.1 First scenario 60
4.2.2 Second scenario 62

5 Operatorial model with cooperation and competition **73**
5.1 The fermionic operatorial model 73
5.2 A simple concrete model: numerical simulations 76
5.2.1 Numerical simulations with the $(\mathcal{H}, \rho)$–induced dynamics approach 78
5.3 An extended spatial model 82

6 Conclusions **87**

Bibliography **89**

List of Figures

1.1 Patterns in animals. 5

1.2 The evolution of ordinary citizens, drug users/dealers, and policemen are shown in the left, center, and right plots, respectively. The chosen parameters are as follows: $\beta = 0.005$, $\mu = 0.5$, $\gamma = 0.03$, $\xi = 0.0001$, $b = 1.0$, $D_{11} = 0.03$, $D_{22} = 0.01$, $D_{33} = 0.02$, $D_{23} = 0.006$, $D_{21} = 0.001$, $D_{32} = 0.006$. 9

1.3 Contour plots of the solution for $t \in [0, 400]$ in (a)-(c)-(e) and for $t \in [400, 3000]$ in (b)-(d)-(f) with the parameters given in (1.20); $d_{31} = 0.075$, $k = 2\pi$. 18

1.4 Contour plots of the solution for $t \in [0, 140]$ in (a)-(c)-(e) and for $t \in [140, 3000]$ in (b)-(d)-(f) with the parameters given in (1.20); $d_{31} = 0.08$, $k = 2\pi$. 19

1.5 Contour plots of the solution for $t \in [0, 1400]$ in (a)-(c)-(e) and for $t \in [1400, 3000]$ in (b)-(d)-(f) with the parameters given in (1.21) and $d_{31} = 0.039$, $k = \pi$. 21

1.6 Contour plots of the solution for $t \in [0, 100]$ in (a)-(c)-(e) and for $t \in [100, 3000]$ in (b)-(d)-(f) with the parameters given in (1.21) and $d_{31} = 0.043$, $k = \pi$. 22

1.7 Plots of the averages (left) and variances (right) of the densities; subfigures (a)-(d) refer to the first scenario with $d_{31} = 0.075$ ((a), (b)), $d_{31} = 0.08$ ((c), (d)); subfigures (e)-(h) refer to the second scenario with $d_{31} = 0.039$ ((e), (f)), $d_{31} = 0.043$ ((g), (h)). . . . 23

1.8 Contour plots of the solution for $t \in [0, 1000]$ in (a)-(c)-(e) and for $t \in [1000, 3000]$ in (b)-(d)-(f) with the parameters given in (1.22) and $d_{31} = 0.055$, $k = 0.7\pi$. 24

1.9 Contour plots of the solution for $t \in [0, 220]$ in (a)-(c)-(e) and for $t \in [220, 3000]$ in (b)-(d)-(f) with the parameters given in (1.22) and $d_{31} = 0.06$, $k = \pi$. 25

1.10 Contour plots of the solution for $t \in [0, 220]$ in (a)-(c)-(e) and for $t \in [220, 3000]$ in (b)-(d)-(f) with the parameters given in (1.23) and $d_{31} = 0.07$, $k = \pi$. 27

1.11 Contour plots of the solution for $t \in [0, 120]$ in (a)-(c)-(e) and for $t \in [120, 3000]$ in (b)-(d)-(f) with the parameters given in (1.23) and $d_{31} = 0.08$, $k = \pi$. 28

1.12 Plots of the averages (left) and variances (right) of the densities; subfigures (a)-(d) refer to the first scenario with $d_{31} = 0.06$ ((a), (b)), $d_{31} = 0.07$ ((c), (d)); subfigures (e)-(h) refer to the second scenario with $d_{31} = 0.07$ ((e), (f)), $d_{31} = 0.08$ ((g), (h)). . . . 29

3.1 Moore neighborhood of the cell α. 42

3.2 Time evolution of the mean values of the number operators of the three subgroups. Only one cell is considered. No rule (subfigures (a), (c) and (e)), and use of the rule with $\tau = 2$ (subfigures (b), (d) and (f)). In all the figures it is $\lambda_1 = 0.04$, $\lambda_2 = 0.025$. As far as the inertia parameters, we have: $\omega_1 = 0.5$, $\omega_2 = 0.2$, $\omega_3 = 0.3$ (subfigures (a) and (b)), $\omega_1 = 0.5$, $\omega_2 = 0.3$, $\omega_3 = 0.2$ (subfigures (c) and (d)), $\omega_1 = 0.5$, $\omega_2 = 0.2$, $\omega_3 = 0.2$ (subfigures (e) and (f)). The initial conditions for all cases are: $n_1^0 = 0.8$, $n_2^0 = 0.08$, $n_3^0 = 0.04$. 47

3.3 Time evolution (left) and contour plots (right) of the densities of the three subgroups in all the cells with classical Heisenberg dynamics: ordinary citizens ((a) and (b)), drug users/dealers ((c) and (d)) and law enforcement personnel ((e) and (f)). The values of the parameters are given in (3.12). The inertia parameters are: $\omega_1 = 0.5$, $\omega_2 = 0.2$, $\omega_3 = 0.3$ The initial conditions are given in (3.11). 48
3.4 Time evolution (left) and contour plots (right) of the densities of the three subgroups in all the cells with classical Heisenberg dynamics: ordinary citizens ((a) and (b)), drug users/dealers ((c) and (d)) and law enforcement personnel ((e) and (f)). The values of the parameters are given in (3.12). The inertia parameters are: $\omega_1 = 0.5$, $\omega_2 = 0.3$, $\omega_3 = 0.2$ The initial conditions are given in (3.11). 49
3.5 Time evolution (left) and contour plots (right) of the densities of the three subgroups in all the cells with classical Heisenberg dynamics: ordinary citizens ((a) and (b)), drug users/dealers ((c) and (d)) and law enforcement personnel ((e) and (f)). The values of the parameters are given in (3.12). The inertia parameters are: $\omega_1 = 0.5$, $\omega_2 = 0.2$, $\omega_3 = 0.2$ The initial conditions are given in (3.11). 50
3.6 Time evolution (left) and contour plots (right) of the densities of the three subgroups in all the cells with $(\mathcal{H}, \rho)$–induced dynamics ($\tau = 2$): ordinary citizens ((a) and (b)), drug users/dealers ((c) and (d)) and law enforcement personnel ((e) and (f)). The values of the parameters are given in (3.12). The inertia parameters are: $\omega_1 = 0.5$, $\omega_2 = 0.2$, $\omega_3 = 0.3$ The initial conditions are given in (3.11). 52
3.7 Time evolution (left) and contour plots (right) of the densities of the three subgroups in all the cells with $(\mathcal{H}, \rho)$–induced dynamics ($\tau = 2$): ordinary citizens ((a) and (b)), drug users/dealers ((c) and (d)) and law enforcement personnel ((e) and (f)). The values of the parameters are given in (3.12). The inertia parameters are: $\omega_1 = 0.5$, $\omega_2 = 0.3$, $\omega_3 = 0.2$ The initial conditions are given in (3.11). 53
3.8 Time evolution (left) and contour plots (right) of the densities of the three subgroups in all the cells with $(\mathcal{H}, \rho)$–induced dynamics ($\tau = 2$): ordinary citizens ((a) and (b)), drug users/dealers ((c) and (d)) and law enforcement personnel ((e) and (f)). The values of the parameters are given in (3.12). The inertia parameters are: $\omega_1 = 0.5$, $\omega_2 = 0.2$, $\omega_3 = 0.2$ The initial conditions are given in (3.11). 54

4.1 Time evolution (standard Heisenberg dynamics with no rule) of the mean local densities in subregion $\mathcal{C}_1$ (a), subregion $\mathcal{C}_2$ (c) and subregion $\mathcal{C}_3$ (e). The subfigures (b), d) and (f) display the time evolution in the framework of (H, ρ)–induced dynamics with rule 1 and $\tau = 1$. . . 61
4.2 First scenario: time evolution of the mean of local densities in the three subregions; rule 2 (subfigures (a), (c) and (e)), and rule 3 (subfigures (b), (d) and (f)); $\tau = 1$. 63
4.3 Second scenario: time evolution of the mean of local densities in the three subregions; classic Heisenberg dynamics (subfigures (a), (c) and (e)), and rule 1 with $\tau = 1$ (subfigures (b), (d) and (f)). 64
4.4 Second scenario: time evolution of the mean of local densities in the three subregions; rule 2 (subfigures (a), (c) and (e)) and rule 3 rule 1 with $\tau = 1$ (subfigures (b), (d) and (f)); the value $\tau = 1$ has been used. 65

4.5 First scenario, $(\mathcal{H},\rho)$–induced dynamics with rule 1: $\tau = 2$ (subfigures (a), (c) and (e)) and $\tau = 4$ (subfigures (b), (d) and (f)). 67
4.6 First scenario, $(\mathcal{H},\rho)$–induced dynamics with rule 2: $\tau = 2$ (subfigures (a), (c) and (e)) and $\tau = 4$ (subfigures (b), (d) and (f)). 68
4.7 First scenario, $(\mathcal{H},\rho)$–induced dynamics with rule 3: $\tau = 2$ (subfigures (a), (c) and (e)) and $\tau = 4$ (subfigures (b), (d) and (f)). 69
4.8 Second scenario, $(\mathcal{H},\rho)$–induced dynamics with rule 1: $\tau = 2$ (subfigures (a), (c) and (e)) and $\tau = 4$ (subfigures (b), (d) and (f)). 70
4.9 Second scenario, $(\mathcal{H},\rho)$–induced dynamics with rule 2: $\tau = 2$ (subfigures (a), (c) and (e)) and $\tau = 4$ (subfigures (b), (d) and (f)). 71
4.10 Second scenario, $(\mathcal{H},\rho)$–induced dynamics with rule 3: $\tau = 2$ (subfigures (a), (c) and (e)) and $\tau = 4$ (subfigures (b), (d) and (f)). 72

5.1 Schematic view of a system with seven agents. 76
5.2 Time evolution of wealth of the agents as a function of time according to the classical Heisenberg dynamics: subfigure (a) is concerned with the competitive subsystem (blue for A_1, red for A_2 and green for A_3); subfigure (b) is concerned with the cooperative subsystem (blue for A_5, red for A_6 and green for A_7); subfigure (c) displays the wealth of the opportunist agent A_4; finally, subfigure (d) displays the average of the wealth of competitive subsystem (blue), cooperative subsystem (green), and opportunist subsystem (red). 77
5.3 Time evolution of wealth of the agents as a function of time using the $(\mathcal{H},\rho)$–induced dynamics approach with $\tau = 1$: subfigure (a) is concerned with the competitive subsystem (blue for A_1, red for A_2 and green for A_3); subfigure (b) is concerned with the cooperative subsystem (blue for A_5, red for A_6 and green for A_7); subfigure (c) displays the wealth of the opportunist agent A_4; finally, subfigure (d) displays the average of the wealth of competitive subsystem (blue), cooperative subsystem (green), and opportunist subsystem (red). . . . 79
5.4 Time evolution of wealth of the agents as a function of time using the $(\mathcal{H},\rho)$–induced dynamics approach with $\tau = 2$: subfigure (a) is concerned with the competitive subsystem (blue for A_1, red for A_2 and green for A_3); subfigure (b) is concerned with the cooperative subsystem (blue for A_5, red for A_6 and green for A_7); subfigure (c) displays the wealth of the opportunist agent A_4; finally, subfigure (d) displays the average of the wealth of competitive subsystem (blue), cooperative subsystem (green), and opportunist subsystem (red). . . . 80
5.5 Time evolution of wealth of the agents as a function of time using the $(\mathcal{H},\rho)$–induced dynamics approach with $\tau = 5$: subfigure (a) is concerned with the competitive subsystem (blue for A_1, red for A_2 and green for A_3); subfigure (b) is concerned with the cooperative subsystem (blue for A_5, red for A_6 and green for A_7); subfigure (c) displays the wealth of the opportunist agent A_4; finally, subfigure (d) displays the average of the wealth of competitive subsystem (blue), cooperative subsystem (green), and opportunist subsystem (red). . . . 81

5.6 Time evolution of wealth of the system with 100 agents: the cooperative (green) and competitive (blue) subgroups contain 45 agents and the opportunist (red) subgroup 10 agents; subfigure (a) displays the results without using the rule, subfigures (b), (c) and (d) the results using the $(\mathcal{H}, \rho)$–induced dynamics approach with $\tau = 1$, $\tau = 2$ and $\tau = 5$, respectively. 83
5.7 Time evolution of wealth of the system with 100 agents: the cooperative (green) and competitive (blue) subgroups contain 42 agents and the opportunist (red) subgroup 16 agents; subfigure (a) displays the results without using the rule, subfigures (b), (c) and (d) the results using the $(\mathcal{H}, \rho)$–induced dynamics approach with $\tau = 1$, $\tau = 2$ and $\tau = 5$, respectively. 84
5.8 Time evolution of wealth of the system with 100 agents: the cooperative (green) and competitive (blue) subgroups contain 40 agents and the opportunist (red) subgroup 20 agents; subfigure (a) displays the results without using the rule, subfigures (b), (c) and (d) the results using the $(\mathcal{H}, \rho)$–induced dynamics approach with $\tau = 1$, $\tau = 2$ and $\tau = 5$, respectively. 85

To my mother and father

Chapter 0

Introduction

Mathematical models for the collective dynamics of interacting and spatially distributed populations find applications in numerous contexts (biology, ecology, social sciences). Their formulation depends primarily on the (continuous or discrete) description of the space (or of the time). In the continuous case, the models are usually expressed in terms of integro-differential equations which, through a mean field approach, can be translated as parabolic coupled reaction-diffusion equations, or, by introducing suitable relaxation times, as hyperbolic systems. By discretizing the space variables, such models take the form of ordinary differential equations (continuous time) or difference equations (discrete time) on a lattice. Reaction-diffusion equations (Lam and Lou, 2022; Murray, 2003) have been widely used in bio-ecology (morphogenesis processes, migration of biological species, tumor growth, neurodegenerative diseases) and in the social sciences (diffusion of opinions or decision-making processes), and may exhibit complex behaviors (propagation of oscillatory phenomena, pattern formation caused by instability, ...).

One of the oldest mathematical models used for describing pattern formation dates back to Alan Turing (1952) and is based on reaction–diffusion mechanisms:

$$\frac{\partial A}{\partial t} - D_A \nabla^2 A = F(A, I), \qquad \frac{\partial I}{\partial t} - D_I \nabla^2 I = G(A, I),$$

where $A(\mathbf{x}, t)$ and $I(\mathbf{x}, t)$ represent the concentrations of an activator and inibitor whose time evolution is affected by diffusion processes along concentration gradients (D_A and D_I are the diffusivity coefficients), whereas $F(A, I)$ and $G(A, I)$ describe the reaction kinetics.

The Turing's idea was that the heterogeneous spatial distribution of activator and inhibitor emerging from the reaction and diffusion processes (the prepattern) *guides* the formation of the patterns in the morphogenesis of a living organism.

In general, we may consider a reaction–diffusion system, say

$$\frac{\partial \mathbf{U}}{\partial t} = \mathbf{R}(\mathbf{U}) + D\frac{\partial^2 \mathbf{U}}{\partial x^2},$$

where $\mathbf{U}$ is the vector of morphogen concentrations, $\mathbf{R}(\mathbf{U})$ represents the reaction kinetics and D is a matrix whose entries are the constant diffusion and cross–diffusion coefficients (the diagonal elements should be positive).

A reaction–diffusion system exhibits diffusion-driven instability, sometimes called Turing instability, if the homogeneous steady state is stable to small perturbations in the absence of diffusion but unstable with respect to small spatial perturbations when diffusion is present.

In this thesis, starting from this classical approach in describing biological phenomena, we move soon to define operatorial models built through the use of some

mathematical apparatus originally introduced in quantum mechanics.

In fact, in the last fifteen years, it became evident that the description of the dynamics of classical complex systems may be profitably carried out with such an operatorial approach, even when dealing with macroscopic systems (see, for instance, Bagarello, 2012; Bagarello, 2019). The underlying idea is that the operatorial framework provides useful tools for describing the interactions occurring within appropriate physical systems in a completely general and precise way.

Areas where these ideas have been used include stock markets, love affairs, population migration phenomena, escape strategies of crowds, desertification processes, microbial ecology, political systems, spread of information in a network, ...(see Bagarello, 2006; Bagarello and Oliveri, 2013; Bagarello and Oliveri, 2014; Gargano, 2014; Bagarello, Gargano, and Oliveri, 2015; Bagarello, Cherubini, and Oliveri, 2016; Bagarello and Haven, 2016; Di Salvo and Oliveri, 2016a; Di Salvo and Oliveri, 2016b; Di Salvo and Oliveri, 2017; Bagarello, Gargano, and Oliveri, 2020; Inferrera and Oliveri, 2022; Gorgone, Inferrera, and Oliveri, 2022, and references therein).

To build an operatorial model describing a macroscopic system $\mathcal{S}$, first of all we associate to the compartments (or agents) we are interested to annihilation and creation operators, together with number operators (our observables). The mean values of the number operators on a given initial condition are used to describe the evolution of our system. The dynamics of the systems we consider is ruled by a suitable Hermitian operator $\mathcal{H} = \mathcal{H}^\dagger$, called the Hamiltonian of $\mathcal{S}$ (in quantum mechanics $\mathcal{H}$ corresponds to the total energy of the system). The time evolution of the system modeled with such operators can be studied using the Schrödinger or the Heisenberg representation as well.

Roughly speaking, in the Schrödinger representation, we have a wave function $\Psi(t)$ associated to $\mathcal{S}$ that evolves in time according to the law

$$\mathrm{i}\frac{d\Psi}{dt} = \mathcal{H}\Psi(t),$$

where $\Psi(0) = \Psi_0$ is the initial status of $\mathcal{S}$. On the contrary, in the Heisenberg representation, a generic observable X evolves according to the law

$$X(t) = \exp(\mathrm{i}\mathcal{H}t)X\exp(-\mathrm{i}\mathcal{H}t),$$

or, equivalently, satisfies the differential equation

$$\frac{dX}{dt} = \mathrm{i}\left[\mathcal{H}, X\right],$$

where $[\mathcal{H}, X] = \mathcal{H}X - X\mathcal{H}$ denotes the commutator. In this thesis, we shall use the Heisenberg representation. Moreover, since our Hamiltonian operators will be time independent and quadratic, whereupon quasi periodic evolutions are often obtained, in order to enrich the dynamics, we will consider the recently introduced $(\mathcal{H}, \rho)$–induced approach (Bagarello et al., 2017; Bagarello et al., 2018). The combined effect of $\mathcal{H}$ with a rule ρ allows us to update the system $\mathcal{S}$ without changing its nature; in particular, the model retains its structure, while the rule explains a kind of dependence on the current state of the system by changing repeatedly, at specific times, the state of the system itself or the value of some parameters entering $\mathcal{H}$ (without changing its functional form). Thus, the model adapts itself as a consequence of its evolution; this approach mimics the changes in the interactions between the actors of the system in different environmental conditions.

The thesis is structured as follows. In Chapter 1, the basic elements for dealing with classical reaction–diffusion equations are briefly recalled. Then, two different variants of a so called *crimo–taxis model* (Epstein, 1997) are introduced and studied. The results presented are contained in a paper which has been submitted for publication (Inferrera et al., 2022).

In Chapter 2, we will move from classical to operatorial models built within the framework of algebra of ladder operators. Thus, the basic notions of the quantum formalism, with special emphasis on the number representation, are also given. Some theoretical elements for the description of the dynamical properties of classical systems described in terms of ladder operators governed by a self-adjoint time independent Hamiltonian operator are introduced. The recently introduced approach of the $(\mathcal{H} - \rho)$-induced dynamics is also exposed. A possible link between operatorial models and classical reaction–diffusion equations is also discussed by means of a simple example.

In Chapter 3, we present a novel operatorial formulation of the *crimo–taxis model* in a street. We also present some numerical simulations.

In Chapter 4, we consider an operatorial model of a couple of populations spatially distributed over a one-dimensional region. The two populations interact with a competitive mechanism and are able to diffuse over the region. A non-local competition effect is also included. The $(\mathcal{H}, \rho)$–induced dynamics approach is also used in order to take into account some changes in time of the attitudes of the two populations and obtain more realistic dynamical outcomes Inferrera and Oliveri, 2022.

In Chapter 5, a fermionic operatorial model of a system with competitive and cooperative agents is presented. In this model, a finite number of agents are examined and the differences between cooperation and competition are underlined by seeing who benefits and who does not, based on which interactive mechanism (purely competitive, purely cooperative or opportunist) is adopted (Gorgone, Inferrera, and Oliveri, 2022).

Finally, Chapter 6 contains our concluding remarks and future research plans.

Chapter 1

Reaction-diffusion systems

1.1 Introduction

The theory of reaction-diffusion equations began in the 1930s with some studies of population dynamics, combustion problems and chemical kinetics (Smoller, 1983; Murray, 2003; Lam and Lou, 2022). Nowadays, it is a well-established research area regarding the qualitative properties of traveling wave solutions, the dynamics of complex nonlinear systems, and the numerous applications in physics, chemistry, biology, medicine and social sciences. Mathematical models for the collective dynamics of interacting and spatially distributed populations find applications in numerous contexts (biology, ecology, social sciences). Their formulation depends primarily on the (continuous or discrete) description of the space and time. In the continuous case, the models are usually expressed in terms of integro-differential equations in which the variation in one of the variables may depend on the variation (instantaneous or delayed) of the same variable and on the superposition of the responses of the other suitably weighted variables. Through a mean field approach, they can be translated as coupled parabolic reaction–diffusion equations. These systems have been used for the modeling of morphogenesis processes, migration of biological species, spread of epidemics, tumor growth, neuro-vegetative diseases, and in socio-economic contexts (diffusion of opinions or decision-making processes); they are also able to describe complex behaviors such as the propagation of oscillatory phenomena and the formation of spatial patterns due to instability. A

FIGURE 1.1: Patterns in animals.

phenomenological concept of pattern formation and differentiation called positional information was proposed by Wolpert (Wolpert, 1969; Wolpert, 1981). He suggested that cells are preprogrammed to react to a chemical (or morphogen) concentration and differentiate accordingly into different kinds of cells such as cartilage cells, providing a description of development of patterns and forms in animals (Figure 1.1).

The increasing use of mathematics in biology has been unavoidable as biology became more quantitative. The complexity of the biological sciences makes interdisciplinary involvement essential. Mathematical biology research, to be useful and interesting, must be relevant from a biological point of view. The best models show how a process works and then predict what may follow. In particular, a fundamental part concerning biology is the description of the pattern formation process. The models built for their study have often been criticized for their lack of inclusion of genes in models. But the critique can be directed to any abstraction of a complex system modeled as a relatively simple one.

Much research in developmental biology, both experimental and theoretical, is dedicated to trying to determine the underlying mechanisms that generate patterns and forms in early development stages. In the following, we shall consider a model where interaction and diffusion mechanisms are concerned with some subgroups of a population sharing the same environment.

This chapter is divided in two parts. In the first part, the very basic theory of reaction–diffusion systems is briefly sketched. In the second part, a model for drug diffusion in a street, which models the interaction among ordinary citizens, drug users/dealers and law enforcement personnel, is considered. We study the linear stability of the system in the spatially homogeneous case and the possibly instabilities due to the diffusive terms. In particular, the Turing instability is possible provided that the original model (see Epstein, 1997) is suitably modified (Inferrera et al., 2022).

1.2 Reaction–diffusion equations

In 1952, Turing, in a seminal paper (Turing, 1952), suggested that, under certain conditions, chemicals can react and diffuse in such a way as to produce steady state heterogeneous spatial patterns of chemical or morphogen concentration.

Let us start by considering a general reaction–diffusion system in one space dimension:

$$\frac{\partial \mathbf{U}}{\partial t} = \mathbf{R}(\mathbf{U}) + D\frac{\partial^2 \mathbf{U}}{\partial x^2} \tag{1.1}$$

where $\mathbf{U}$ is the column vector of unknowns, $\mathbf{R}(\mathbf{U})$ represents the reaction terms, and D is a (possibly constant) matrix whose diagonal entries are positive.

First of all, we need to compute the homogeneous equilibrium solutions, represented by constant vectors $\mathbf{U}^\star$ such that

$$\mathbf{R}(\mathbf{U}^\star) = \mathbf{0}. \tag{1.2}$$

If such equilibria exist and are physically admissible, then we can study their linear stability. This is ascertained by computing for each equilibrium $\mathbf{U}^\star$ the eigenvalues of the Jacobian matrix $J = \nabla_{\mathbf{U}}\mathbf{R}(\mathbf{U})|_{\mathbf{U}^\star}$. If all the eigenvalues have negative real parts then $\mathbf{U}^\star$ is asymptotically stable with respect to small perturbations; then, we may consider the complete system and check if this equilibrium may lose its stability for non homogeneous small perturbations due to the spatial diffusive terms. In such a case, the diffusion-driven instability is called *Turing instability*.

1.2.1 General conditions for diffusion–driven instability

The concept of instability often occurs in ecological contexts, where a uniform steady state becomes unstable with respect to small perturbations and the populations typically exhibit some time oscillatory behavior. The main process driving the spatially inhomogeneous instability is diffusion, and this mechanism determines a spatial pattern.

Let us consider the full reaction–diffusion system (1.1), and consider the perturbation around a stable homogeneous equilibrium $\mathbf{U}^\star$, say

$$\mathbf{U} = \mathbf{U}^\star + \mathbf{U}_0 \exp(\lambda t + \mathrm{i}kx), \tag{1.3}$$

where $\mathbf{U}_0$ is a constant vector such that $\|\mathbf{U}_0\|$ is small. Linearizing the system (1.1), it is $\mathbf{U}_0 \neq \mathbf{0}$ provided that

$$\det\left(-\lambda\mathcal{I} + J - Dk^2\right) = 0, \tag{1.4}$$

where $\mathcal{I}$ is the identity matrix.

The instability arises if equation (1.4) admits at least a solution for λ with positive real part, that is, there is a diffusion–driven instability if some eigenvalue of the matrix $J - Dk^2$ has a real positive part for some wave numbers k.

In the next Section, we will investigate the Turing instability of a reaction–diffusion model involving three scalar equations.

1.3 The crimo–taxis model in a street

Urban crime is a very common social problem, and its prevention is one of the fundamental tasks of law enforcement activities, (Short, Bertozzi, and Brantingham, 2010; Short et al., 2008). The formation of "hot-spots" of crime suggests that this phenomenon does not occur uniformly in space and time; in some cases, it is concentrated in relatively small places that generate more than half of crime events such as drugs, robbery, theft. The description of criminal activity through models of reaction–diffusion, in which actors interact, can be a suitable tool to analyze crime patterns and consequently provide police strategies on the crime hot-spots. Such reaction–diffusion systems can be able to explain how the density of various subgroups of a population is distributed in the space at various times due to the local interaction and diffusion processes. There are many mathematical model, which describe similar phenomena, such as reaction-diffusion equations (Murray, 2003; Lam and Lou, 2022), kinetic models (Arlotti, Bellomo, and Lachowicz, 2000; Bianca and Menale, 2021), and even operatorial models based on the mathematical apparatus of quantum mechanics (Bagarello and Oliveri, 2013; Bagarello and Oliveri, 2014; Bagarello, Gargano, and Oliveri, 2015; Bagarello, Cherubini, and Oliveri, 2016; Inferrera and Oliveri, 2022).

The main results that will be presented in the following are concerned with two generalizations of a model proposed by Epstein (Epstein, 1997) that are susceptible of presenting persistent spatial patterns.

Let us start from the original model proposed in 1997 by Epstein, and named *crimo–taxis model*. The population is divided in three subgroups, whose densities and spatial distributions evolve in time. We imagine that events unfold on a one-dimensional interval — a "street." Let us define $u(x,t)$, $v(x,t)$, and $w(x,t)$ as the susceptible (ordinary citizens), infectious/infective (drug users/dealers), and law enforcement personnel, respectively, at street position x and time t; of course, a more

sophisticated model involving a fourth subgroup (the removed, *i.e.*, arrested) could be considered, but this extension will not be considered here.

The model equations (Epstein, 1997) read:

$$\begin{aligned}
\frac{\partial u}{\partial t} &= \mu u - \beta uv + D_{11}\frac{\partial^2 u}{\partial x^2},\\
\frac{\partial v}{\partial t} &= \beta uv - \gamma vw - D_{21}\frac{\partial^2 u}{\partial x^2} + D_{22}\frac{\partial^2 v}{\partial x^2} + D_{23}\frac{\partial^2 w}{\partial x^2},\\
\frac{\partial w}{\partial t} &= -bw + \xi uvw - D_{32}\frac{\partial^2 v}{\partial x^2} + D_{33}\frac{\partial^2 w}{\partial x^2},
\end{aligned} \tag{1.5}$$

where all the parameters therein involved are assumed to be positive.

As far as the *reaction* terms are concerned, ordinary citizens and drug users/dealers interact with a prey predator mechanism (Murray, 2002); on the contrary, the interaction between drug users/dealers and law enforcement personnel is a little bit different: the term $-\gamma vw$ is standard, whereas the term ξuvw describes the growth in the number of police forces in parallel with the increase of the level of social alarm, due to the spread of the drug problem. In particular, μ is the susceptible reproduction rate, β the rate of infected, γ the police arrest rate, b the natural police decay rate, and ξ the police growth rate.

As far as the diffusion terms are concerned, the terms $D_{11}\frac{\partial^2 u}{\partial x^2}$, $D_{22}\frac{\partial^2 v}{\partial x^2}$ and $D_{33}\frac{\partial^2 w}{\partial x^2}$ model the self-diffusion of the three classes of individuals. In the second and third equation we have some cross-diffusion terms:

- the terms $-D_{21}\frac{\partial^2 u}{\partial x^2}$ and $D_{23}\frac{\partial^2 w}{\partial x^2}$ represent that drug users/dealers spread in the areas occupied by the susceptible individuals and far away from the areas occupied by the police, respectively;

- the term $-D_{32}\frac{\partial^2 v}{\partial x^2}$, models the diffusion of the police towards the areas where there is a high concentration of drug users/dealers.

It is reasonable to assume $D_{23} > D_{21}$, at least if drug users/dealers give less importance to convert a susceptible subject with respect to the risk of being arrested. However, we shall consider also scenarios where $D_{23} < D_{21}$ so simulating situations where drug users/dealers move fearless towards ordinary citizens.

Figure 1.2 displays the numerical simulations that can be found in Epstein's paper. The street was divided into 12 blocks, and the initial distribution of the various classes was assumed as follows: the susceptible individuals occupy the four central blocks (1000 in each block), in blocks 8-12 there are the infected individuals (100 in each block), and the policemen are in blocks 1-3 (25 in each block).

The results therein presented show that the infected individuals diffuse toward the central blocks, and peddle with many susceptible individuals, so that the latter become part of the crime: consequently, it is observed a decrease in the population density of the ordinary citizens and an increase in that of the infected in the central blocks. This bulge induces a police reaction, that spread from the barracks at the end of the road to the center, the heart of the problem. Thereafter, the police "wither away" letting the susceptible individuals to continue their undisturbed spread.

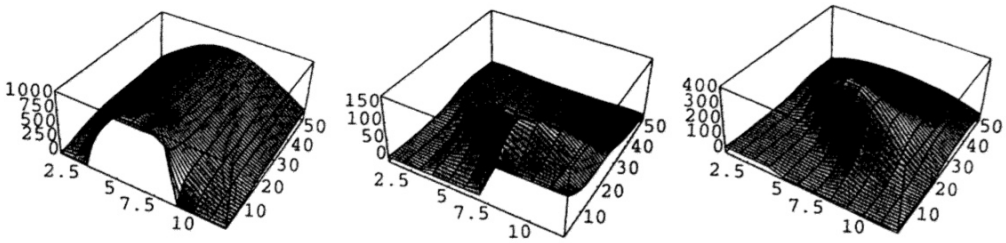

FIGURE 1.2: The evolution of ordinary citizens, drug users/dealers, and policemen are shown in the left, center, and right plots, respectively. The chosen parameters are as follows: $\beta = 0.005$, $\mu = 0.5$, $\gamma = 0.03$, $\xi = 0.0001$, $b = 1.0$, $D_{11} = 0.03$, $D_{22} = 0.01$, $D_{33} = 0.02$, $D_{23} = 0.006$, $D_{21} = 0.001$, $D_{32} = 0.006$.

Let us analyze the homogeneous equilibrium points of the system (neglecting diffusive terms). There are three equilibria, say

$$P_1 = (0,0,0), \quad P_2 = (0,v^\star,0), \quad P_3 = \left(\frac{b\beta}{\xi\mu}, \frac{\mu}{\beta}, \frac{b\beta^2}{\xi\gamma\mu}\right), \tag{1.6}$$

where $v^\star > 0$ is arbitrary.

Linearizing the system around each equilibrium and computing the eigenvalues of the corresponding Jacobian matrix J, the following results are easily deduced:

1. the equilibrium P_1 is unstable since J has the eigenvalues
$$\lambda_1 = \mu, \quad \lambda_2 = 0, \quad \lambda_3 = -b;$$

2. the equilibrium P_2 is not asymptotically stable (possibly unstable if $\mu - \beta v^\star > 0$ since the eigenvalues of J are
$$\lambda_1 = \mu - \beta v^*, \quad \lambda_2 = 0, \quad \lambda_3 = -b;$$

3. the coexistence equilibrium P_3 is not stable because there is a positive real eigenvalue and two complex conjugate eigenvalues with negative real part, say
$$\begin{aligned}\lambda_1 &= \ell_1 + \ell_2\\ \lambda_2 &= -\frac{1}{2}(\ell_1+\ell_2) + \frac{\sqrt{3}}{2}(\ell_1-\ell_2)\mathrm{i}\\ \lambda_3 &= -\frac{1}{2}(\ell_1+\ell_2) + \frac{\sqrt{3}}{2}(\ell_2-\ell_1)\mathrm{i},\end{aligned}$$
where
$$\ell_1 = \sqrt[3]{\frac{b^2\beta^2}{2\xi} + \sqrt{\Delta_{III}}}, \quad \ell_2 = \sqrt[3]{\frac{b^2\beta^2}{2\xi} - \sqrt{\Delta_{III}}},$$
$$\Delta_{III} = \frac{b^2\beta^4}{4\xi^2}\left(\frac{1}{4} + \frac{b\beta^2(b+mu)^3}{27\mu^3\xi}\right).$$

The simple analysis above described forces us to propose some variants of the model in order to have asymptotically stable coexistence equilibria able of losing their stability as a consequence of the diffusive terms, and obtain the emergence of some patterns (Inferrera et al., 2022).

1.4 Modified models

The first variant we propose is the following one:

$$\begin{aligned}
\frac{\partial u}{\partial t} &= ru\left(1-\frac{u}{\kappa_1}\right)-\beta uv+D_{11}\frac{\partial^2 u}{\partial x^2},\\
\frac{\partial v}{\partial t} &= \beta uv-\gamma vw-D_{21}\frac{\partial^2 u}{\partial x^2}+D_{22}\frac{\partial^2 v}{\partial x^2}+D_{23}\frac{\partial^2 w}{\partial x^2},\\
\frac{\partial w}{\partial t} &= -bw+\xi uvw-D_{31}\frac{\partial^2 u}{\partial x^2}-D_{32}\frac{\partial^2 v}{\partial x^2}+D_{33}\frac{\partial^2 w}{\partial x^2}.
\end{aligned} \tag{1.7}$$

where the constant parameters therein involved are all positive. The rationale of this model is that we assume a maximum number of ordinary people in the street (say, κ_1), so that we have a more realistic logistic growth for the susceptible people; moreover, we introduce a cross diffusion term in the third equation ($-D_{31}\frac{\partial^2 u}{\partial x^2}$) to account for the diffusion of the police towards the areas where there is a high concentration of susceptible individuals (for instance, this may occur when there are some events, like concerts of political demonstrations that may cause possible problems).

The second variant, still retaining the modifications above described, modifies the *crimo–taxis* term of the original model; in fact, we assume that the reaction term responsible for the growth of police tends to decrease as w approaches κ_2; this means that there is a limit, κ_2, to the number of law enforcement personnel.

Thus, we are led to consider the equations

$$\begin{aligned}
\frac{\partial u}{\partial t} &= ru\left(1-\frac{u}{\kappa_1}\right)-\beta uv+D_{11}\frac{\partial^2 u}{\partial x^2},\\
\frac{\partial v}{\partial t} &= \beta uv-\gamma vw-D_{21}\frac{\partial^2 u}{\partial x^2}+D_{22}\frac{\partial^2 v}{\partial x^2}+D_{23}\frac{\partial^2 w}{\partial x^2},\\
\frac{\partial w}{\partial t} &= -bw+\xi uv\left(1-\frac{w}{\kappa_2}\right)-D_{31}\frac{\partial^2 u}{\partial x^2}-D_{32}\frac{\partial^2 v}{\partial x^2}+D_{33}\frac{\partial^2 w}{\partial x^2}.
\end{aligned} \tag{1.8}$$

Before analyzing these two models, let us introduce dimensionless variables,

$$\begin{aligned}
&\widehat{u}=\frac{u}{\kappa_1}, \qquad \widehat{v}=\frac{v}{\kappa_1}, \qquad \widehat{w}=\frac{w}{\kappa_1},\\
&\widehat{t}=\frac{t}{T}, \qquad \widehat{x}=\frac{x}{L},
\end{aligned} \tag{1.9}$$

where $T=\dfrac{1}{\beta\kappa_1}$ and L are characteristic quantities having the dimensions of time and length, respectively.

To simplify the notation let us drop the hats; by setting

$$\mathbf{U}=\begin{pmatrix} u\\ v\\ w\end{pmatrix}, \qquad \mathcal{D}=\begin{pmatrix} d_{11} & 0 & 0\\ -d_{21} & d_{22} & d_{23}\\ -d_{31} & -d_{32} & d_{33}\end{pmatrix}, \tag{1.10}$$

we may write both dimensionless models in compact form as

$$\frac{\partial \mathbf{U}}{\partial t}=\mathbf{R}(\mathbf{U})+\mathcal{D}\frac{\partial^2 \mathbf{U}}{\partial x^2}, \tag{1.11}$$

where

$$\mathbf{R}(\mathbf{U}) = \begin{pmatrix} m_1 u(1-u) - uv \\ uv - m_2 vw \\ -m_3 w + m_4 uvw \end{pmatrix} \tag{1.12}$$

for the first variant, and

$$\mathbf{R}(\mathbf{U}) = \begin{pmatrix} m_1 u(1-u) - uv \\ uv - m_2 vw \\ -m_3 w + m_5 uv(1 - m_6 w) \end{pmatrix} \tag{1.13}$$

for the second variant.

The parameters therein involved have the following expressions:

$$\begin{aligned} &m_1 = \frac{r}{\beta\kappa_1}, \quad m_2 = \frac{\gamma}{\beta}, \quad m_3 = \frac{b}{\beta\kappa_1}, \quad m_4 = \frac{\xi\kappa_1}{\beta}, \\ &m_5 = \frac{\xi}{\beta}, \quad m_6 = \frac{\kappa_1}{\kappa_2}, \quad d_{ij} = \frac{D_{ij}}{\beta\kappa_1 L^2}. \end{aligned} \tag{1.14}$$

1.5 Linear stability analysis

In this Section, let us consider the models where the spatial terms are neglected, say

$$\frac{d\mathbf{U}}{dt} = \mathbf{R}(\mathbf{U}). \tag{1.15}$$

Both models possess the physically admissible equilibria

$$P_1 \equiv (0,0,0), \qquad P_2 \equiv (1,0,0), \qquad P_3 \equiv (0,v^\star,0),$$

where $v^\star$ is an arbitrary positive value. Linearizing system (1.15) around an equilibrium, and setting $J_k = \nabla_{\mathbf{U}}\mathbf{R}(\mathbf{U})|_{P_k}$ $(k = 1,2,3)$, we easily deduce the following results:

1. P_1 is not stable since J_1 has the eigenvalues

$$\lambda = 0, \qquad \lambda = m_1, \qquad \lambda = -m_3;$$

2. P_2 is not stable since J_2 has the eigenvalues

$$\lambda = 1, \qquad \lambda = -m_1, \qquad \lambda = -m_3;$$

3. P_3 is not asymptotically stable (not stable if $m_1 - v^\star > 0$) since J_3 has the eigenvalues

$$\lambda = 0, \qquad \lambda = m_1 - v^\star, \qquad \lambda = -m_3.$$

Moreover, the first model admits the coexistence equilibria

$$P_\pm \equiv \left(u_\pm, m_1(1-u_\pm), \frac{u_\pm}{m_2}\right),$$

where

$$u_\pm = \frac{1}{2}\left(1 \pm \sqrt{1 - \frac{4m_3}{m_1 m_4}}\right),$$

provided that the parameters m_1, m_3 and m_4 satisfy the constraint

$$m_1 m_4 \geq 4m_3,$$

and collapse in the same equilibrium

$$P^\star \equiv \left(\frac{1}{2}, \frac{m_1}{2}, \frac{1}{2m_2}\right)$$

when $m_1 m_4 - 4m_3 = 0$. The constraint on the dimensionless parameters, expressed in terms of the original parameters, reads

$$b \leq \frac{\kappa_1 r \xi}{4\beta}.$$

As far as the linear stability analysis is concerned, we have that

1. P_+ is asymptotically stable: using Routh–Hurwitz criterion, it is proved that all the eigenvalues have negative real part;
2. P_- is not stable;
3. when $m_1 m_4 - 4m_3 = 0$, the equilibrium $P^\star$ is stable, and the eigenvalues of the Jacobian matrix are:

$$\lambda = 0, \qquad \lambda_{2,3} = \frac{-m_1 m_2 \pm \sqrt{m_1 m_2^2 (m_1 - 2m_4 - 4)}}{4m_2}.$$

As far as the second model is concerned, we have the following coexistence equilibrium solution:

$$P^\star \equiv \left(u^\star, \frac{m_3}{m_5(m_2 - m_6 u^\star)}, \frac{u^\star}{m_2}\right),$$

where

$$u^\star = \frac{1}{2m_6}\left(m_2 + m_6 - \sqrt{(m_2 - m_6)^2 + \frac{4m_3 m_6}{m_1 m_5}}\right).$$

This equilibrium exists if

$$m_1 m_2 m_5 - m_3 > 0,$$

that, in terms of the original parameters, becomes

$$b \leq \frac{\kappa_1 r \gamma \xi}{\beta^2}.$$

Furthermore, $P^\star$ is asymptotically stable, as it can be proved by using Routh–Hurwitz criterion.

1.6 Analysis of the complete system: Turing instability

The effect of self- and cross-diffusive terms in a reaction-diffusion system may imply the loss of stability of an equilibrium point and lead to the emergence of special patterns. This is a well known phenomenon described for the first time in 1952 by Alan Turing in a pioneering paper (Turing, 1952), and investigated in several contexts by many authors (Vanag and Epstein, 2009; Xie, 2012; Hao and Xue, 2020;

Giunta, Lombardo, and Sammartino, 2021; Zincenko et al., 2021; Chakraborty, Baek, and Bairagi, 2021; DellaMarca et al., 2022; Aymard, 2022).

Since both models above introduced admit an asymptotically stable equilibrium, let $\mathbf{U}^\star \equiv (u^\star, v^\star, w^\star)^T$ be an asymptotic stable equilibrium of the system without spatial terms ($\mathbf{U}^\star$ coincides with P_+ for the first variant, and with $P^\star$ for the second variant), $\mathbf{U}_0 \equiv (u_0, v_0, w_0)^T$, and consider the following non homogeneous perturbation:

$$\mathbf{U} = \mathbf{U}^\star + \mathbf{U}_0 \exp(\lambda t + \mathrm{i}kx). \tag{1.16}$$

As outlined in subsection 1.2.1, we have Turing instability when the matrix

$$\mathcal{A} = \nabla_{\mathbf{U}} \mathbf{R}(\mathbf{U})|_{\mathbf{U}=\mathbf{U}^\star} - Dk^2 \tag{1.17}$$

possesses at least one eigenvalue with positive real part.

1.6.1 First variant

As far as the first proposed variant is concerned, we consider the coexistence equilibrium point

$$P_+ \equiv \left(u_+, m_1(1-u_+), \frac{u_+}{m_2}\right),$$

where

$$u_+ = \frac{1}{2}\left(1 + \sqrt{1 - \frac{4m_3}{m_1 m_4}}\right),$$

that is asymptotically stable. Let us write the characteristic polynomial of matrix $\mathcal{A}$,

$$-\lambda^3 + a_2(k)\lambda^2 + a_1(k)\lambda + a_0(k),$$

where

$$\begin{aligned}
a_2(k) &= -(d_{11}+d_{22}+d_{33})k^2 - \frac{m_1}{2}\left(1 + \sqrt{1 - \frac{4m_3}{m_1 m_4}}\right),\\
a_1(k) &= -\left(d_{11}d_{22} + d_{23}d_{32} + (d_{11}+d_{22})d_{33}\right)k^4\\
&\quad - \left(\left(\frac{d_{21}}{2} + \frac{m_1}{2}(d_{22}+d_{33}) + \frac{m_4 d_{23}}{2m_2}\right)\left(1 + \sqrt{1 - \frac{4m_3}{m_1 m_4}}\right)\right.\\
&\qquad \left. + \frac{m_1 m_2 d_{32}}{2}\left(1 - \sqrt{1 - \frac{4m_3}{m_1 m_4}}\right) - \frac{d_{23}m_3}{m_1 m_2}\right)k^2\\
&\quad - \frac{m_3}{2}\left(\left(1 + \frac{2}{m_4} + \sqrt{1 - \frac{4m_3}{m_1 m_4}}\right)\right),\\
a_0(k) &= a_{01}k^6 + a_{02}k^4 + a_{03}k^2 + a_{04},
\end{aligned}$$

along with the positions

$$a_{01} = -d_{11}(d_{22}d_{33} + d_{23}d_{32}),$$

$$
\begin{aligned}
a_{02} &= -\frac{d_{23}}{2}\left(1+\sqrt{1-\frac{4m_3}{m_1m_4}}\right)d_{31}+\frac{m_3d_{11}d_{23}}{m_1m_2}\\
&\quad -\frac{1}{2}d_{11}d_{32}m_1m_2\left(1-\sqrt{1-\frac{4m_3}{m_1m_4}}\right)\\
&\quad -\frac{1}{2}\left(1+\sqrt{1-\frac{4m_3}{m_1m_4}}\right)\left(d_{21}d_{33}+(d_{22}d_{33}+d_{23}d_{32})m_1+d_{11}d_{23}\frac{m_4}{m_2}\right),\\
a_{03} &= \frac{m_2m_3}{m_4}d_{31}-\frac{m_3}{2}\left(1+\sqrt{1-\frac{4m_3}{m_1m_4}}\right)d_{11}\\
&\quad -\frac{1}{2m_2}\left((m_1m_4-4m_3)+(m_1m_4-2m_3)\sqrt{1-\frac{4m_3}{m_1m_4}}\right)d_{23}\\
&\quad -\frac{m_1m_2m_3}{m_4}d_{32}-\frac{m_3}{m_4}d_{33},\\
a_{04} &= -\frac{m_1m_3}{2}\left(1-\frac{4m_3}{m_1m_4}+\sqrt{1-\frac{4m_3}{m_1m_4}}\right).
\end{aligned}
$$

It is easily recognized that the coefficients $a_2(k)$ and $a_1(k)$ are negative, the latter due to the constraint ensuring the existence of the equilibrium point. Therefore, the condition for the Turing instability is that $a_0(k)$ be positive for some values of k. Since $a_0(k)$ is a polynomial of degree 3 in k^2, we can proceed by substituting $\kappa = k^2$, whereupon we can write

$$a_0(\kappa) = a_{01}\kappa^3 + a_{02}\kappa^2 + a_{03}\kappa + a_{04}. \tag{1.18}$$

Though this polynomial has to be considered for $\kappa \geq 0$, let us study its trend in $\mathbb{R}$. It is $a_{01} < 0$ so that

$$\lim_{\kappa\to-\infty} a_0(\kappa) = +\infty;$$

moreover, because $a_{04} < 0$, it is $a_0(0) < 0$. Thus, there exists a value $\kappa_1 < 0$ such that $a_0(\kappa_1) = 0$. For the existence of the Turing instability we need that $a_0(\kappa)$ possesses also two distinct positive roots. The roots of the polynomial (1.18) are real and distinct if the condition

$$\frac{1}{27}\left(\frac{a_{03}}{a_{01}}-\frac{1}{3}\left(\frac{a_{02}}{a_{01}}\right)^2\right)^3+\frac{1}{4}\left(\frac{a_{04}}{a_{01}}+\frac{2}{27}\left(\frac{a_{02}}{a_{01}}\right)^3-\frac{1}{3}\frac{a_{02}a_{03}}{a_{01}^2}\right)^2 < 0 \tag{1.19}$$

is satisfied.

Both a_{02} and a_{03} are linear in d_{31}; let $d_{31}^\star$ and $d_{31}^{\star\star}$ the (positive) values of d_{31} annihilating a_{02} and a_{03}, respectively, and let

$$\delta_1 = \min\left(d_{31}^\star, d_{31}^{\star\star}\right), \quad \delta_2 = \max\left(d_{31}^\star, d_{31}^{\star\star}\right).$$

We may have two positive roots of (1.18) in the following two cases:

A_1: $a_{02}a_{03} < 0$, whereupon d_{31} cannot lie outside the open interval $]\delta_1, \delta_2[$;

A_2: $a_{02} > 0$ and $a_{03} > 0$, whereupon it has to be $d_{31} > \delta_2$.

Nevertheless, we have to take into account the constraint coming from (1.19) that poses an additional restriction to the variability of d_{31}; therefore, merging the condition $d_{31} > \delta_1$ with the constraint (1.19), the range for the parameter d_{31} where the diffusion driven instability arises can be determined. Once we choose the parameter d_{31} in such a way Turing instability may occur, the real positive roots of (1.18) determine the interval where the wave number k can be taken.

1.6.2 Second variant

As far as the second proposed variant is concerned, we consider the coexistence equilibrium point

$$P^\star \equiv \left(u^\star, \frac{m_3}{m_5(m_2 - m_6u^\star)}, \frac{u^\star}{m_2}\right),$$

where

$$u^\star = \frac{1}{2m_6}\left(m_2 + m_6 - \sqrt{(m_2 - m_6)^2 + \frac{4m_3m_6}{m_1m_5}}\right),$$

that is asymptotically stable. Let us write the characteristic polynomial of matrix $\mathcal{A}$,

$$-\lambda^3 + a_2(k)\lambda^2 + a_1(k)\lambda + a_0(k),$$

where

$$\begin{aligned}
a_2(k) &= -2k^2(d_{11} + d_{22} + d_{33}) - \frac{1}{2}m_1(1 + m_2m_5) \\
&\quad - \frac{1 - m_2m_5}{2m_6}\left(m_1m_2 - \sqrt{\frac{m_1(m_5(m_2 - m_6)^2 + 4m_3m_6)}{m_5}}\right), \\
a_1(k) &= -\frac{m_1m_2(1 + m_1m_2m_5) - m_3m_6}{2m_6^2}\sqrt{(m_2 - m_6)^2 + \frac{4m_3m_6}{m_1m_5}} \\
&\quad + \frac{m_1m_2}{2m_6^2}(m_1m_2m_5(m_2 - m_6) + m_2 + m_6(2m_3 - 1)) \\
&\quad - \frac{m_3}{2m_5m_6}(m_5(m_2 - m_6) - 2) \\
&\quad - \left(\left(\frac{d_{23}}{2m_2} + \frac{m_2(d_{32} + m_5(d_{11} + d_{22})) - d_{21} - m_1(d_{22} + d_{33})}{2m_6}\right) \times \right. \\
&\qquad \times \sqrt{(m_2 - m_6)^2 + \frac{4m_3m_6}{m_1m_5}} + \frac{d_{21}}{2} \\
&\quad + \frac{m_1m_2(d_{22} + d_{33} - m_2d - 32 - m_2m_5(d_{11} + d_{22})) + m_2d_{21}}{2m_6} \\
&\quad \left. + \frac{(m_1m_5(m_2 - m_6) - m_3)d_{23}}{2m_1m_2}\right)k^2 - (d_{11}d_{22} + d_{23}d_{32} + (d_{11} + d_{22})d_{33})k^4, \\
a_0(k) &= a_{01}k^6 + a_{02}k^4 + a_{03}k^2 + a_{04},
\end{aligned}$$

along with

$$a_0^{(1)} = -d_{11}(d_{22}d_{33} + d_{23}d_{32}),$$

$$
\begin{aligned}
a_0^{(2)} &= \frac{m_2(d_{21}d_{33}+m_1(d_{22}d_{33}+d_{23}d_{32}))-d_{11}(m_1m_2^2(m_5d_{22}+d_{32})+m_5m_6d_{23})}{2m_2m_6}\times \\
&\quad\times\sqrt{(m_2-m_6)^2+\frac{4m_3m_6}{m_1m_5}}-\frac{1}{2m_6}(m_2+m_6)(m_1(d_{22}d_{33}+d_{23}d_{32})+d_{21}d_{33}) \\
&\quad+\frac{d_{11}(m_1^2m_2^2(m_2-m_6)d_{32}+2m_3m_6d_{23}+m_1m_5(m_2-m_6)(m_1m_2^2d_{22}-m_6d_{23}))}{2m_1m_2m_6}, \\
a_0^{(3)} &= \left(\frac{m_3}{2m_6}d_{11}-\frac{m_1m_2^2m_5}{2m_6^2}(d_{21}+m_1d_{22})-\frac{2m_3+m_1m_5m_6}{2m_2m_6}d_{23}\right. \\
&\quad\left.+\frac{m_1m_2}{2m_6^2}(m_2d_{31}-m_1m_2d_{32}-d_{33})\right)\sqrt{(m_2-m_6)^2+\frac{4m_3m_6}{m_1m_5}} \\
&\quad-\frac{m_3(m_2+m_6)}{2m_6}d_{11}-\frac{m_2(2m_3m_6+m_1m_2m_5(m_2-m_6))}{2m_6^2}d_{21} \\
&\quad+\frac{m_1m_2(2m_3m_6+m_1m_2m_5(m_2-m_6))}{2m_6^2}d_{22} \\
&\quad-\frac{m_1m_5m_6(m_2-m_6)-2m_3(m_2+2m_6)}{2m_2m_6}d_{23} \\
&\quad-\frac{m_2(2m_3m_6+m_1m_2m_5(m_2-m_6))}{2m_5m_6^2}d_{31} \\
&\quad+\frac{m_1m_2(m_1m_2m_5(m_2-m_6)+2m_3m_6)}{2m_5m_6^2}d_{32} \\
&\quad+\frac{m_1m_2m_5(m_2-m_6)+2m_3m_6}{2m_5m_6^2}d_{33}, \\
a_0^{(4)} &= \frac{m_1((m_1m_2^2m_5+m_3m_6)(m_2-m_6)+2m_3m_6(m_2+m_6))}{2m_6^3}\times \\
&\quad\times\sqrt{(m_2-m_6)^2+\frac{4m_3m_6}{m_1m_5}} \\
&\quad-\frac{(m_1m_5(m_2-m_6)^2+4m_3m_6)(m_1m_2^2m_5+m_3m_6)}{2m_5m_6^3}
\end{aligned}
$$

The coefficients $a_2(k)$ and $a_1(k)$ are always negative (with the constraint ensuring the existence of the equilibrium point), so that Turing instability may arise if the coefficient a_0 is positive for some values of k.

The same analysis done in the previous subsection applies to this case, the only difference being that we have to impose the following additional constraints:

$$
m_2 > \frac{m_6}{2}, \qquad m_1 \geq \frac{4m_3}{m_5(2m_2-m_6)}.
$$

Thus, the range for the parameter d_{31} where the diffusion driven instability arises can be determined. Once we choose the parameter d_{31} in such a way Turing instability may occur, the range where the wave number can be chosen is determined as well.

1.7 Numerical results

In this Section, we present some numerical computations, and the solutions clearly exhibit the formation of well recognized patterns. For both variants of (1.11) with (1.12) or (1.13), we take the initial condition

$$\mathbf{U}(x,0) = \mathbf{U}^* + \mathbf{U_0}\cos(kx), \qquad x \in [0,1],$$

$\mathbf{U}^*$ being the asymptotically stable equilibrium of the homogeneous model and $\mathbf{U_0} = (0.01, 0.01, 0.01)^T$; moreover, Neumann boundary conditions at $x = 0$ and $x = 1$ are used. Numerical integrations are performed by using an implicit central finite difference scheme (Mitchell and Griffiths, 1980) with steps $\delta x = 0.01$ and $\delta t = 0.01$. We also considered smaller steps and the accuracy of the results has not been affected.

1.7.1 First variant

Here, we present the numerical solutions of the system (1.11) along with (1.12) in two different scenarios characterized by different values of some of the parameters and possessing qualitatively different equilibrium solutions.

In the first scenario, the equilibrium values for drug users/dealers and law enforcement personnel are very close, so that we can describe a situation where the street is mainly occupied by ordinary people. Moreover, we take the coefficient d_{23} larger than the coefficient d_{21}; this means that criminals prefer to avoid arrest rather than convert ordinary citizens. More in detail, let us choose the set of parameters

$$\begin{aligned} &m_1 = 1, \quad m_2 = 8, \quad m_3 = 0.2, \quad m_4 = 2, \\ &d_{11} = 0.055, \quad d_{21} = 0.0018, \quad d_{22} = 0.004, \\ &d_{23} = 0.011, \quad d_{32} = 0.011, \quad d_{33} = 0.036, \end{aligned} \tag{1.20}$$

whereupon the stable homogeneous equilibrium is

$$\mathbf{U}^\star \equiv (0.887298, 0.112782, 0.110912);$$

to ensure Turing instability it is required $d_{31} > 0.0532081$.

Figures 1.3 and 1.4 show the contour plots of the solution in correspondence of the parameters (1.20) for two different values of d_{31} greater than the critical value. Each figure displays on the left the evolution in the time interval needed for the emergence of the pattern, whereas on the right the asymptotic solution after the transient evolution. For large values of time it can be observed the formation of *strips*. There is a sort of segregation of the three subgroups: ordinary citizens and law enforcement personnel are more abundant far from the center of the domain, whereas drug users/dealers remain concentrated (and isolated) in the central part of the domain.

In the second scenario, let us choose the set of parameters

$$\begin{aligned} &m_1 = 1, \quad m_2 = 11, \quad m_3 = 0.25, \quad m_4 = 1.5, \\ &d_{11} = 0.055, \quad d_{21} = 0.03, \quad d_{22} = 0.004, \\ &d_{23} = 0.011, \quad d_{32} = 0.011, \quad d_{33} = 0.036, \end{aligned} \tag{1.21}$$

whence the stable homogeneous equilibrium turns out to be

$$\mathbf{U}^\star \equiv (0.788675, 0.211325, 0.0716977);$$

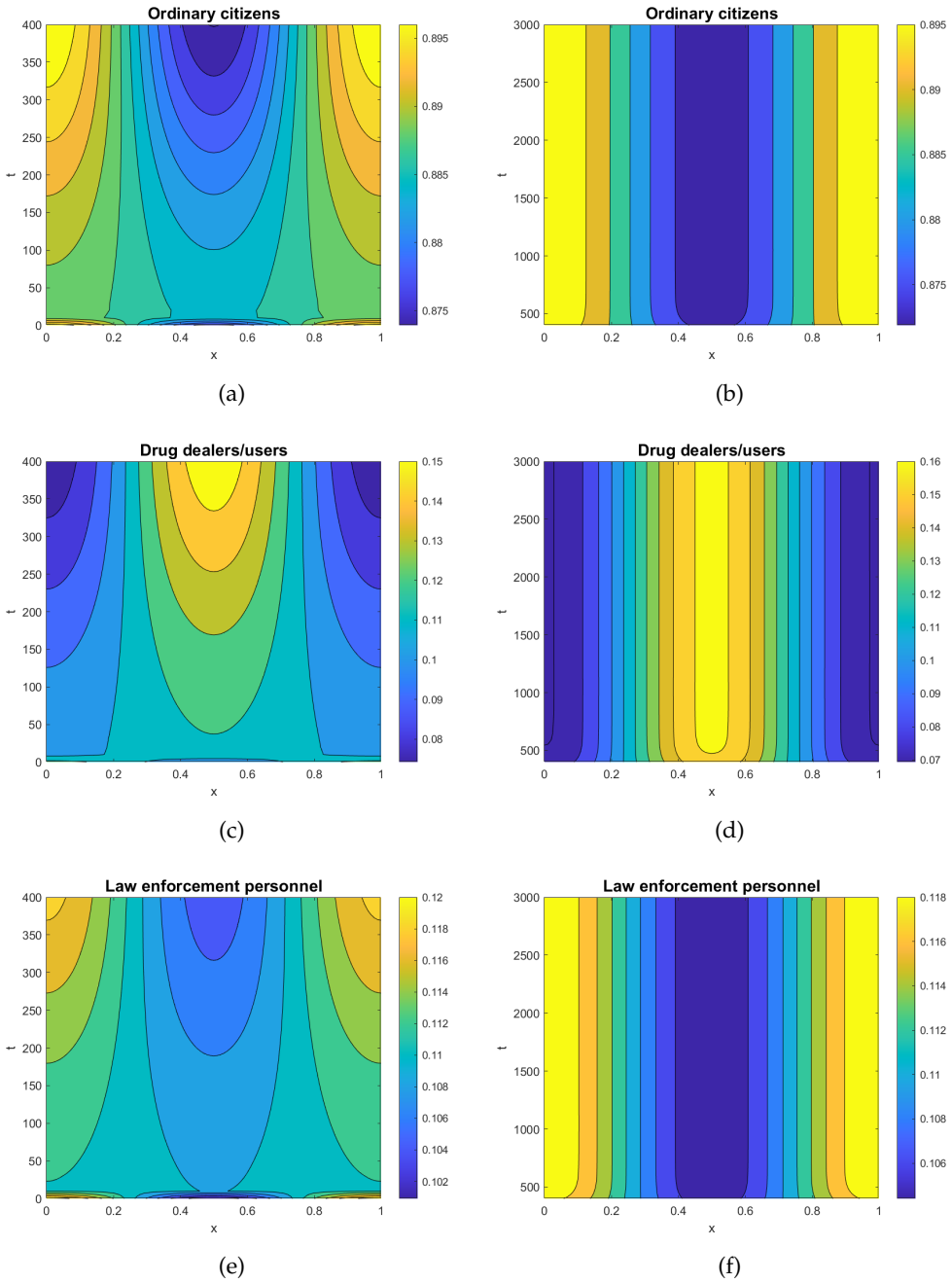

FIGURE 1.3: Contour plots of the solution for $t \in [0, 400]$ in (a)-(c)-(e) and for $t \in [400, 3000]$ in (b)-(d)-(f) with the parameters given in (1.20); $d_{31} = 0.075$, $k = 2\pi$.

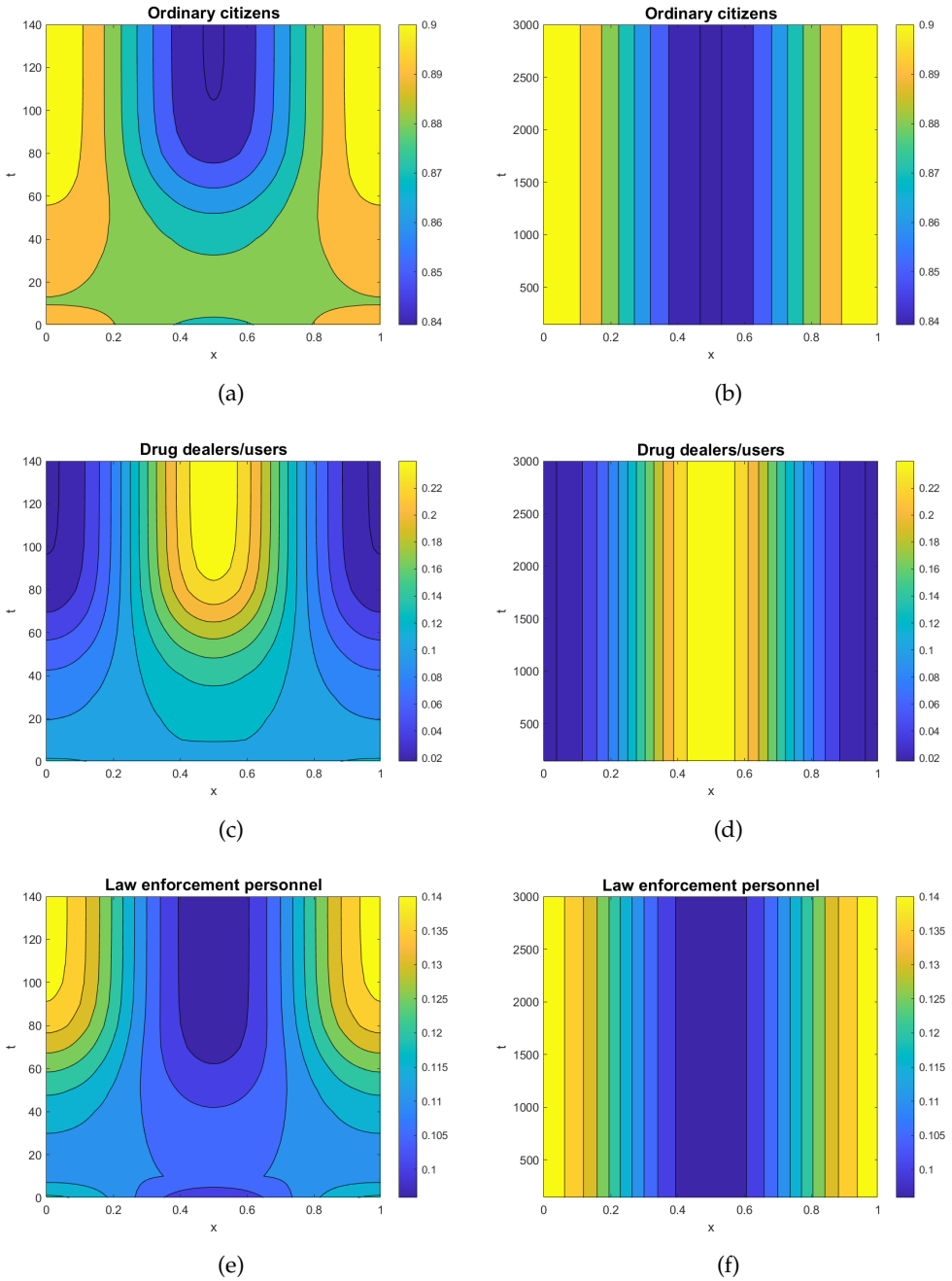

FIGURE 1.4: Contour plots of the solution for $t \in [0, 140]$ in (a)-(c)-(e) and for $t \in [140, 3000]$ in (b)-(d)-(f) with the parameters given in (1.20); $d_{31} = 0.08$, $k = 2\pi$.

the constraint $d_{31} > 0.0378693$ guarantees the rise of diffusion driven instability. In this scenario, at the equilibrium, the value for drug users/dealers is about three times the value of law enforcement personnel. Because of this, to mimic the situation where drug users/dealers do not care about the risk of being arrested in trying to convert ordinary citizens, we take a value of d_{23} smaller than that of d_{21}.

Figures 1.5 and 1.6 show the contour plots of the solution in correspondence of the parameters (1.21) for two different values of d_{31} greater than the critical value. As done above, each figure displays on the left the evolution in the time interval needed for the emergence of the pattern, whereas on the right the asymptotic solution after the transient evolution. Also in this scenario, for large values of time we observe the formation of *strips*. Nevertheless, differently from the first scenario, for large values of time, ordinary citizens and law enforcement personnel concentrate in the left part of the street, whereas drug dealers are concentrated in the right part of the domain.

Figure 1.7 displays the time evolution of averages and variances of the densities of the three subgroups all over the spatial domain in all the cases considered. It can be observed that, after the transient phase, as one expects, the variances stay constant in time, and this corresponds to the fact that the strips remain stationary even for a long time. In both scenarios, we notice that, increasing the value of d_{31} the duration of the transient phase is shortened.

1.7.2 Second variant

For the system (1.11), along with (1.13), we consider two different scenarios too. The first scenario uses the following set of parameters

$$\begin{aligned} &m_1 = 1, \quad m_2 = 10, \quad m_3 = 0.05, \quad m_5 = 0.3, \quad m_6 = 9, \\ &d_{11} = 0.06, \quad d_{21} = 0.001, \quad d_{22} = 0.02, \\ &d_{23} = 0.012, \quad d_{32} = 0.012, \quad d_{33} = 0.04; \end{aligned} \tag{1.22}$$

the stable homogeneous equilibrium is

$$\mathbf{U}^\star \equiv (0.908569, 0.0914306, 0.0908569),$$

and, in order to have Turing instability, it is required $d_{31} > 0.0503979$.

Figures 1.8 and 1.9 show the contour plots of the solution according to the parameters in (1.22) for two different values of d_{31} greater than the critical value. Each figure exibits on the left the evolution in the time interval needed for the emergence of the pattern, whereas on the right the stationary solution. Also in this case hot *strips* originate for large values of time. It is highlighted the formation of aggregations of the three subgredoups on the sides of the domain. In particular, citizens and policemen are shifted on the left side of the domain while drug users/dealers concentrate on the right side. The formation of pattern takes longer with respect to what observed in the first variant.

On the contrary, the second scenario uses the set of parameters

$$\begin{aligned} &m_1 = 1, \quad m_2 = 10, \quad m_3 = 0.07, \quad m_5 = 0.2, \quad m_6 = 10, \\ &d_{11} = 0.06, \quad d_{21} = 0.05, \quad d_{22} = 0.02, \\ &d_{23} = 0.012, \quad d_{32} = 0.012, \quad d_{33} = 0.04; \end{aligned} \tag{1.23}$$

the stable homogeneous equilibrium is

$$\mathbf{U}^\star \equiv (0.687868, 0.312132, 0.0859835),$$

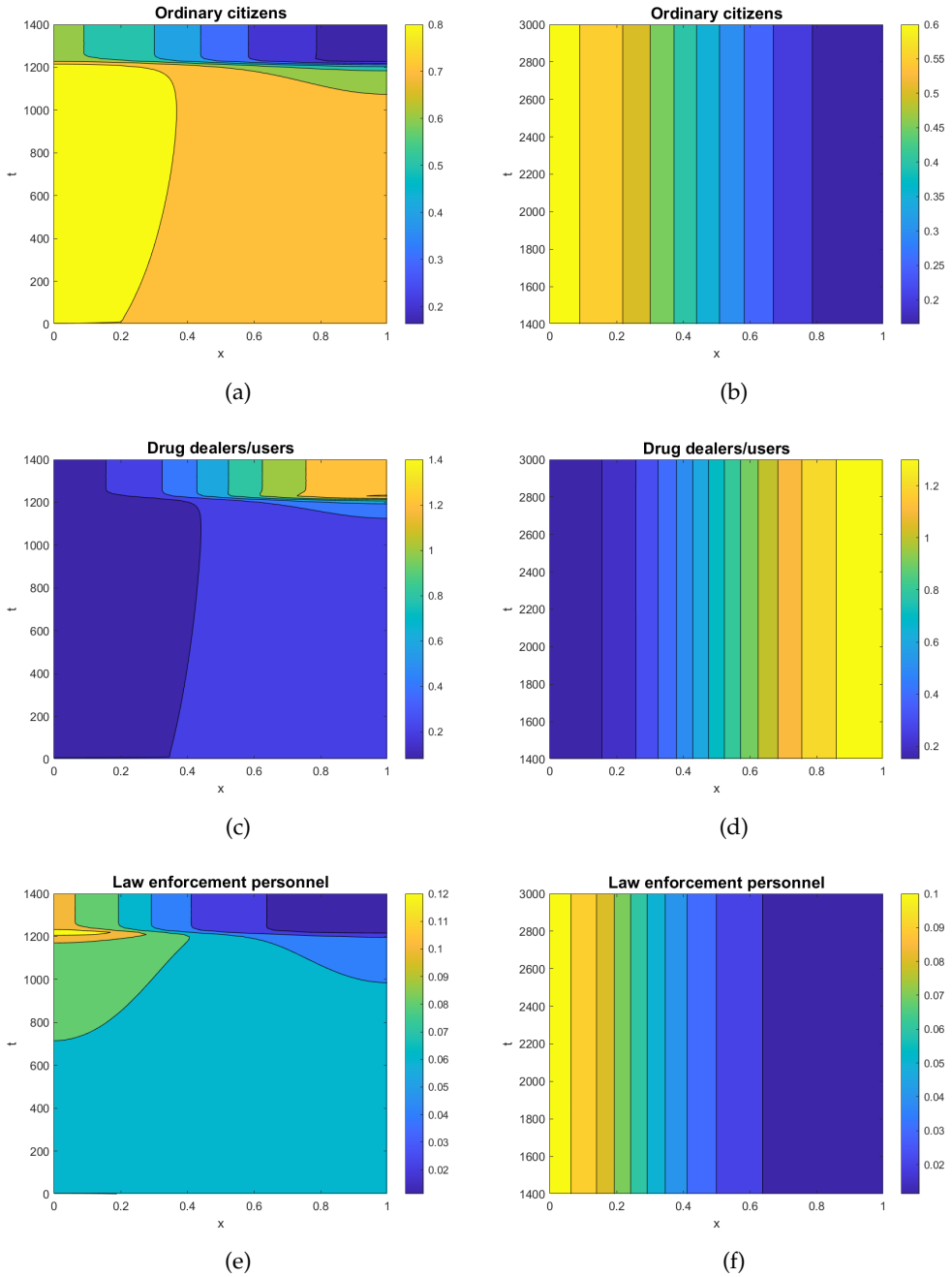

FIGURE 1.5: Contour plots of the solution for $t \in [0, 1400]$ in (a)-(c)-(e) and for $t \in [1400, 3000]$ in (b)-(d)-(f) with the parameters given in (1.21) and $d_{31} = 0.039$, $k = \pi$.

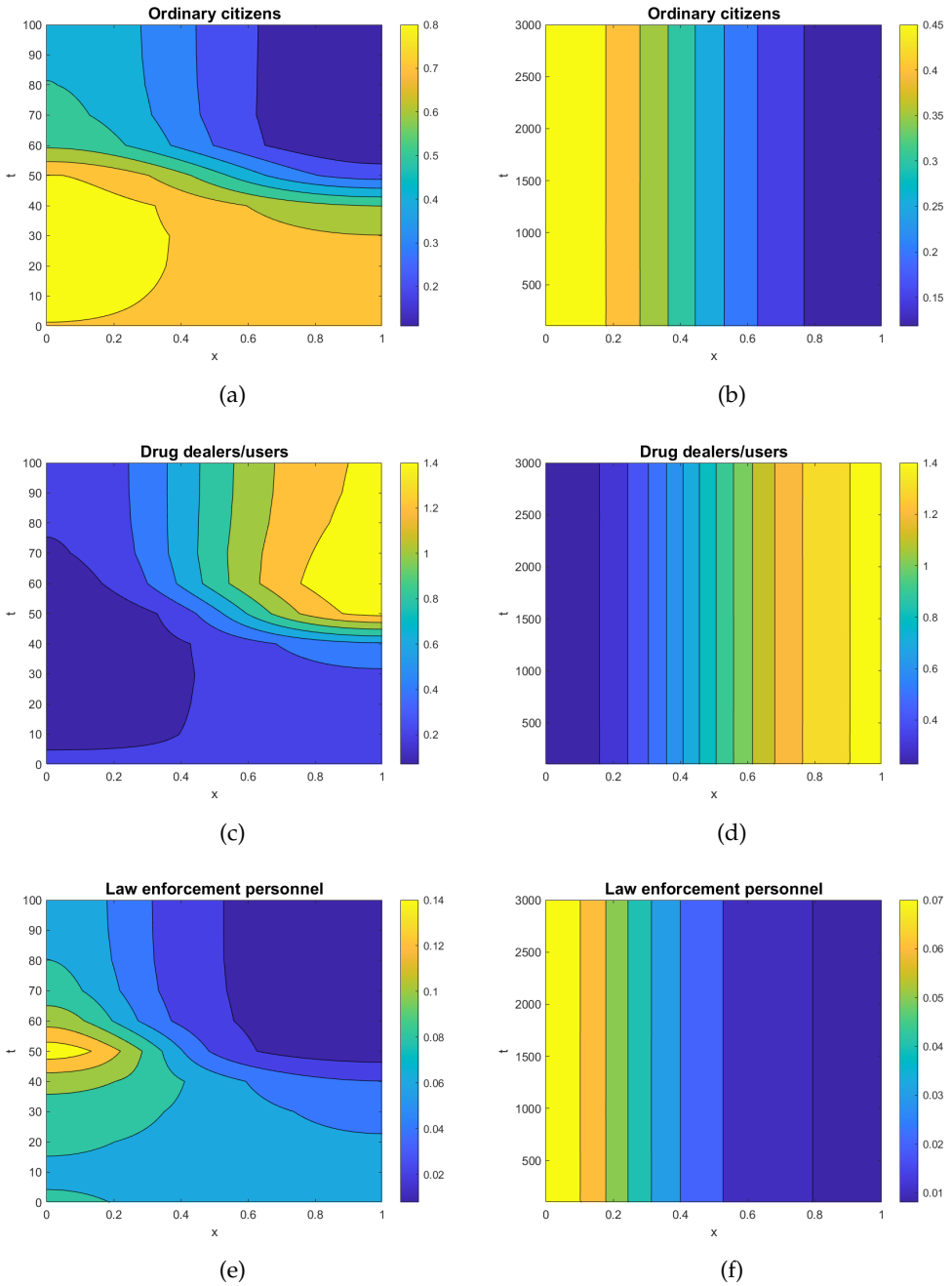

FIGURE 1.6: Contour plots of the solution for $t \in [0, 100]$ in (a)-(c)-(e) and for $t \in [100, 3000]$ in (b)-(d)-(f) with the parameters given in (1.21) and $d_{31} = 0.043$, $k = \pi$.

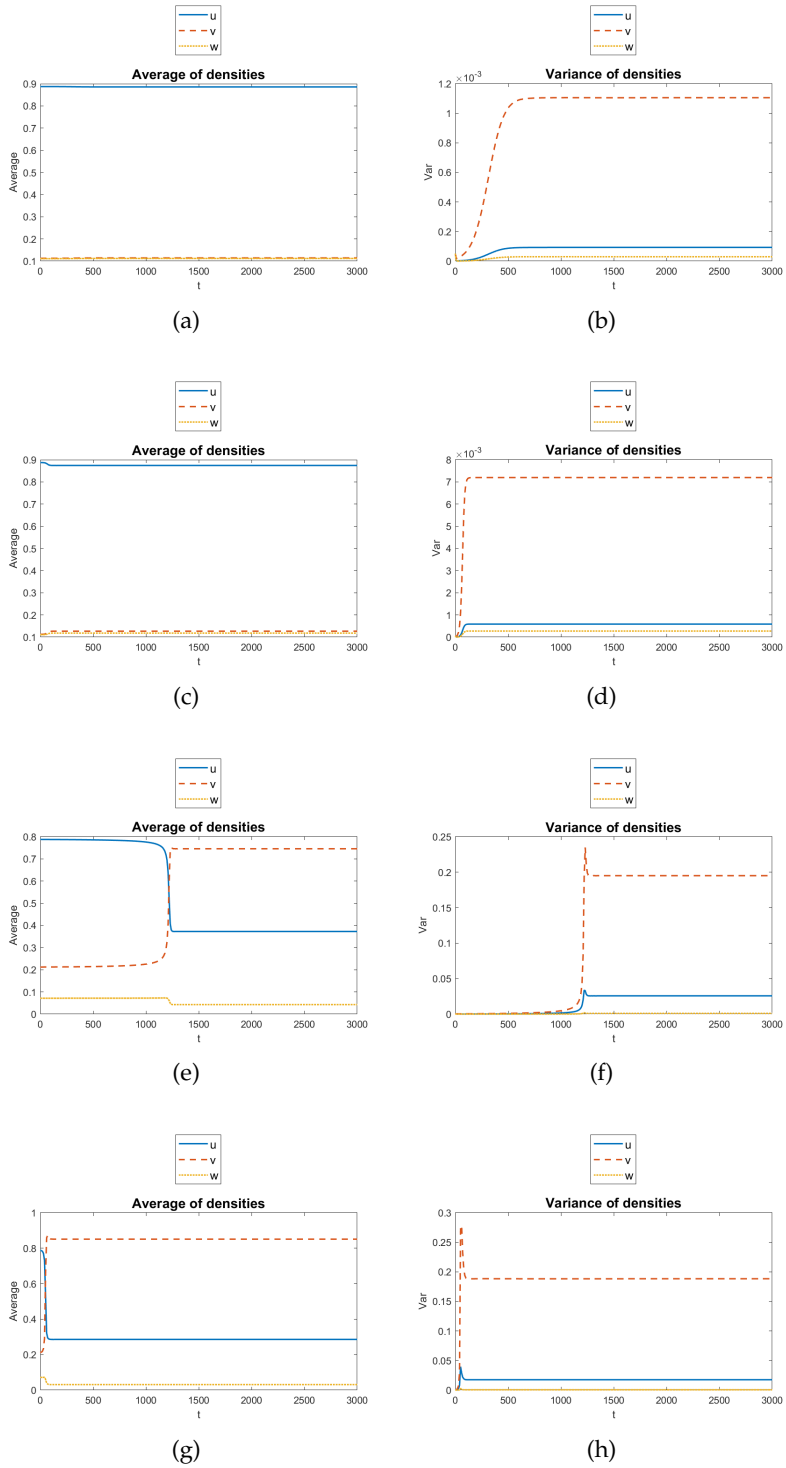

FIGURE 1.7: Plots of the averages (left) and variances (right) of the densities; subfigures (a)-(d) refer to the first scenario with $d_{31} = 0.075$ ((a), (b)), $d_{31} = 0.08$ ((c), (d)); subfigures (e)-(h) refer to the second scenario with $d_{31} = 0.039$ ((e), (f)), $d_{31} = 0.043$ ((g), (h)).

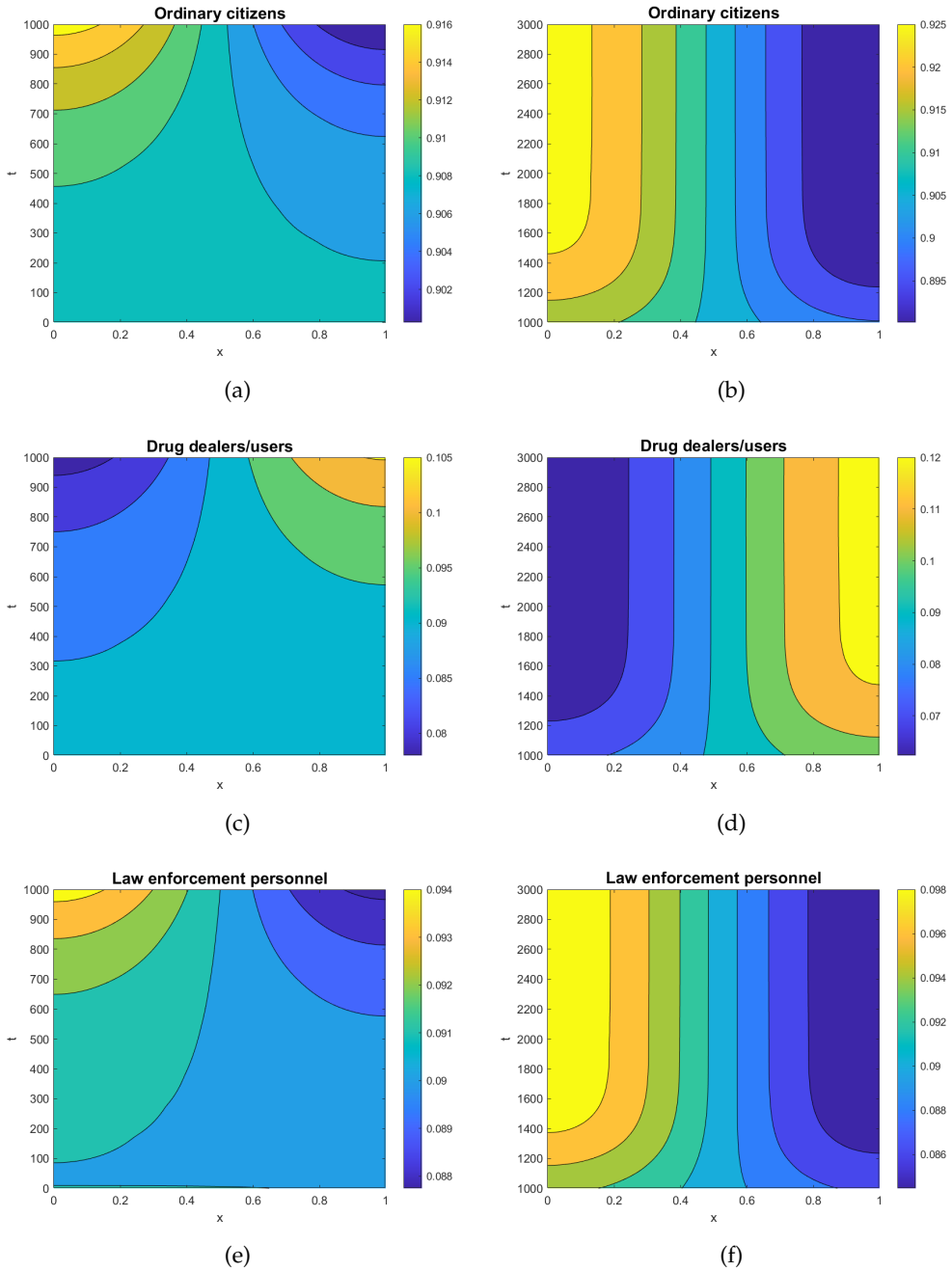

FIGURE 1.8: Contour plots of the solution for $t \in [0, 1000]$ in (a)-(c)-(e) and for $t \in [1000, 3000]$ in (b)-(d)-(f) with the parameters given in (1.22) and $d_{31} = 0.055$, $k = 0.7\pi$.

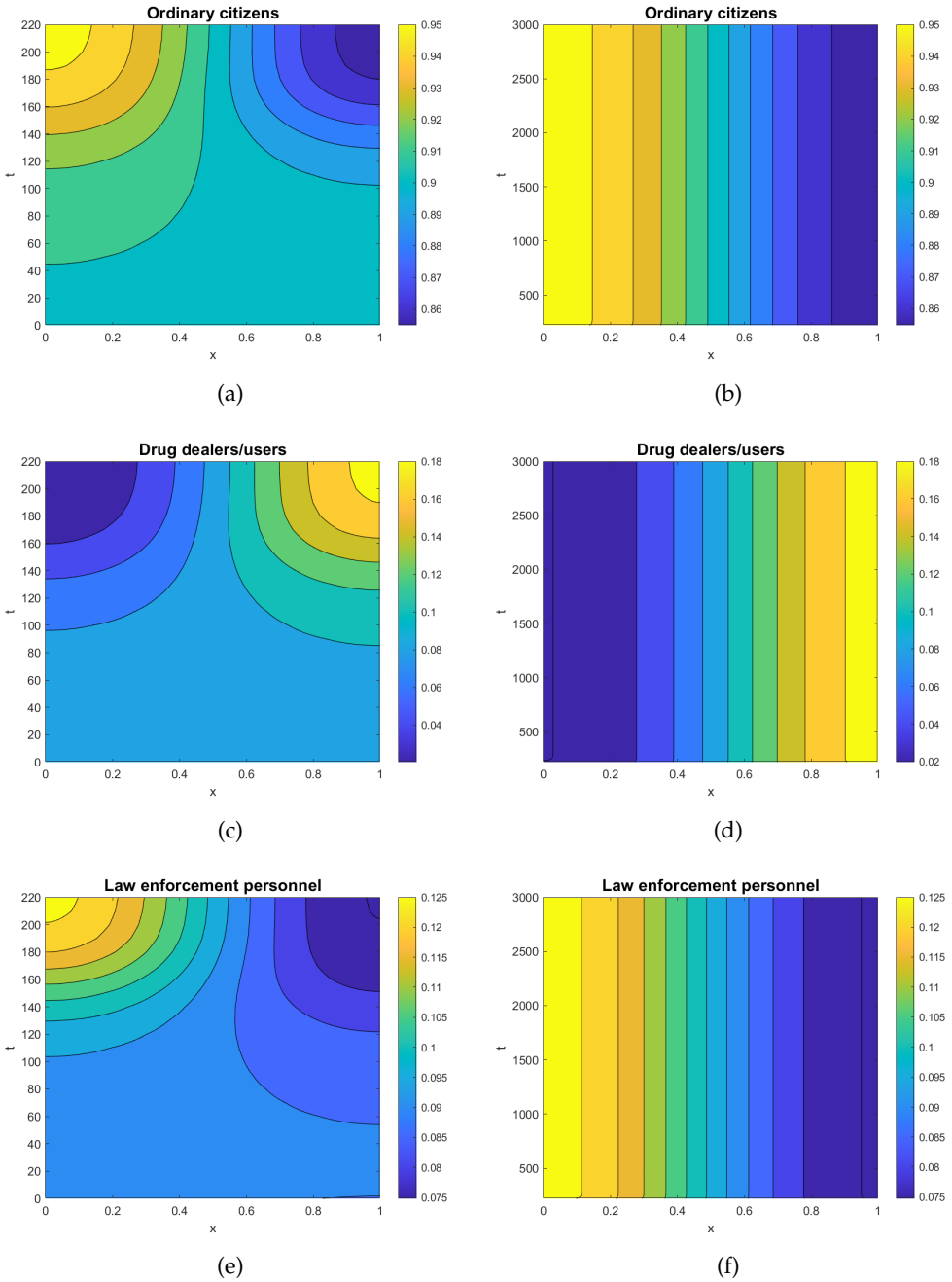

FIGURE 1.9: Contour plots of the solution for $t \in [0, 220]$ in (a)-(c)-(e) and for $t \in [220, 3000]$ in (b)-(d)-(f) with the parameters given in (1.22) and $d_{31} = 0.06$, $k = \pi$.

and, in order to have Turing instability, it is required $d_{31} > 0.0595941$.

In this scenario, at the equilibrium, the value for drug users/dealers is about four times the value of law enforcement personnel. Therefore, by assigning a value of d_{23} less than d_{21}, this allows the drug users/dealers to move fearless towards ordinary citizens.

Figures 1.10 and 1.11 depict the contour plots of the solution in correspondence of the parameters (1.23) for two different values of d_{31} greater than the critical value. As in the previous cases, on the left it is represented the evolution of the solution up to the formation of the pattern, while on the right is is shown the stationary state exhibiting the pattern with strips. Ordinary citizens and law enforcement personnel definitely concentrate on the same side (left), while drug users/dealers are more abundant on the opposite part (right) of the street.

Figure 1.12 illustrates the time evolution of averages and variances of the densities of the three subgroups all over the spatial domain in all the cases considered. As seen in the first variant, once the transient is over, the variance remains constant in time, thence the strips are stationary. Finally, the time required for the formation of Turing patterns decreases as the diffusion coefficient d_{31} increases.

1.8 Conclusions

In this Chapter, we implemented and investigated two variants of a model originally proposed by Epstein, named crimo-taxis. The models consist of three coupled reaction-diffusion equations involving self- and cross-diffusion coefficients. The modifications to the Epstein model consist in adding a logistic effect in the susceptible population and a cross-diffusion coefficient in order to describe a sort of *citizens' protection* made by the policemen. The second variant modifies also the original term accounting for the growth in the number of police forces in parallel with the increase of the level of social alarm.

Both models here studied admit asymptotically stable homogeneous coexistence equilibria, susceptible of losing their stability due to the self- and cross-diffusive terms. We analytically prove that the models may experience Turing instability depending on the value of a control parameter. The numerical simulations show the emergence of some characteristic patterns that remain stationary over time. The stationary non homogeneous solutions show that the models definitely allow for a distribution of the three subgroups in such a way law enforcement personnel is able to protect ordinary citizens, whereas drug users/dealers are isolated.

We must recognize that at the moment we do not have at the present rigorous results establishing the conditions for the positivity of the solutions; nevertheless, we notice that the parameters we used and the numerical solutions above presented describe physically meaningful solutions.

We are conscious that further investigations are needed, for instance considering an extension of the models to a two–dimensional spatial setting modeling a neighborhood of a town, or considering a generalization including an additional subgroup (the arrested individuals) so that the action of the law enforcement personnel is not limited to protect ordinary citizens but also to actively crack down on illegal behavior.

In Chapter 3, we will implement an operatorial model where the actors of the system here considered are represented by annihilation, creation and number fermionic operators whose evolution is ruled by a time-independent Hermitian Hamiltonian

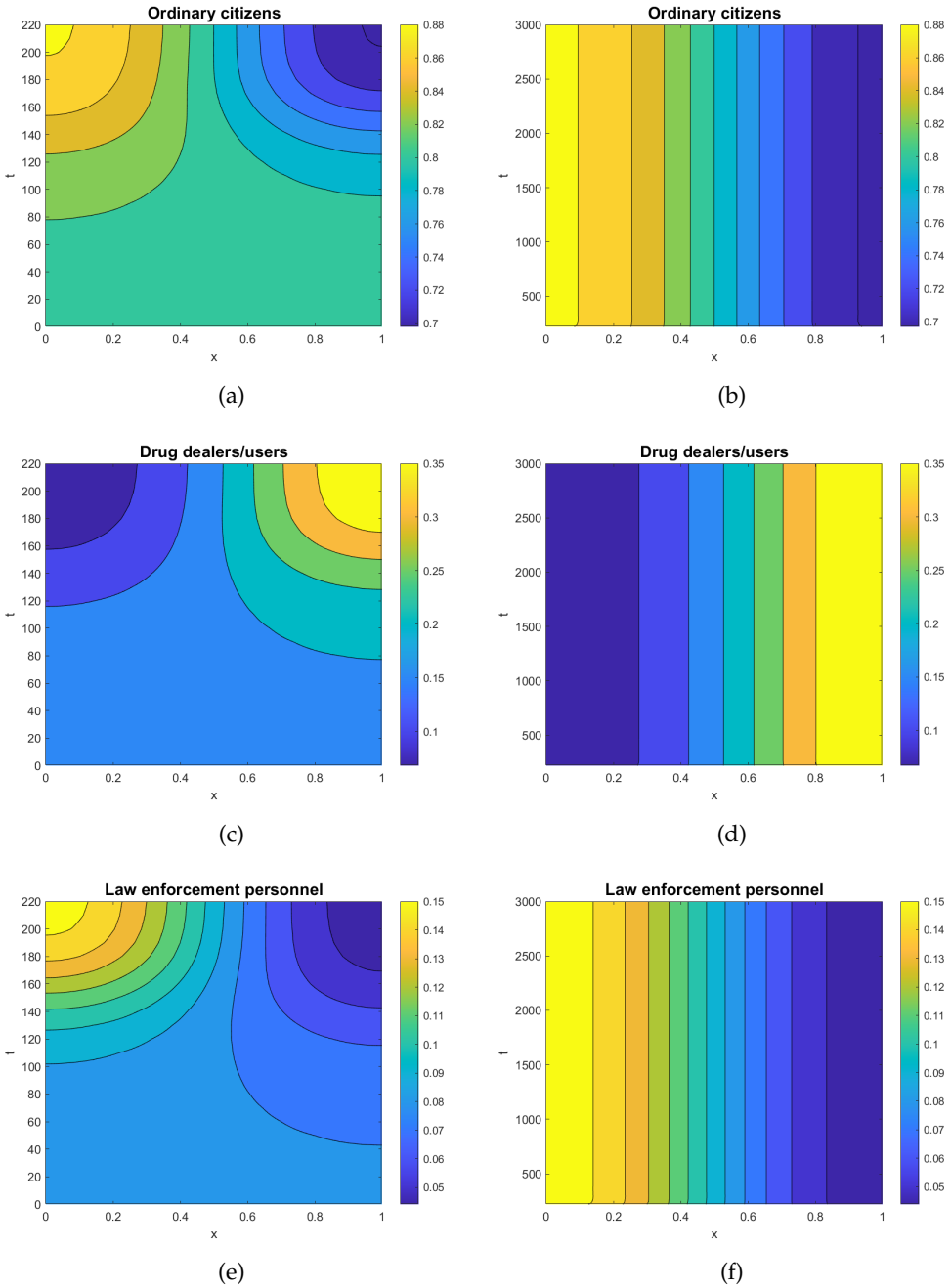

FIGURE 1.10: Contour plots of the solution for $t \in [0, 220]$ in (a)-(c)-(e) and for $t \in [220, 3000]$ in (b)-(d)-(f) with the parameters given in (1.23) and $d_{31} = 0.07, k = \pi$.

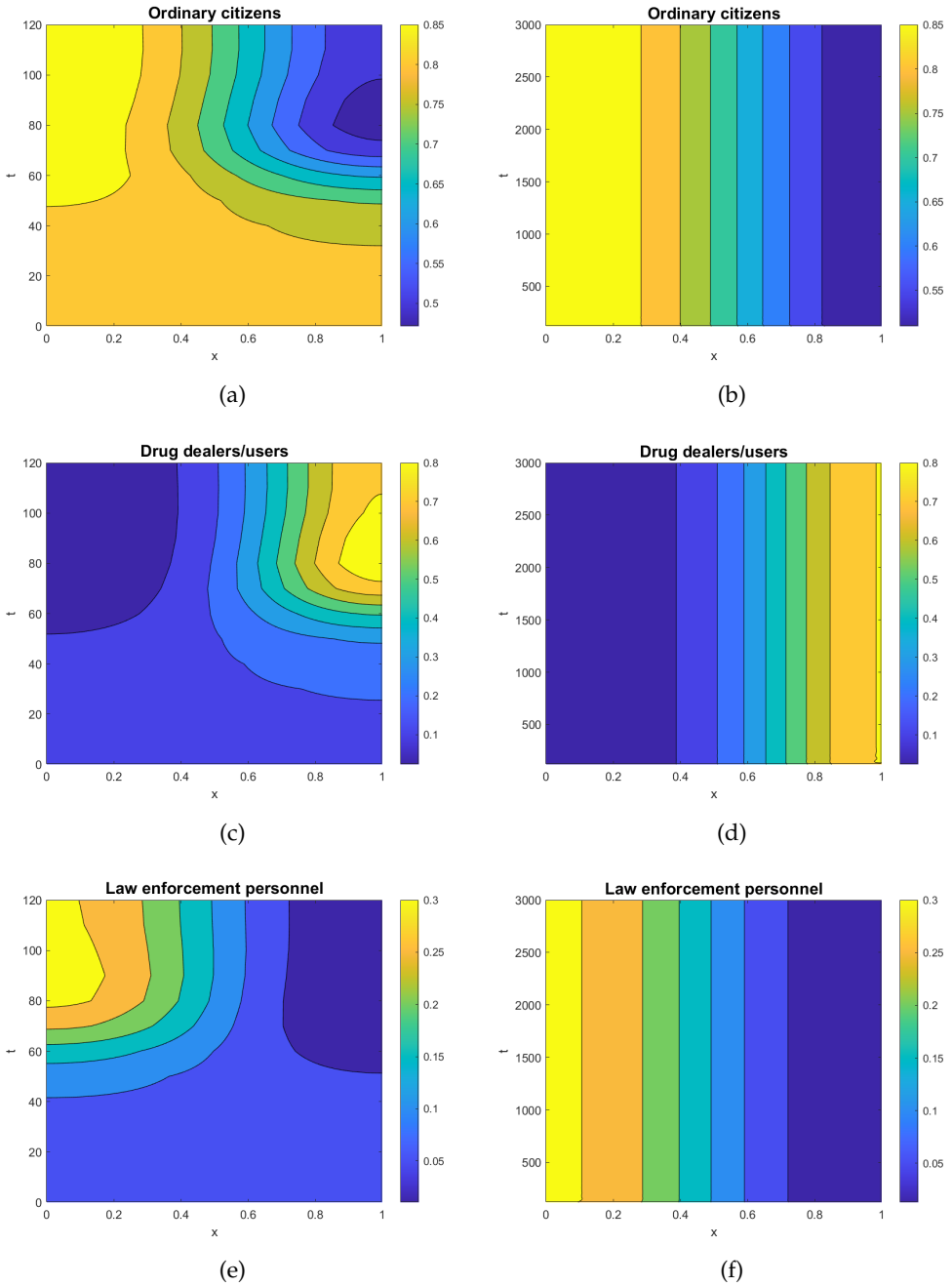

(a) (b) (c) (d) (e) (f)

FIGURE 1.11: Contour plots of the solution for $t \in [0, 120]$ in (a)-(c)-(e) and for $t \in [120, 3000]$ in (b)-(d)-(f) with the parameters given in (1.23) and $d_{31} = 0.08, k = \pi$.

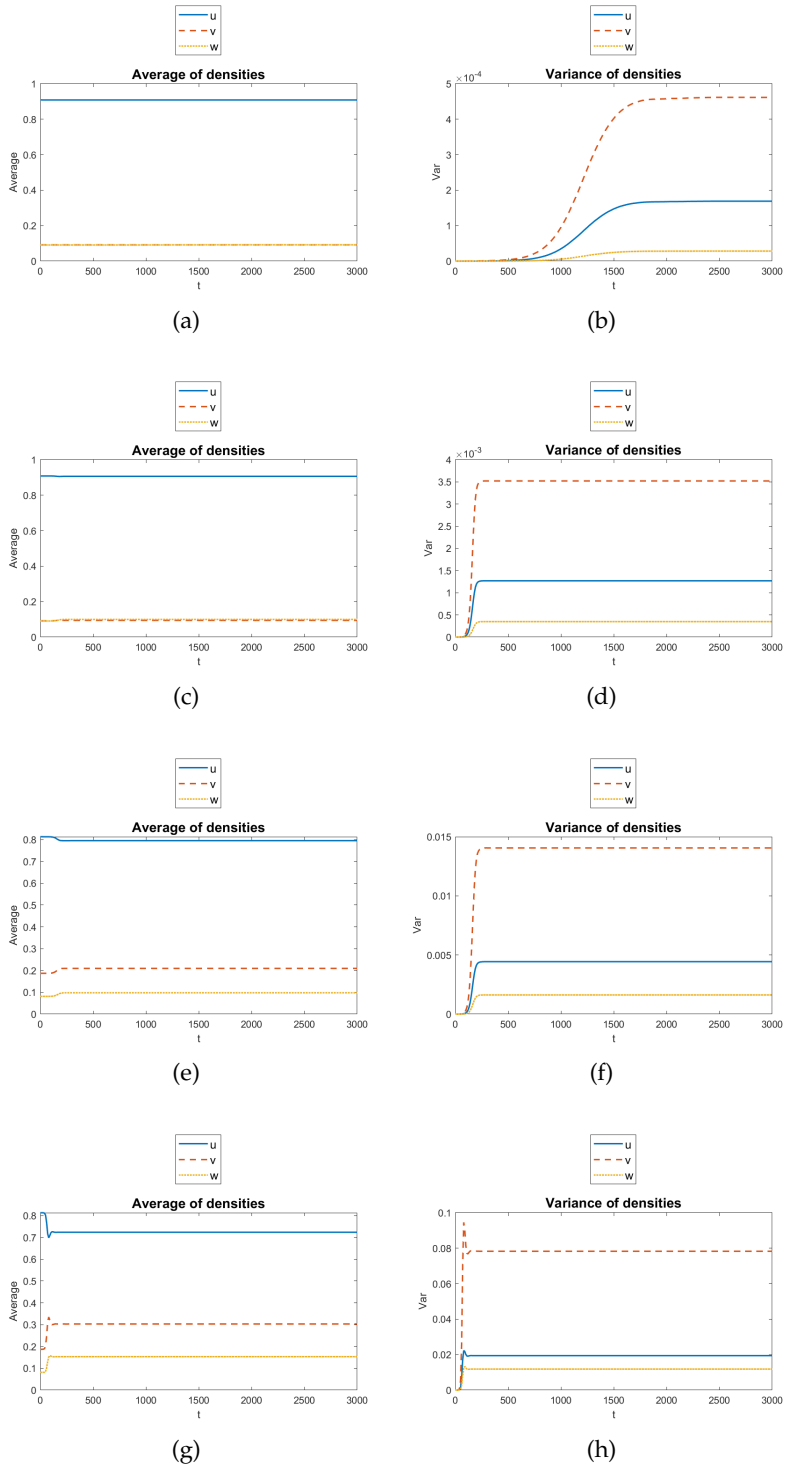

FIGURE 1.12: Plots of the averages (left) and variances (right) of the densities; subfigures (a)-(d) refer to the first scenario with $d_{31} = 0.06$ ((a), (b)), $d_{31} = 0.07$ ((c), (d)); subfigures (e)-(h) refer to the second scenario with $d_{31} = 0.07$ ((e), (f)), $d_{31} = 0.08$ ((g), (h)).

$\mathcal{H}$ within the recently introduced framework of $(\mathcal{H}, \rho)$–induced dynamics (Bagarello et al., 2018).

Chapter 2

The quantum framework

In the first part of this Chapter, to fix the language, the basic formalism used in quantum mechanics and essential for the subsequent developments is presented, and some aspects of the theory are briefly illustrated. In particular, we focus on occupation numbers, used for the definition of the theoretical framework that provides in a logically satisfying way the conceptual setting for the various applications. In the second part of the Chapter, we sketch the theoretical framework for the description of the dynamical properties of macroscopic systems by means of operatorial methods. The disquisition is carried out in very general terms, leaving aside the interpretation that can be attributed to the various models. Moreover, the approach of $(\mathcal{H}, \rho)$–induced-dynamics (Bagarello et al., 2018) is illustrated. The concluding Section shows a possible relation between terms in an operatorial model and the ones occurring in a classical model.

2.1 Background and preliminaries

During the twentieth century, scientists began to approach the microscopic world with the laws of physics introduced up to that moment. The first difficulties began because the laws for macroscopic phenomena were unable to satisfactorily describe the properties of matter at the microscopic level; in particular, classical mechanics appeared unable to describe the behavior of matter and electromagnetic radiation at the length scale of the order of the atom or at the energy scale of interatomic interactions; furthermore, the experimental reality of light and the electron was inexplicable. The limit of classical laws was the main motivation that led to the development of a new physics completely different from the one developed up to then. Some paradoxes related to microscopic phenomena have already been reported during nineteenth century. An example was the evidence that, according to the classical theory, a black body capable of absorbing all the incident radiation should emit electromagnetic waves with infinite intensity at short wavelengths. This devastating paradox, although not immediately deemed of great importance, was called the "ultraviolet catastrophe". The first physicist who introduced the concept of *quantum* was Max Planck in 1900 with his "*Über die Elementar quanta der Materie und der Elektrizitaet* (Planck, 1900). Planck's law states that the energy associated with electromagnetic radiation is transmitted in discrete units or quanta, subsequently identified with photons, $E = h\nu$, where E is the energy of a quantum, ν the frequency of radiation and h the Planck's constant. From these results, Werner Heisenberg and Erwin Schrödinger developed matrix mechanics and wave mechanics, two different formulations of quantum mechanics that lead to the same results. The Schrödinger equation, in particular, is similar to wave equation, and its stationary solutions represent the possible states of the particles and therefore also of the electrons in the hydrogen atom. The structure of quantum mechanics differs strongly from that of the

classical theory. In particular, the algebra of observables is no longer commutative, but, instead, position and momentum (q and p) satisfy the **canonical commutation relations**

$$[q, p] := qp - pq = \mathrm{i}\tilde{h}$$

where i is the imaginary unit, and $\tilde{h} = \frac{h}{2\pi} = 1.054 \times 10^{-34} Joule \cdot sec.$ is the reduced Planck's constant. The Schrödinger equation depends on the interactions between the various components of the system. In the general case, the equation is written as:

$$\mathrm{i}\tilde{h}\frac{\partial \Psi}{\partial t}(\mathbf{x}, t) = \mathcal{H}\Psi(\mathbf{x}, t).$$

where $\mathbf{x} = (x_1, x_2, x_3) \in \mathbb{R}^3$, Ψ is the wave function, that is the probability amplitude for the different configurations of the system; $\mathcal{H}$ is the Hamiltonian operator, which has the property of being Hermitian. The Schrödinger equation is the fundamental equation of quantum mechanics. One method to solve this equations is the Fourier method, which allows to obtain important information about the system.

The Hamiltonian operator plays a very important role, providing the time dependence of the wave function, and allowing, through the solution of the Schrödinger equation, to solve the eigenvalue problem for energy. The double slit experiment shows that the wave function can be considered as probability amplitude and its square modulus as probability density. It follows that the continuity equation expresses the conservation of probability. The class of functions acceptable as solutions of the Schrödinger equation is given by the complex square-integrable function defined on $\mathbb{R}^3$. In particular, the functions Ψ that are acceptable as solutions are the functions that belong to a complex linear space called the Hilbert space.

All the operators that we use in the following to build operatorial models will be defined on Hilbert spaces.

2.2 Canonical relations and number representation

In physics, fermions, so called in honor of Enrico Fermi, are the particles that follow the Fermi-Dirac statistics and consequently, according to the spin-statistics theorem, have half integer spin. Together with bosons, they are one of the two fundamental families into which particles are divided. The main distinctive elements of fermions are that they are subject to the Pauli exclusion principle and that they always possess mass, of which elementary bosons in several cases lack. All known matter is made up of fermions, responsible, directly or through their attractive force, for the mass detectable in nature.

The fermionic and bosonic operators are defined in a Hilbert space. In particular, let $\mathbb{H}$ be a Hilbert space and $\mathcal{B}(\mathbb{H})$ the set of all the bounded operators on $\mathbb{H}$. $\mathcal{B}(\mathbb{H})$ is a so-called $C^\star$*–algebra*, that is, an algebra with involution that is complete under a norm, $||\cdot||$, satisfying the $C^\star$*–property*: $||A^\star A|| = ||A||^2$, for all $A \in \mathcal{B}(\mathbb{H})$. As a matter of fact, $\mathcal{B}(\mathbb{H})$ is usually seen as a *concrete realization* of an abstract $C^\star$–algebra.

Let $\mathcal{S}$ be the physical system under consideration, and $\mathcal{A}$ the set of all the operators useful for a complete description of $\mathcal{S}$, which includes the observables of $\mathcal{S}$. For simplicity, it is convenient to assume that $\mathcal{A}$ is a $C^\star$–algebra by itself, possibly coinciding with the original set $\mathcal{B}(\mathbb{H})$, or, at least, with some closed subset of $\mathcal{B}(\mathbb{H})$. All definitions apply only if bounded operators are used. However, if $X : \mathbb{H} \to \mathbb{H}$ is an operator, and if it is self–adjoint, then $\exp(\mathrm{i}Xt)$ is unitary and, therefore, bounded.

The formalism of second quantization (Paar, 2010) starts by postulating the Canonical Commutation Relations (CCR):

$$[a_j, a_k] = [a_j^\dagger, a_k^\dagger] = 0, \qquad [a_j, a_k^\dagger] = \delta_{j,k}\mathcal{I}, \tag{2.1}$$

$j, k = 1, \dots L$ (in case of a system $\mathcal{S}$ with L independent bosonic modes), where $\mathcal{I}$ is the identity operator on $\mathbb{H}$, $\delta_{j,k}$ is the Kronecker symbol, and $[u, v] := uv - vu$ is the commutator between the operators u and v.

In the equations (2.1) the operators a_j, and their adjoints $a_j^\dagger$, represent the annihilation and creation operators of the bosons, respectively (the annihilation and creation operators are operators that respectively decrease or increase the number of particles of a quantum state by one. For example, they are comparable to the operators for the quantum harmonic oscillator, which remove or add a quantum of energy to the system). From these operators we can construct another important and self–adjoint operator, the *number operator* for the j–th mode, say

$$\widehat{n}_j = a_j^\dagger a_j, \qquad j = 1, \dots, L, \tag{2.2}$$

whose eigenvalues are the occupation numbers n_j for the L modes of the system. The operator

$$\widehat{N} = \sum_{j=1}^{L} \widehat{n}_j \tag{2.3}$$

is called the *number operator* of $\mathcal{S}$.

Once the operators have been defined, it is necessary to construct an orthonormal basis of $\mathbb{H}$. Let us start introducing the *vacuum* of the theory, that is, a vector φ_0 that is annihilated by all the operators a_j, $a_j\varphi_0 = 0$ for $j = 1, \dots, L$. Then we act on φ_0 with the operators $a_l^\dagger$ and with their powers,

$$\varphi_{n_1,n_2,\dots,n_L} := \frac{1}{\sqrt{n_1!, n_2!, \dots, n_L!}} (a_1^\dagger)^{n_1} (a_2^\dagger)^{n_2} \dots (a_L^\dagger)^{n_L} \varphi_0, \tag{2.4}$$

$n_j = 0, 1, \dots,$ for all j. The set of the vectors $\varphi_{n_1,n_2,\dots,n_L}$ forms a complete and orthonormal set in $\mathbb{H}$, and they are eigenstates of both $\widehat{n}_j$ and $\widehat{N}$:

$$\widehat{n}_j \varphi_{n_1,n_2,\dots,n_L} = n_j \varphi_{n_1,n_2,\dots,n_L}, \qquad \widehat{N}\varphi_{n_1,n_2,\dots,n_L} = N\varphi_{n_1,n_2,\dots,n_L},$$

where $N = \sum_{j=1}^{L} n_l$. Hence, n_j and N are eigenvalues of $\widehat{n}_j$ and $\widehat{N}$, respectively. Moreover, using the CCR we deduce that

$$\widehat{n}_j(a_l \varphi_{n_1,n_2,\dots,n_L}) = (n_j - 1)(a_j \varphi_{n_1,n_2,\dots,n_L}),$$

for $n_j \leq 1$, whereas if $n_j = 0$, a_j annihilates the vector, and

$$\widehat{n}_j(a_j^\dagger \varphi_{n_1,n_2,\dots,n_L}) = (n_j + 1)(a_j^\dagger \varphi_{n_1,n_2,\dots,n_L}),$$

for all j and for all n_j.

The operator $\widehat{n}_j$ acts on $\varphi_{n_1,n_2,\dots,n_L}$ and return n_j, which is exactly the number of bosons in the j-th mode. The operator $\widehat{N}$ counts the total number of bosons. Moreover, the operator a_j destroys a boson in the j–th mode, whereas $a_j^\dagger$ creates a boson in the same mode. This is why in the physical literature a_j and $a_j^\dagger$ are called the *annihilation* and the *creation* operators, respectively.

Thus, the Hilbert Space $\mathbb{H}$ is infinite dimensional, and the operators introduced so far are all unbounded.

The vector $\varphi_{n_1,n_2,\dots,n_L}$ has to be intended as a descriptor of the L different modes of bosons of $\mathcal{S}$ in the sense that n_1 bosons are in the first mode, n_2 in the second mode, and so on.

Analogously to the case of bosons, fermions are annihilated and created by similar operators, b_j and $b_j^\dagger$, but these operators satisfy different rules, called the *Canonical Anticommutation Relations* (CAR)

$$\{b_j, b_k\} = \{b_j^\dagger, b_k^\dagger\} = 0, \qquad \{b_j, b_k^\dagger\} = \delta_{j,k}\mathcal{I}, \tag{2.5}$$

$j,k = 1,\dots L$ (in case of a system $\mathcal{S}$ with L independent fermionic modes), where $\{u,v\} := uv + vu$ is the anticommutator between the operators u and v. These operators are used to describe L different *modes* of fermions. As for bosons, it is possible to construct $\widehat{n}_j = b_j^\dagger b_j$ and $\widehat{N} = \sum_{j=1}^L \widehat{n}_j$, which are both self–adjoint. Also in this case, $\widehat{n}_j$ is the *number operator* for the j-th mode, while $\widehat{N}$ is *number operator* for $\mathcal{S}$.

A very important difference between bosonic and fermionic operators is that if we try to square fermionic operators (or to rise them to higher powers), we simply get zero; for instance, from equations (2.5), we have $b_j^2 = 0$. This happens because the fermions satisfy the Pauli exclusion principle (Roman, 1965), whereas bosons do not.

The Hilbert space $\mathbb{H}$ of the system $\mathcal{S}$ is constructed as for bosons, with the difference that we can act on the vacuum φ_0 with the operators $b_j^\dagger$ but not with higher powers because these powers are simply zero. Let us construct the vector

$$\varphi_{n_1,n_2,\dots,n_L} = (b_1^\dagger)^{n_1}(b_2^\dagger)^{n_2}\cdots(b_L^\dagger)^{n_L}\varphi_0 \tag{2.6}$$

$n_j = 0, 1$ for all j (here it is $\sqrt{n_1!n_2!\cdots n_L!} = 1$).

A major difference with respect to what happens for bosons is the property, following from the idempotence of $\widehat{n}_j$,

$$\widehat{n}_j^2 = b_j^\dagger b_j b_j^\dagger b_j = b_j^\dagger(1 - b_j^\dagger b_j)b_j = b_j^\dagger b_j - b_j^\dagger b_j^\dagger b_j b_j = \widehat{n}_j, \tag{2.7}$$

and the consequence of this is that the eigenvalues of $\widehat{n}_j$ are simply 0 and 1.

Moreover, using the CAR, we deduce that

$$\widehat{n}(b_j\varphi_{n_1,n_2,\dots,n_L}) = \begin{cases} (n_j - 1)(b_j\varphi_{n_1,n_2,\dots,n_L}), & n_j = 1 \\ 0, & n_j = 0, \end{cases}$$

and

$$\widehat{n}(b_j^\dagger\varphi_{n_1,n_2,\dots,n_L}) = \begin{cases} (n_j + 1)(b_j^\dagger\varphi_{n_1,n_2,\dots,n_L}), & n_j = 0 \\ 0, & n_j = 1, \end{cases},$$

for all j. The interpretation of the annihilation and the creation operators for fermions is not different from the one for bosons, except from the fact that the annihilation operator $b_j^\dagger$ acting on a state with $n_j = 1$ destroys that state. Of course, the dimension of the Hilbert space of the fermionic systems is finite. In particular, for just one mode of fermions, $\dim(\mathbb{H}) = 2$, and for L modes of fermions $\dim(\mathbb{H}) = 2^L$. This also implies that, contrarily to what happens for bosons, all the fermionic operators are bounded and can be represented by matrices of finite order.

In this thesis, the operatorial models we introduce use fermionic operators.

2.3 Heisenberg representation

In this Section, some useful notions to describe a system $\mathcal{S}$, whose actors are represented by ladder operators, are recalled. In particular, we will limit ourselves to fermionic operators.

The description of the time evolution of $\mathcal{S}$ involving L modes is assumed to be ruled by a self–adjoint and time independent operator $\mathcal{H}$, the Hamiltonian; in standard quantum mechanics, it is the observable operator corresponding to the total energy of the system.

The time evolution of a self–adjoint operator X in the associated Hilbert space $\mathbb{H}$, in the Heisenberg representation, is given by the relation

$$X(t) = \exp(\mathrm{i}\mathcal{H}t)X\exp(-\mathrm{i}\mathcal{H}t), \tag{2.8}$$

or equivalently by the solution of

$$\frac{dX(t)}{dt} = \mathrm{i}[\mathcal{H}, X(t)]. \tag{2.9}$$

Once defined a vector state $\varphi_{n_1,n_2,\ldots,n_L}$ representing the initial configuration of the system, we compute the mean values

$$x(t) = \langle \varphi_{n_1,n_2,\ldots,n_L}, X(t)\varphi_{n_1,n_2,\ldots,n_L}\rangle, \tag{2.10}$$

where $\langle , \rangle$ is the scalar product in $\mathbb{H}$. For the description of a macroscopic system, the operator X that we will consider is the number operator of the generic j-th mode.

2.4 Operatorial models of macroscopic systems

In this Section, we present a general operatorial model for the description of a macroscopic system made by L compartments or agents; the dynamics is assumed to be ruled by a quadratic Hamiltonian. For this reason the interpretation of the models at the moment is left free in order to analyze the theoretical aspects. In the following chapters we will specialize these results by considering well defined systems.

2.4.1 Systems modeled by quadratic Hamiltonians

Let us consider at first a simple model describing the dynamics of a certain physical system $\mathcal{S}$ in terms of L different fermionic modes, and let us introduce the fermionic annihilation and creation operators a_j and $a_j^\dagger$ ($j = 1, 2, \ldots, L$). These operators satisfy the canonical anticommutation relations (2.5). Let us assume the existence of the following Hamiltonian operator

$$\begin{aligned} \mathcal{H} &= \mathcal{H}_0 + \mathcal{H}_I, \qquad \text{with} \\ \mathcal{H}_0 &= \sum_{i=1}^{L} \omega_i a_i^\dagger a_i, \\ \mathcal{H}_I &= \sum_{i,j=1\ i<j}^{L} \lambda_{i,j}(a_i a_j^\dagger + a_j a_i^\dagger) + \sum_{i,j=1\ i<j}^{L} \mu_{i,j}(a_i^\dagger a_j^\dagger + a_j a_i), \end{aligned} \tag{2.11}$$

where ω_i, $\lambda_{i,j}$, $\mu_{i,j}$ are positive real parameters. The operator $\mathcal{H}$ includes a free standard part, $\mathcal{H}_0$, and a contribution, $\mathcal{H}_I$, related to the interaction among the components. In particular, the parameters in $\mathcal{H}_0$ can be thought of as a measure of the inertia of the different compartments (Bagarello, 2012): the higher the value of a certain ω_i , the higher the tendency of the corresponding mode to stay constant in time. On the other hand, the contribution $\mathcal{H}_I$, which is quadratic in the raising and lowering operators, describes the interactions among the different modes. In particular, the term $a_i^\dagger a_j$, makes the number of particles of the i-th compartment of S to increase and that of the j-th one to decrease, while the adjoint contribution, $a_j^\dagger a_i$, is responsible for the opposite phenomenon. Similarly, the terms $a_i^\dagger a_j^\dagger$ or $a_j a_i$ are intended to produce a simultaneous increase or decrease of particles both the i-th and the j-th compartment of $\mathcal{S}$. The parameters $\lambda_{i,j}$ measure the strength of the competition between the i-th and the j-th compartment, whereas the parameters $\mu_{i,j}$ the strength of cooperation. When the components of the system do not interact, the parameters $\lambda_{i,j}$ and $\mu_{i,j}$ must be zero and no dynamics occurs.

In the Heisenberg representation, we are led to the following system of (linear) ordinary differential equations

$$\begin{aligned}
\dot{a}_i &= \mathrm{i}\left(-\omega_i a_i + \sum_{1\le k<i} \lambda_{k,i} a_k \sum_{i<j\le L} \lambda_{i,j} a_j - \sum_{1\le k<i} \mu_{k,i} a_k^\dagger + \sum_{i<j\le L} \mu_{i,j} a_j^\dagger\right), \\
\dot{a}_i^\dagger &= \mathrm{i}\left(\omega_i a_i^\dagger - \sum_{1\le k<i} \lambda_{k,i} a_k^\dagger - \sum_{i<j\le L} \lambda_{i,j} a_j^\dagger + \sum_{1\le k<i} \mu_{k,i} a_k - \sum_{i<j\le L} \mu_{i,j} a_j\right).
\end{aligned} \tag{2.12}$$

The unknowns in (2.12) are operators represented by $2^L \times 2^L$ matrices with complex entries, whereupon, at least in principle, we have to solve a system of $2L \cdot 2^{2L}$ scalar ordinary differential equations in the complex domain. Nevertheless, because of the linearity of equation (2.12), we are able to reduce drastically the computational complexity.

Introducing the formal column vector

$$\mathbf{A} = \left[a_1, \ldots, a_L, a_1^\dagger, \ldots, a_L^\dagger\right]^T,$$

(^{T} stands for the transposition operator), and a suitable $2L \times 2L$ real matrix Γ (whose entries, once we fix L, can be constructed from (2.12), the evolution equations for the annihilation operators can be written in the compact form as

$$\frac{d\mathbf{A}}{dt} = \mathrm{i}\Gamma\mathbf{A}, \tag{2.13}$$

whose solution is

$$\mathbf{A}(t) = \exp(\mathrm{i}\Gamma t)\mathbf{A}_0 = \mathcal{B}(t)\mathbf{A}_0, \tag{2.14}$$

whereupon we can compute the number operators and their mean values on an initial condition. Let n_i^0 $(i = 1, \ldots, L)$ be the initial mean value of the number operators, and let $\mathbf{n}^0$ the vector with L components

$$\mathbf{n}^0 = \left(\sqrt{n_1^0}, \ldots, \sqrt{n_L^0}\right);$$

denoting with $B_{j,k}$ the generic entry of the $2L \times 2L$ matrix $\mathcal{B}(t)$, it is not difficult

to derive, by using the canonical anticommutation relations (2.5), the formula giving the mean values of the number operators at time t (Inferrera and Oliveri, 2022; Gorgone, Inferrera, and Oliveri, 2022):

$$\begin{aligned} n_i(t) = &\sum_{j=1}^{L} \left(n_j^0\right)^2 \sum_{\ell=1}^{L} \left(B_{i,f(\ell,j)} B_{i+L,g(\ell,j)}\right) \\ &+ \sum_{j=1}^{L-1} \sum_{k=j+1}^{L} n_j^0 n_j k^0 \left(B_{i,j} B_{i+L,k+L} + B_{i,k} B_{i+L,j+L}\right. \\ &\left. - B_{i,j+L} B_{i+L,k} - B_{i,k+L} B_{i+L,j}\right), \end{aligned} \tag{2.15}$$

where

$$f(\ell,j) = \begin{cases} j & \text{if} \quad j = \ell, \\ j+L & \text{if} \quad j \neq \ell, \end{cases} \qquad g(\ell,j) = \begin{cases} j+L & \text{if} \quad j = \ell, \\ j & \text{if} \quad j \neq \ell. \end{cases}$$

In general, the dynamics when we take a quadratic Hamiltonian with only competitive interaction terms, is at most quasi-periodic, and this behavior is not always the result we expect. For this reason, if we want to obtain more interesting behaviors, we need to include in the Hamiltonian other ingredients (for example, time dependent parameters), or something else. There are various possibilities; however, they often determine an increase of the technical difficulties or a huge amount of the computational complexity.

There has been proposed recently a method, named $(\mathcal{H}, \rho)$-induced dynamics (see Section 2.6) that, still retaining a time independent quadratic Hamiltonian, use some *rules*, and allow for dynamical behaviors that can admit asymptotic equilibrium states.

2.5 Spatial models

In this Section, we introduce the possibility that the agents of a system $\mathcal{S}$ are spatially distributed. These models are very important since it is possible to model migration phenomena (Bagarello and Oliveri, 2013; Inferrera and Oliveri, 2022), for instance when a population can move from a poor place to a richer region already occupied by a second population, or desertification processes (Bagarello, Cherubini, and Oliveri, 2016), or models with crowds and their escaping strategies (Bagarello, Gargano, and Oliveri, 2015), ...

To describe these systems, it is necessary to introduce additional terms in the Hamiltonian operator able to describe the diffusion over a region. This implies to consider a high number of modes, in each cell of the spatial region where the L actors of the system interact, we have L modes; therefore, if the spatial region contains N cells, we have $L \times N$ modes.

Let us start by considering a region $\mathcal{R}$ made by N cells, where L actors live. In each cell α we have annihilation operators $a_{j,\alpha}$ ($j = 1, \ldots, L$, $\alpha = 1, \ldots, N$). In the Hamiltonian operator, besides the terms $\mathcal{H}_0$ and $\mathcal{H}_I$ (for local interaction), we may include *migration* terms ($\mathcal{H}_M$) as well as terms describing nonlocal interaction

mechanisms ($\mathcal{H}_C$):

$$\begin{aligned}\mathcal{H}_M &= \sum_{\alpha=1}^{N}\sum_{i=1}^{L}\left(\mu_{i,\alpha}\sum_{\beta=1}^{N}p_{\alpha\beta}(a_{i,\alpha}a_{i,\beta}^{\dagger}+a_{i,\beta}a_{i,\alpha}^{\dagger})\right),\\ \mathcal{H}_C &= \sum_{\alpha=1}^{N}\sum_{i,j=1,i<j}^{L}\left(\nu_{ij,\alpha}\sum_{\beta=1}^{N}p_{\alpha\beta}(a_{i,\alpha}a_{j,\beta}^{\dagger}+a_{j,\beta}a_{i,\alpha}^{\dagger})\right),\end{aligned} \tag{2.16}$$

where $\mu_{i,\alpha}$, $\nu_{ij,\alpha}$, $p_{\alpha,\beta}$ are real constants. All the parameters entering the spatial model are, in general, assumed to be cell dependent. The coefficients $p_{\alpha,\beta}$, symmetric with respect to their indices, are equal to 1 if β denotes a cell in a suitable neighborhood of the cell α (for instance, it is in the Moore neighborhood of the cell α), and 0 elsewhere, and the parameters $\mu_{i,\alpha}$ are the mobilities. Therefore, if $p_{\alpha,\beta} = 1$, the term $a_{i,\alpha}a_{i,\beta}^{\dagger}$ produces a migration from cell α to cell β. For this reason, $p_{\alpha,\beta}$'s, with the parameters $\mu_{i,\alpha}$ measure the diffusion coefficients.

The same reasoning leads to say that $p_{\alpha,\beta}$, with the parameters $\nu_{ij,\alpha}$ measure the non-local competition.

2.6 $(\mathcal{H},\rho)$–induced dynamics

In this Section, we explain the possibility to expand the description of the time evolution of a macroscopic system by using some tools arising from quantum mechanics together with some specific rules. This innovative approach, called $(\mathcal{H},\rho)$–induced dynamics, was introduced for the first time in (Bagarello et al., 2017), then applied in several papers (Bagarello, Gargano, and Oliveri, 2015; Di Salvo and Oliveri, 2016a; Di Salvo and Oliveri, 2017; Di Salvo, Gorgone, and Oliveri, 2017a; Di Salvo, Gorgone, and Oliveri, 2017b; Bagarello, Gargano, and Oliveri, 2020; Inferrera and Oliveri, 2022; Gorgone, Inferrera, and Oliveri, 2022), and analyzed in general in (Bagarello et al., 2018). This approach allows to derive the time evolution of a given system governed not only by a Hamiltonian operator, but also by some external/internal actions periodically acting to the system that are not easy to include in any Hamiltonian. In the next Chapters, we will show that by replacing the Heisenberg classical dynamics with the $(\mathcal{H},\rho)$–induced dynamics, some relevant dynamic variables of the system may converge, for large times, to some asymptotic values.

The *rule* we consider is nothing more than a law that modifies periodically some of the values of the parameters involved in the Hamiltonian as a consequence of the evolution of the system. The underlying idea is that the model adjusts itself during the time evolution; since the model involves some actors, the modifications of some of the parameters entering the Hamiltonian reflect some changes in the intensity of the interactions according to the evolution of their state. In other words, the modifications of some of the parameters of the model may be thought of as a surreptitious way to take into account the influence of the external world, even if this action is induced by the evolution of the model itself; actually, the evolution of the state of the system does influence the attitudes of the different actors!

2.6.1 The rule ρ as a map in the space of the parameters of $\mathcal{H}$

In the models that will be discussed in the following Chapters of the thesis we will therefore use the rule ρ as a map in the space of the parameters of $\mathcal{H}$.

Thus, we sketch briefly how the procedure works (see Bagarello et al., 2018, and references therein, for further details).

Let us start considering a self–adjoint time–independent quadratic Hamiltonian operator $\mathcal{H}^{(1)}$; according to Heisenberg view, we can compute, in a time interval of length $\tau > 0$, the evolution of annihilation and creation operators, whereupon, choosing an initial condition for the mean values of the number operators, obtain their time evolution (our observables). According to the values of the observables at time τ, or to their variations in the time interval $[0, \tau]$, we modify some of the parameters involved in $\mathcal{H}^{(1)}$. In this way, we get a new Hamiltonian operator $\mathcal{H}^{(2)}$, having the same functional form as $\mathcal{H}^{(1)}$, but (in general) with different values of (some of) the involved parameters, and follow the continuous evolution of the system under the action of this new Hamiltonian for the next time interval of length τ. Actually, we do not restart the evolution of the system from a new initial condition, but simply continue to follow the evolution with the only difference that for $t \in]\tau, 2\tau]$ a new Hamiltonian $\mathcal{H}^{(2)}$ rules the process. And so on.

From a mathematical point of view, the rule is just a map from $\mathbb{R}^p$ into $\mathbb{R}^p$ acting on the space of the p parameters involved in the Hamiltonian. The global evolution is governed by a sequence of similar Hamiltonian operators, and the parameters entering the model can be considered stepwise (in time) constant. More specifically, let us consider a time interval $[0, T]$ where we follow the evolution of the system, and split it in $n = T/\tau$ subintervals of length τ. Assume for simplicity n to be integer. In the k–th subinterval $[(k-1)\tau, k\tau[$ consider an Hermitian Hamiltonian $H^{(k)}$ ruling the dynamics and apply Heisenberg view. Therefore, the global dynamics comes from the sequence of Hamiltonians

$$\mathcal{H}^{(1)} \xrightarrow{\tau} \mathcal{H}^{(2)} \xrightarrow{\tau} \mathcal{H}^{(3)} \xrightarrow{\tau} \cdots \xrightarrow{\tau} \mathcal{H}^{(n)}, \tag{2.17}$$

and the complete evolution in the interval $[0, T]$ is obtained by glueing the local evolutions in each subinterval.

This kind of rule-induced stepwise dynamics clearly may generate discontinuities in the first order derivatives of the operators, but prevents the occurrence of jumps in their evolutions and, consequently, in the mean values of the number operators. By adopting this rule, we are implicitly considering the possibility of having a time dependent Hamiltonian. However, the time dependence is, in our case, of a very special form: in each interval $[(k-1)\tau, k\tau[$ the Hamiltonian does not depend on time, but in $k\tau$ some changes may occur, according to how the system is evolving. For this reason, our Hamiltonian can be considered piecewise constant in time. A comparison of this approach with that related to an explicitly time dependent Hamiltonian is discussed in Bagarello et al., 2018.

2.7 Similitudes between a reaction-diffusion system and an operatorial model

Consider a system of two populations, whose numbers and spatial distributions evolve in time. For simplicity, imagine to study their evolution in a one-dimensional region. Let $u(x,t)$ and $v(x,t)$ positive real functions describing the densities of two populations, for instance interacting with a prey-predator mechanism. A possible reaction-diffusion model could be

$$\begin{aligned}
\frac{\partial u}{\partial t} &= \mu u - \lambda uv + D_{11}\frac{\partial^2 u}{\partial x^2} + D_{12}\frac{\partial^2 v}{\partial x^2}, \\
\frac{\partial v}{\partial t} &= -\gamma v + \lambda uv + D_{21}\frac{\partial^2 u}{\partial x^2} + D_{22}\frac{\partial^2 v}{\partial x^2}.
\end{aligned}$$

Now, let us construct a similar operatorial model ruled by a quadratic time independent self-adjoint Hamiltonian. Let us divide the region $\mathcal{C}$ where the two populations live and interact in N cells labeled with a greek letter. To each population in the cell α let us associate an annihilation $(a_{j,\alpha})$ and a creation $(a^\dagger_{j,\alpha})$ operator. The interpretation we give to the number operators $\widehat{n}_{j,\alpha}$ is that of the density of the j-th actor in the cell α.

Let us define the following Hamiltonian:

$$\mathcal{H} = \mathcal{H}_0 + \mathcal{H}_I + \mathcal{H}_M + \mathcal{H}_C,$$

where

$$\begin{aligned}
\mathcal{H}_0 &= \sum_{\alpha=1}^{N}\sum_{j=1}^{2}\left(\omega_j a^\dagger_{j,\alpha}a_{j,\alpha}\right),\\
\mathcal{H}_I &= \sum_{\alpha=1}^{N}\lambda(a_{1,\alpha}a^\dagger_{2,\alpha} + a_{2,\alpha}a^\dagger_{1,\alpha}),\\
\mathcal{H}_M &= \sum_{\alpha=1}^{N}\sum_{j=1}^{2}\left(\mu_j\sum_{\beta=1}^{N}p_{\alpha\beta}(a_{j,\alpha}a^\dagger_{j,\beta} + a_{j,\beta}a^\dagger_{j,\alpha})\right),\\
\mathcal{H}_C &= \sum_{\alpha=1}^{N}\left(\nu\sum_{\beta=1}^{N}p_{\alpha\beta}(a_{1,\alpha}a^\dagger_{2,\beta} + a_{2,\beta}a^\dagger_{1,\alpha})\right).
\end{aligned}$$

Adopting the Heisenberg view of dynamics, we are led to the following evolution equations for the annihilation operators in the cell α:

$$\begin{aligned}
\dot{a}_{1,\alpha} =& \mathrm{i}(-\omega_1 a_{1,\alpha} + \lambda a_{2,\alpha} + 2\mu_1(a_{1,\alpha-1} + a_{1,\alpha+1}) + \nu(a_{2,\alpha+1} + a_{2,\alpha-1})),\\
\dot{a}_{2,\alpha} =& \mathrm{i}(-\omega_2 a_{2,\alpha} + \lambda a_{1,\alpha} + 2\mu_2(a_{2,\alpha-1} + a_{2,\alpha+1}) + \nu(a_{1,\alpha+1} + a_{1,\alpha-1})).
\end{aligned}$$

With a suitable substitution it is possible to rewrite the above system in the following form :

$$\begin{aligned}
\dot{a}_{1,\alpha} =& \mathrm{i}\left(-\widetilde{\omega}_{1,\alpha}a_{1,\alpha} + \widetilde{\lambda}_\alpha a_{2,\alpha} + \widetilde{\mu}_1\frac{(a_{1,\alpha-1} - 2a_{1,\alpha} + a_{1,\alpha+1})}{\Delta x^2}\right.\\
&\left.\widetilde{\nu}\frac{(a_{2,\alpha-1} - 2a_{2,\alpha} + a_{2,\alpha+1})}{\Delta x^2}\right),\\
\dot{a}_{2,\alpha} =& \mathrm{i}\left(-\widetilde{\omega}_{2,\alpha}a_{2,\alpha} + \widetilde{\lambda}_\alpha a_{1,\alpha} + \widetilde{\mu}_2\frac{(a_{2,\alpha-1} - 2a_{2,\alpha} + a_{2,\alpha+1})}{\Delta x^2}\right.\\
&\left.\widetilde{\nu}\frac{(a_{1,\alpha-1} - 2a_{1,\alpha} + a_{1,\alpha+1})}{\Delta x^2}\right),
\end{aligned}$$

with

$$\begin{aligned}
&\widetilde{\omega}_1 = \omega_1 - 2\mu_1, \quad \widetilde{\omega}_2 = \omega_2 - 2\mu_2, \quad \widetilde{\lambda}_\alpha = \lambda_\alpha + 2\nu,\\
&\widetilde{\mu}_1 = 2\mu_1\Delta x^2, \quad \widetilde{\mu}_2 = 2\mu_2\Delta x^2, \quad \widetilde{\nu} = \nu\Delta x^2.
\end{aligned}$$

Terms in red and blue can be interpreted as the spatial discretization (with step Δx) of self- and cross-diffusion terms, respectively; thus, an operatorial model of a lattice can be though of as the spatial discretization of a system of partial differential equations of reaction-diffusion type.

Chapter 3

Operatorial Model of crimo-taxis in a street

In this Chapter, using the elements introduced in the previous Chapter, an operatorial version of the crimo-taxis model in a street, considered in Chapter 1, is proposed. The model consists of N cells distributed over a one–dimensional region where the ordinary citizens, drug users/dealers and law enforcement personnel, represented by annihilation, creation and number fermionic operators, interact. The dynamics is governed by a self-adjoint and time independent Hamiltonian operator describing the various interactions. The results of some numerical simulations are presented and discussed. The recently introduced variant of the standard Heisenberg approach, named $(\mathcal{H}, \rho)$–induced dynamics, is also taken into account in order to enrich the dynamical outcome.

3.1 The model

We label the cells of the spatial region with a greek letter, and represent ordinary citizens with annihilation fermionic operators $a_{1,\alpha}$, the drug users/dealers with $a_{2,\alpha}$, and law enforcement personnel with $a_{3,\alpha}$ ($\alpha = 1, \dots N$, where N is the number of the cells in the domain). The annihilation operators, together with the associated creation operators of course satisfy the canonical anticommutation relations (2.5). The fermionic operators representing the system $\mathcal{S}$ are defined in the Hilbert space $\mathbb{H}$ such that $\dim(\mathbb{H}) = 2^{3N}$.

The mean values of number operators $\widehat{n}_{j,\alpha}$ over an assigned initial condition

$$\varphi \equiv \varphi_{n_{1,1},\dots,n_{1,N},n_{2,1},\dots,n_{2,N},n_{3,1},\dots,n_{3,N}},$$

say

$$n_{j,\alpha} = \langle \varphi, \widehat{n}_{j,\alpha}\varphi \rangle, \qquad j = 1, \dots, 3, \quad \alpha = 1, \dots, N \tag{3.1}$$

are interpreted as the local density of the corresponding population subgroup in the cell α.

Let us assume the dynamics be governed by the following Hamiltonian operator:

$$\mathcal{H} = \mathcal{H}_0 + \mathcal{H}_I + \mathcal{H}_M + \mathcal{H}_C, \tag{3.2}$$

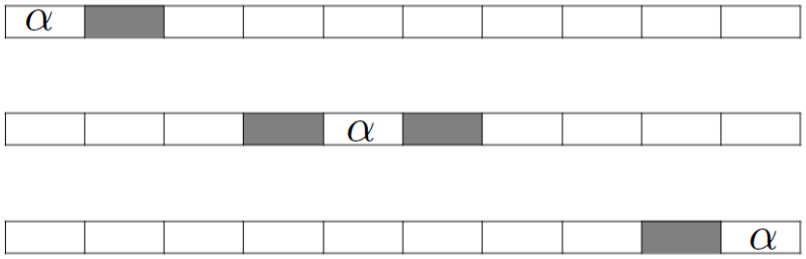

FIGURE 3.1: Moore neighborhood of the cell α.

where

$$
\begin{aligned}
\mathcal{H}_0 &= \sum_{j=1}^{3}\sum_{\alpha=1}^{N} \omega_{j,\alpha} a_{j,\alpha}^{\dagger} a_{j,\alpha}, \\
\mathcal{H}_I &= \sum_{\alpha=1}^{N} \lambda_{1,\alpha}(a_{1,\alpha}a_{2,\alpha}^{\dagger} + a_{2,\alpha}a_{1,\alpha}^{\dagger}) + \lambda_{2,\alpha}(a_{2,\alpha}a_{3,\alpha}^{\dagger} + a_{3,\alpha}a_{2,\alpha}^{\dagger}), \\
\mathcal{H}_M &= \sum_{j=1}^{3}\sum_{\alpha=1}^{N} \left(\mu_{j,\alpha} \sum_{\beta=1}^{N} p_{\alpha,\beta}(a_{j,\alpha}a_{j,\beta}^{\dagger} + a_{j,\beta}a_{j,\alpha}^{\dagger}) \right), \\
\mathcal{H}_C &= \sum_{\alpha,\beta=1}^{N} p_{\alpha,\beta} \Big(\nu_{1,\alpha}(a_{1,\alpha}a_{2,\beta}^{\dagger} + a_{2,\beta}a_{1,\alpha}^{\dagger}) + \nu_{2,\alpha}(a_{2,\alpha}a_{3,\beta}^{\dagger} + a_{3,\beta}a_{2,\alpha}^{\dagger}) \\
&\quad \nu_{3,\alpha}(a_{1,\alpha}a_{3,\beta}^{\dagger} + a_{3,\beta}a_{1,\alpha}^{\dagger}) \Big),
\end{aligned}
\tag{3.3}
$$

with $\omega_{j,\alpha}$, $\lambda_{j,\alpha}$, $\mu_{j,\alpha}$, $\nu_{j,\alpha}$ ($\alpha = 1,\dots,N$, $j = 1,\dots,3$) positive constants; moreover, the coefficients $p_{\alpha,\beta}$ ($\alpha,\beta = 1,\dots,N$), symmetric with respect to their indices, are equal to 1 if β denotes a cell in the Moore neighborhood M_α and 0 elsewhere (Figure 3.1). Therefore, the cells in the Moore neighborhood of the cell $\alpha \neq 1, N$ are labeled as $\alpha - 1$ and $\alpha + 1$, whereas the cells labeled with 1 and N have only one neighbor (labeled 2 and $N - 1$, respectively) (Figure 3.1).

Some comments about the various contributions in the Hamiltonian are in order:

- $\mathcal{H}_0$ is the free part of the Hamiltonian, and $\omega_{i,\alpha}$ are parameters somehow related to the inertia of the operators associated to the agents of $\mathcal{S}$: in fact, they can be thought of as a measure of the tendency of each degree of freedom to stay constant in time (Bagarello, 2012).

- $\mathcal{H}_I$ rules the local (i.e., in the same cell α) competitive interaction between the three subgroups of population; the coefficients $\lambda_{1,\alpha}$ and $\lambda_{2,\alpha}$ give a measure of the strength of the interaction between $(a_{1,\alpha}, a_{2,\alpha})$ and $(a_{2,\alpha}, a_{3,\alpha})$, respectively: the contribution $a_{1,\alpha}a_{2,\alpha}^{\dagger}$ is a competition term since a *particle* associated to $a_{1,\alpha}$ is *destroyed* and a *particle* associated to $a_{2,\alpha}$ is *created*; the adjoint term $a_{2,\alpha}a_{1,\alpha}^{\dagger}$ swaps the roles of the two modes. The second term has the same interpretation.In particular, in this Hamiltonian we have two competitions since in Epstein's system (1.5) we find the two prey-predator interactions (uv and vw).

- $\mathcal{H}_C$ takes into account a nonlocal competitive interaction between the three subgroups of population, and $\nu_{j,\alpha}$ measure the strength of nonlocal interaction

(absent if $\nu_{j,\alpha} = 0$, $j = 1,\dots,3$, $\alpha = 1,\dots,N$): in fact the competition between the three populations occurs in adjacent cells. This contribution is introduced to represent the cross-diffusion terms of the Epstein's system (1.5).

- $\mathcal{H}_M$ is responsible for the diffusion of the three subgroups of population in the region, and $\mu_{j,\alpha}$ is the mobility coefficient of population $\mathcal{P}_j$ in the cell α: for example, the contribution $a_{1,\alpha}a^\dagger_{1,\beta}$ is such that for the actor associated to $a_{1,\alpha}$ a *particle* is *destroyed* and for the actor associated to $a_{1,\beta}$ *created*; the adjoint term $a_{1,\beta}a^\dagger_{1,\alpha}$ swaps the roles of the two modes. The interpretation is the same for the other contributions.

Adopting the Heisenberg representation, the operators $a_{j,\alpha}$ evolve in time according to the differential equations

$$\frac{da_{j,\alpha}}{dt} = \mathrm{i}[\mathcal{H}, a_{j,\alpha}], \qquad j = 1,\dots,3, \quad \alpha = 1,\dots,N,$$

that is

$$\begin{aligned}
\frac{da_{1,1}}{dt} &= \mathrm{i}\left(-\omega_{1,1}a_{1,1} + \lambda_{1,1}a_{2,1} + (\mu_{1,1}+\mu_{1,2})a_{1,2} + \nu_{1,1}a_{2,2} + \nu_{3,1}a_{3,2}\right),\\
\frac{da_{1,\alpha}}{dt} &= \mathrm{i}\left(-\omega_{1,\alpha}a_{1,\alpha} + \lambda_{1,\alpha}a_{2,\alpha} + (\mu_{1,\alpha}+\mu_{1,\alpha-1})a_{1,\alpha-1}\right.\\
&\quad + (\mu_{1,\alpha}+\mu_{1,\alpha+1})a_{1,\alpha+1} + \nu_{1,\alpha}(a_{2,\alpha-1}+a_{2,\alpha+1})\\
&\quad \left.+\nu_{3,\alpha}(a_{3,\alpha-1}+a_{3,\alpha+1})\right), \qquad \alpha = 2,\dots,N-1,\\
\frac{da_{1,N}}{dt} &= \mathrm{i}\left(-\omega_{1,N}a_{1,N} + \lambda_{1,N}a_{2,N} + (\mu_{1,N}+\mu_{1,N-1})a_{1,N-1}\right.\\
&\quad \left.+\nu_{1,N}a_{2,N-1} + \nu_{3,N}a_{3,N-1}\right),\\
\frac{da_{2,1}}{dt} &= \mathrm{i}\left(-\omega_{2,1}a_{2,1} + \lambda_{1,1}a_{1,1} + \lambda_{2,1}a_{3,1}\right.\\
&\quad \left.+(\mu_{2,1}+\mu_{2,2})a_{2,1} + \nu_{1,2}a_{1,2} + \nu_{2,1}a_{3,2}\right),\\
\frac{da_{2,\alpha}}{dt} &= \mathrm{i}\left(-\omega_{2,\alpha}a_{2,\alpha} + \lambda_{1,\alpha}a_{1,\alpha} + \lambda_{2,\alpha}a_{3,\alpha}\right.\\
&\quad + (\mu_{2,\alpha}+\mu_{2,\alpha-1})a_{2,\alpha-1} + (\mu_{2,\alpha}+\mu_{2,\alpha+1})a_{2,\alpha+1}\\
&\quad +\nu_{1,\alpha-1}a_{1,\alpha-1} + \nu_{1,\alpha+1}a_{1,\alpha+1}\\
&\quad \left.+\nu_{3,\alpha}(a_{3,\alpha-1}+a_{3,\alpha-1})\right), \qquad \alpha = 2,\dots,N-1,\\
\frac{da_{2,N}}{dt} &= \mathrm{i}\left(-\omega_{2,N}a_{2,N} + \lambda_{1,N}a_{1,N} + \lambda_{2,N}a_{3,N}\right.\\
&\quad \left.+(\mu_{2,N}+\mu_{2,N-1})a_{2,N-1} + \nu_{1,N-1}a_{1,N-1} + \nu_{3,N}a_{3,N-1}\right),\\
\frac{da_{3,1}}{dt} &= \mathrm{i}\left(-\omega_{3,1}a_{3,1} + \lambda_2 a_{2,1} + (\mu_{3,1}+\mu_{3,2})a_{3,2} + \nu_{3,2}a_{1,2} + \nu_{2,2}a_{2,2}\right),\\
\frac{da_{3,\alpha}}{dt} &= \mathrm{i}\left(-\omega_{3,\alpha}a_{3,\alpha} + \lambda_{2,\alpha}a_{2,\alpha} + (\mu_{3,\alpha}+\mu_{3,\alpha-1})a_{3,\alpha-1}\right.\\
&\quad + (\mu_{3,\alpha}+\mu_{3,\alpha+1})a_{3,\alpha+1} + \nu_{3,\alpha-1}a_{1,\alpha-1} + \nu_{3,\alpha+1}a_{1,\alpha+1}\\
&\quad \left.+\nu_{2,\alpha-1}a_{2,\alpha-1} + \nu_{2,\alpha+1}a_{2,\alpha+1}\right), \qquad \alpha = 2,\dots,N-1,\\
\frac{da_{3,N}}{dt} &= \mathrm{i}\left(-\omega_{2,N}a_{3,N} + \lambda_{2,N}a_{2,N}\right.\\
&\quad \left.+(\mu_{3,N}+\mu_{3,N-1})a_{3,N-1} + \nu_{3,N-1}a_{1,N-1} + \nu_{2,N-1}a_{2,N-1}\right).
\end{aligned} \tag{3.4}$$

Because of the linearity of equation (3.4), we introduce the formal column vector

$$\mathbf{A} = \left[a_{1,1}, \ldots, a_{1,N}, a_{2,1}, \ldots, a_{2,N}, a_{3,1}, \ldots, a_{3,N}\right]^T,$$

and a suitable $3N \times 3N$ real matrix Γ (whose entries, once we fix N, can be constructed from (3.4)), the evolution equations for the annihilation operators can be written in the compact form as

$$\frac{d\mathbf{A}}{dt} = \mathrm{i}\Gamma\mathbf{A}. \tag{3.5}$$

Let us now consider the compact version of the evolution equations for the creation operators, say

$$\frac{d\mathbf{A}^\dagger}{dt} = -\mathrm{i}\Gamma\mathbf{A}^\dagger; \tag{3.6}$$

coupling (3.5) and (3.6), we have the system

$$\frac{d}{dt}\begin{bmatrix} \mathbf{A} \\ \mathbf{A}^\dagger \end{bmatrix} = \begin{bmatrix} \mathrm{i}\Gamma & \mathbf{0}_{3N} \\ \mathbf{0}_{3N} & -\mathrm{i}\Gamma \end{bmatrix}\begin{bmatrix} \mathbf{A} \\ \mathbf{A}^\dagger \end{bmatrix}, \tag{3.7}$$

$\mathbf{0}_{3N}$ being a zero matrix of order $3N$; the formal solution to system (3.7) is

$$\begin{bmatrix} \mathbf{A}(t) \\ \mathbf{A}^\dagger(t) \end{bmatrix} = \exp\left(\begin{bmatrix} \mathrm{i}\Gamma t & \mathbf{0}_{3N} \\ \mathbf{0}_{3N} & -\mathrm{i}\Gamma t \end{bmatrix}\right)\begin{bmatrix} \mathbf{A}_0 \\ \mathbf{A}_0^\dagger \end{bmatrix} = \mathcal{B}(t)\begin{bmatrix} \mathbf{A}_0 \\ \mathbf{A}_0^\dagger \end{bmatrix}. \tag{3.8}$$

Let $n^0_{i,\alpha}$ $(i = 1, 2, 3, \alpha = 1, \ldots, N)$ be the initial density of population $\mathcal{P}_i$ in the cell α, and let $\mathbf{n}^0$ the vector with $3N$ components

$$\mathbf{n}^0 = \left(\sqrt{n^0_{1,1}}, \ldots, \sqrt{n^0_{1,N}}, \sqrt{n^0_{2,1}}, \ldots, \sqrt{n^0_{2,N}}, \sqrt{n^0_{3,1}}, \ldots, \sqrt{n^0_{3,N}}\right);$$

denoting with $B_{j,k}$ the generic entry of the $6N \times 6N$ matrix $\mathcal{B}(t)$, it is easy to derive, by using the canonical anticommutation relations (2.5), the formula giving the mean values of the number operators at time t:

$$\begin{aligned}
n_{1,\alpha}(t) &= \sum_{i=1}^{3N}\left(n_i^0\right)^2\sum_{\ell=1}^{3N}\left(B_{\alpha,f(\ell,i)}B_{\alpha+3N,g(\ell,i)}\right) \\
&\quad + \sum_{i=1}^{3N-1}\sum_{j=i+1}^{3N} n_i^0 n_j^0\left(B_{\alpha,i}B_{\alpha+3N,j+3N} + B_{\alpha,j}B_{\alpha+3N,i+3N}\right. \\
&\qquad \left. - B_{\alpha,i+3N}B_{\alpha+3N,j} - B_{\alpha,j+3N}B_{\alpha+3N,i}\right), \\
n_{2,\alpha}(t) &= \sum_{i=1}^{3N}\left(n_i^0\right)^2\sum_{\ell=1}^{3N}\left(B_{\alpha+N,f(\ell,i)}B_{\alpha+4N,g(\ell,i)}\right) \\
&\quad + \sum_{i=1}^{3N-1}\sum_{j=i+1}^{3N} n_i^0 n_j^0\left(B_{\alpha+N,i}B_{\alpha+4N,j+3N} + B_{\alpha+N,j}B_{\alpha+4N,i+3N}\right. \\
&\qquad \left. - B_{\alpha+N,i+3N}B_{\alpha+4N,j} - B_{\alpha+N,j+3N}B_{\alpha+4N,i}\right), \\
n_{3,\alpha}(t) &= \sum_{i=1}^{3N}\left(n_i^0\right)^2\sum_{\ell=1}^{3N}\left(B_{\alpha+2N,f(\ell,i)}B_{\alpha+5N,g(\ell,i)}\right) \\
&\quad + \sum_{i=1}^{3N-1}\sum_{j=i+1}^{3N} n_i^0 n_j^0\left(B_{\alpha+2N,i}B_{\alpha+5N,j+3N} + B_{\alpha+2N,j}B_{\alpha+5N,i+3N}\right. \\
&\qquad \left. - B_{\alpha+2N,i+3N}B_{\alpha+5N,j} - B_{\alpha+2N,j+3N}B_{\alpha+5N,i}\right),
\end{aligned}$$

where

$$f(\ell,i)=\begin{cases} i & \text{if} \quad i=\ell,\\ i+3N & \text{if} \quad i\neq\ell,\end{cases} \qquad g(\ell,i)=\begin{cases} i+3N & \text{if} \quad i=\ell,\\ i & \text{if} \quad i\neq\ell.\end{cases}$$

Let us divide the region $\mathcal{C}$ in three different subregions: a left region ($\mathcal{C}_1$), a central region ($\mathcal{C}_2$), and a right region ($\mathcal{C}_3$); this distinction is because we assume that some of the parameters entering the Hamiltonian are somehow different in the three subregions. Moreover, we will distinguish two different cases in order to simulate two different realistic scenarios.

The quadratic form of the Hamiltonian has an immediate consequence: the dynamic behavior that we can obtain in each cell is at most quasiperiodic. Furthermore, due to the relation

$$\left[\mathcal{H},\sum_{\alpha=1}^{N}(\widehat{n}_{1,\alpha}+\widehat{n}_{2,\alpha}+\widehat{n}_{3,\alpha})\right]=0,$$

the Hamiltonian possesses a first integral, expressing the fact that the sum of the densities of the three subgroups all over the cells of the domain is constant in time.

More complex outcomes (not necessarily quasiperiodic) could be recovered including in the Hamiltonian terms more than quadratic. Nevertheless, in such a case we would be forced to solve numerically a very huge number of differential equations. Another strategy to enrich the dynamics without rendering the problem computationally hard, if not impossible from a practical point of view, is the one introduced in a series of recent papers (Di Salvo and Oliveri, 2017; Di Salvo, Gorgone, and Oliveri, 2017b; Di Salvo, Gorgone, and Oliveri, 2017a; Bagarello et al., 2017; Bagarello et al., 2018), where it was shown how to obtain more interesting dynamics still retaining a quadratic and time-independent Hamiltonian.

With this approach we were able to build a model based on the theory of fermionic operators comparable with the reaction–diffusion crimo–taxis model, even if the nonlinear reaction terms cannot be described with fermions; for this reason, we use the theory $(\mathcal{H},\rho)$–induced dynamics Bagarello et al., 2018, which allows us to introduce surreptitiously nonlinearities.

In this model, after fixing the value of τ (*i.e.*, the length of the subintervals), we update at instants $k\tau$ (k integer) the inertia parameters as follows. Let us define

$$\begin{aligned}\delta_{j,\alpha}^{(k)}&=n_{j,\alpha}(k\tau)-n_{j,\alpha}((k-1)\tau), \qquad j=1,2,3, \quad \alpha=1,\dots,N,\\ \delta_{\alpha}^{(k)}&=n_{2,\alpha}(k\tau)n_{1,\alpha}(k\tau)-n_{2,\alpha}((k-1)\tau)n_{1,\alpha}((k-1)\tau).\end{aligned} \tag{3.9}$$

Then, at instants $k\tau$, we made the substitutions

$$\begin{aligned}\omega_{1,\alpha}&\to\omega_{1,\alpha}(1-\delta_{2,\alpha}^{(k)}+\delta_{3,\alpha}^{(k)}),\\ \omega_{2,\alpha}&\to\omega_{2,\alpha}(1+\delta_{1,\alpha}^{(k)}-\delta_{3,\alpha}^{(k)}),\\ \omega_{3,\alpha}&\to\omega_{3,\alpha}(1-\delta_{3,\alpha}^{(k)}-\delta_{\alpha}^{(k)}).\end{aligned} \tag{3.10}$$

This rule modifies the propensity to change of the subgroups. In particular, $\omega_{1,\alpha}$ increases if the density of drug users/dealers in the cell α decreases and that of policemen increases (ordinary citizens go far away the infected and feel secure with policemen); $\omega_{2,\alpha}$ increases if the density of ordinary citizens in the cell α increases and that of policemen decreases (drug users/dealers go where there are ordinary citizens to convert and far away the policemen); finally, $\omega_{3,\alpha}$ increases if the density of drug users/dealers in the cell α decreases and the same occurs to the variation of

the product of densities of ordinary citizens and drug users/dealers (policemen are attracted where the two other subgroups increase their density).

Next Section will present some numerical simulations of the model.

3.2 Numerical results

In the first part of this Section, we neglect spatial inhomogeneities, in the sense that all the interactions occur just in one cell. The second part will deal with the complete model, and the one–dimensional region will be considered made by $N = 50$ cells. We present two scenarios. In both situations, we compare the numerical results obtained by the standard Heisenberg dynamics and those coming from the superposition of the Heisenberg dynamics with the rules above described.

3.2.1 Simplified model in one cell

We see in Figure 3.2 that, without the rule the evolution exhibits a never ending oscillatory trend, as expected. On the contrary, when the rule is used, the amplitude of the oscillations tends to decrease and the densities of the three subgroups tends to reach a sort of asymptotic equilibrium (this is more evident in subfigures Figure 3.2(b) and Figure 3.2(f)). In the same subfigures Figure 3.2(b) and Figure 3.2(f) it is also evident that policemen are able to keep better drug users/dealers under control. Note also that the time needed to get a stationary behavior after the transient behavior depends on the values of the parameters.

3.2.2 Spatial model

Let us assume the one–dimensional region $\mathcal{C}$ divided in three subregions. Drug users/dealers are initially more abundant in the left subregion, ordinary citizens in the central part, and law enforcement personnel in the right part. Therefore, we choose the following initial local densities for the three subgroups:

$$\begin{aligned} n^0_{1,\alpha} &= \quad 0.8\exp(-(\alpha-25)^2/39), \\ n^0_{2,\alpha} &= \quad 0.08\exp(-(\alpha-10)^2/19), \\ n^0_{3,\alpha} &= \quad 0.04\exp(-(\alpha-35)^2/19). \end{aligned} \tag{3.11}$$

We choose the parameters of the spatial effects similar to the diffusion and cross-diffusion of the model (1.5), say

$$\begin{aligned} &\lambda_{1,\alpha} = 0.04, \quad \lambda_{2,\alpha} = 0.025, \\ &\mu_{1,\alpha} = 0.07, \quad \mu_{2,\alpha} = 0.05, \quad \mu_{3,\alpha} = 0.035, \\ &\nu_{1,\alpha} = 0.006, \quad \nu_{2,\alpha} = 0.006, \quad \nu_{3,\alpha} = 0.003, \end{aligned} \tag{3.12}$$

where ($\alpha \in \mathcal{C}$); three different combinations of the inertia parameters $\omega_{1,\alpha}$, $\omega_{2,\alpha}$ and $\omega_{3,\alpha}$ are chosen and reported in the captions of the figures.

Comparing the plots in Figures 3.3, 3.4 and 3.5 (where the classical Heisenberg dynamics is applied) with the plots in Figures 3.6, 3.7 and 3.8 (where the $(\mathcal{H}, \rho)$–induced dynamics approach is used) we observe some differences. At the instant $t = 0$ the ordinary citizens are distributed in the central part of the domain, the drug users/dealers on the left and the policemen on the right.Without rules we have an oscillatory trend for all three subgroups of populations. During the time evolution

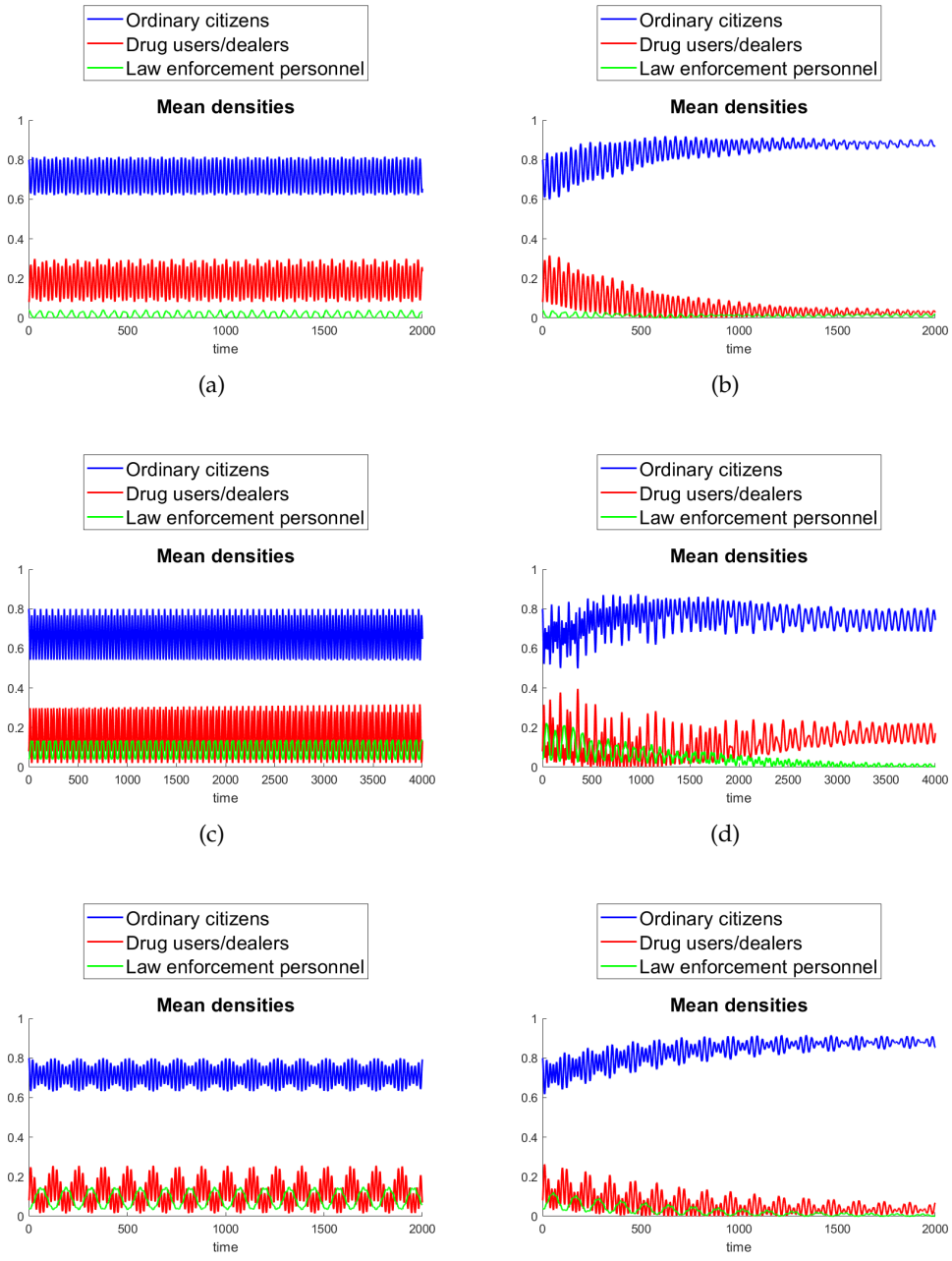

FIGURE 3.2: Time evolution of the mean values of the number operators of the three subgroups. Only one cell is considered. No rule (subfigures (a), (c) and (e)), and use of the rule with $\tau = 2$ (subfigures (b), (d) and (f)). In all the figures it is $\lambda_1 = 0.04$, $\lambda_2 = 0.025$. As far as the inertia parameters, we have: $\omega_1 = 0.5$, $\omega_2 = 0.2$, $\omega_3 = 0.3$ (subfigures (a) and (b)), $\omega_1 = 0.5$, $\omega_2 = 0.3$, $\omega_3 = 0.2$ (subfigures (c) and (d)), $\omega_1 = 0.5$, $\omega_2 = 0.2$, $\omega_3 = 0.2$ (subfigures (e) and (f)). The initial conditions for all cases are: $n_1^0 = 0.8$, $n_2^0 = 0.08$, $n_3^0 = 0.04$.

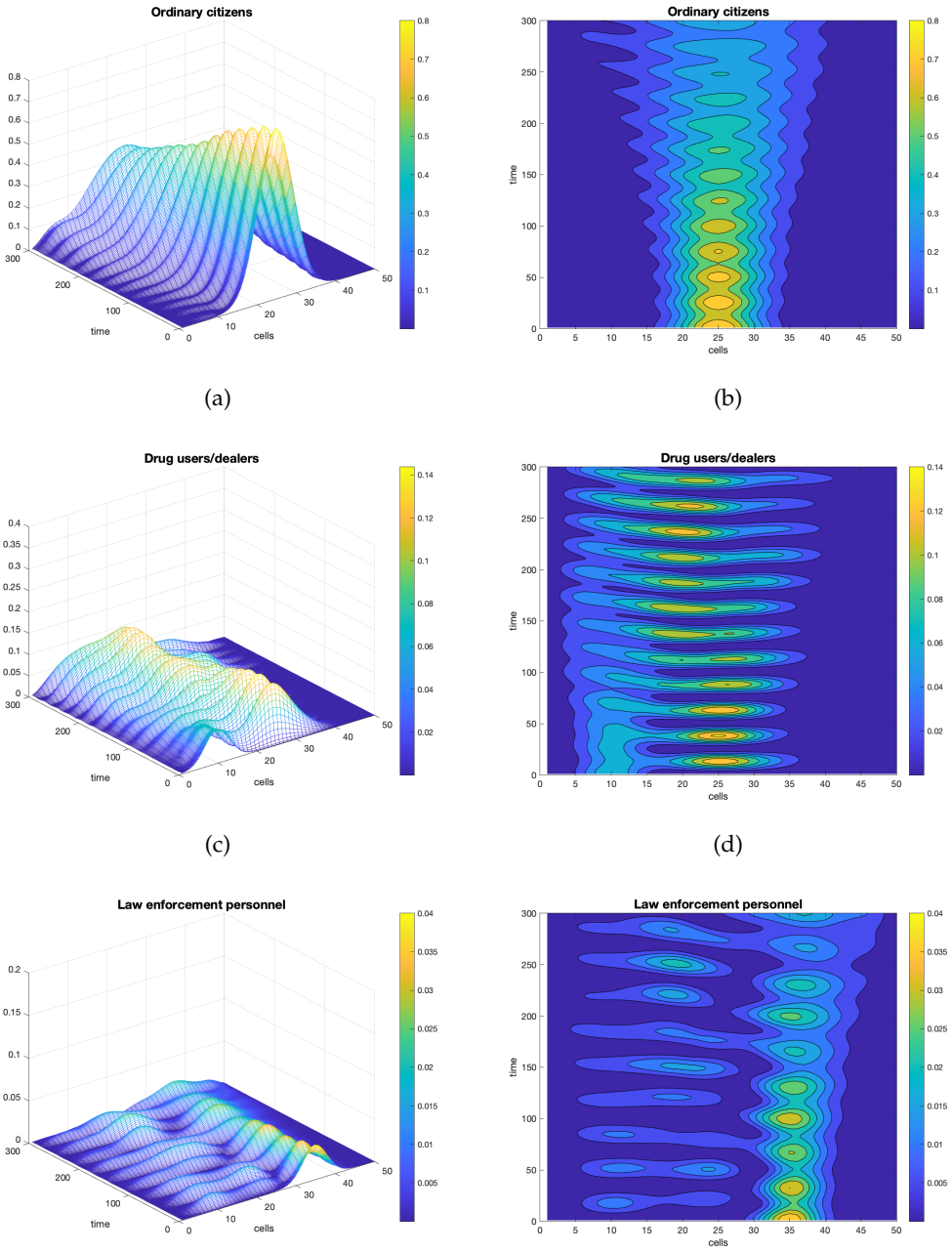

(a) (b)

(c) (d)

(e) (f)

FIGURE 3.3: Time evolution (left) and contour plots (right) of the densities of the three subgroups in all the cells with classical Heisenberg dynamics: ordinary citizens ((a) and (b)), drug users/dealers ((c) and (d)) and law enforcement personnel ((e) and (f)). The values of the parameters are given in (3.12). The inertia parameters are: $\omega_1 = 0.5$, $\omega_2 = 0.2$, $\omega_3 = 0.3$ The initial conditions are given in (3.11).

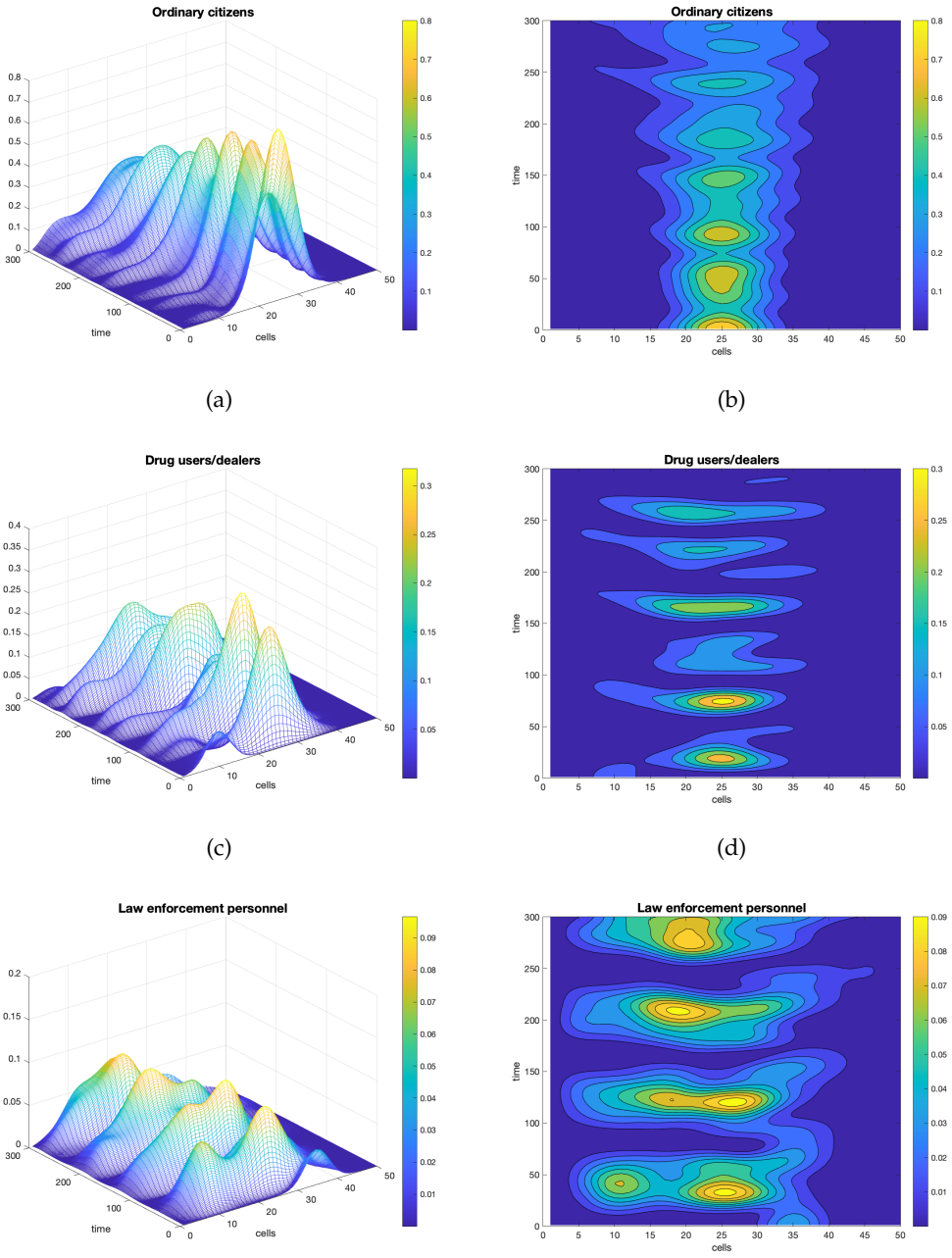

(a) (b)

(c) (d)

(e) (f)

FIGURE 3.4: Time evolution (left) and contour plots (right) of the densities of the three subgroups in all the cells with classical Heisenberg dynamics: ordinary citizens ((a) and (b)), drug users/dealers ((c) and (d)) and law enforcement personnel ((e) and (f)). The values of the parameters are given in (3.12). The inertia parameters are: $\omega_1 = 0.5$, $\omega_2 = 0.3$, $\omega_3 = 0.2$ The initial conditions are given in (3.11).

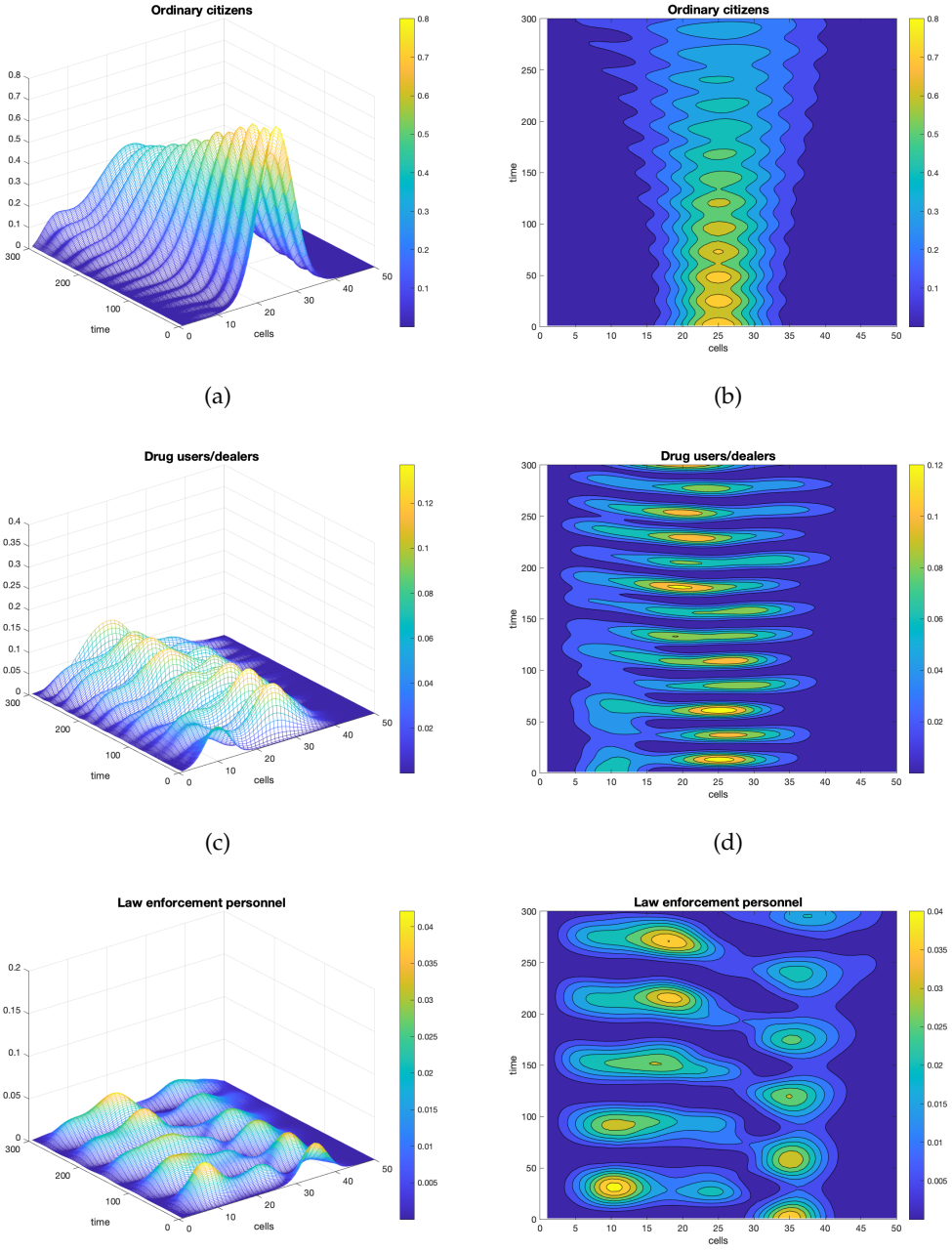

(a) (b)

(c) (d)

(e) (f)

FIGURE 3.5: Time evolution (left) and contour plots (right) of the densities of the three subgroups in all the cells with classical Heisenberg dynamics: ordinary citizens ((a) and (b)), drug users/dealers ((c) and (d)) and law enforcement personnel ((e) and (f)). The values of the parameters are given in (3.12). The inertia parameters are: $\omega_1 = 0.5$, $\omega_2 = 0.2$, $\omega_3 = 0.2$ The initial conditions are given in (3.11).

using the rules, we observe that the drug users/dealers move from their neighborhood towards the central part of the domain with the aim of converting the ordinary citizens; and the same is observed for policemen. One of the effects of the rule is that ordinary citizens come back to the central domain defended by policemen, while the drug users/dealers migrate far away.

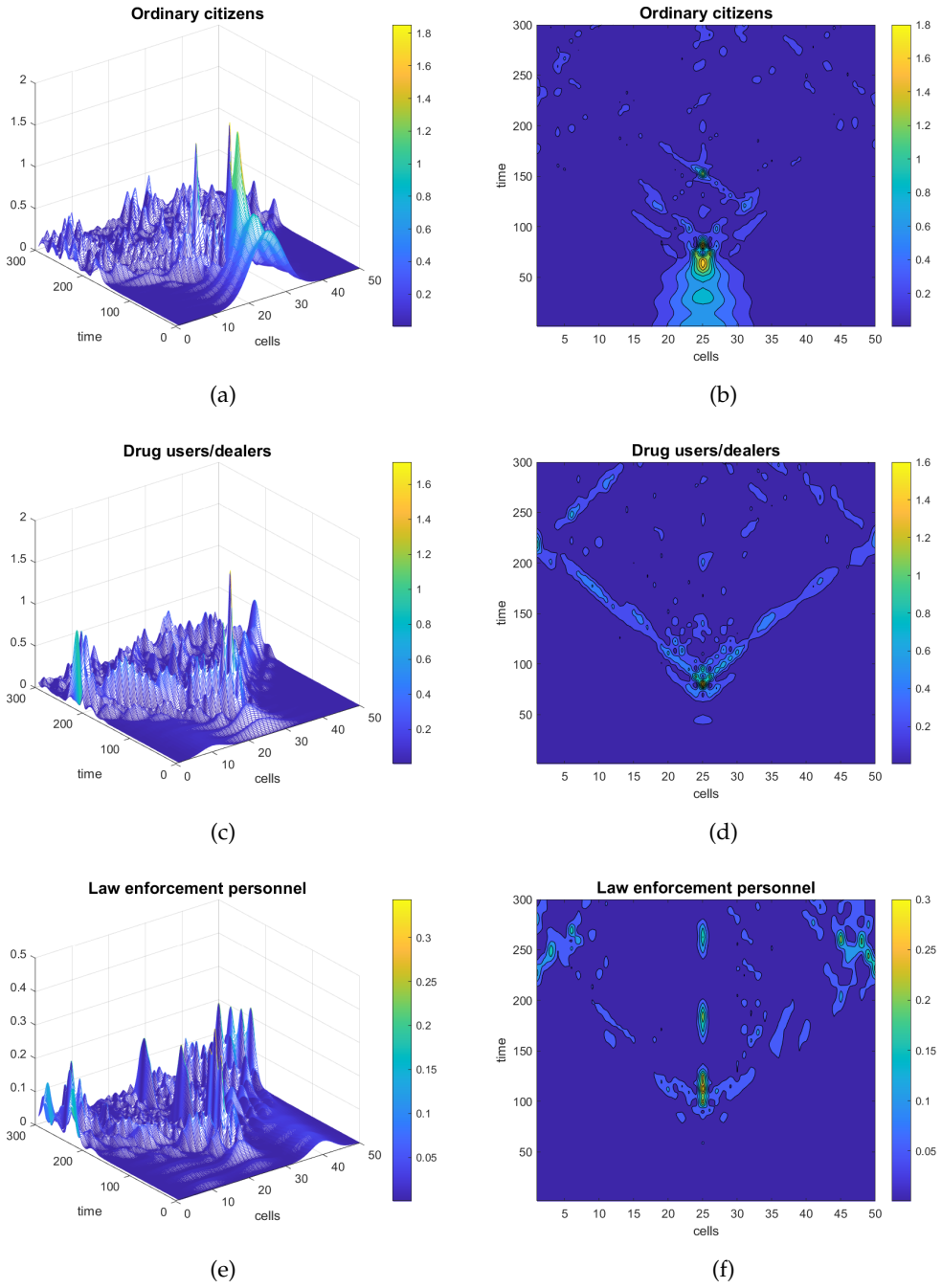

(a) (b)

(c) (d)

(e) (f)

FIGURE 3.6: Time evolution (left) and contour plots (right) of the densities of the three subgroups in all the cells with $(\mathcal{H}, \rho)$–induced dynamics ($\tau = 2$): ordinary citizens ((a) and (b)), drug users/dealers ((c) and (d)) and law enforcement personnel ((e) and (f)). The values of the parameters are given in (3.12). The inertia parameters are: $\omega_1 = 0.5, \omega_2 = 0.2, \omega_3 = 0.3$ The initial conditions are given in (3.11).

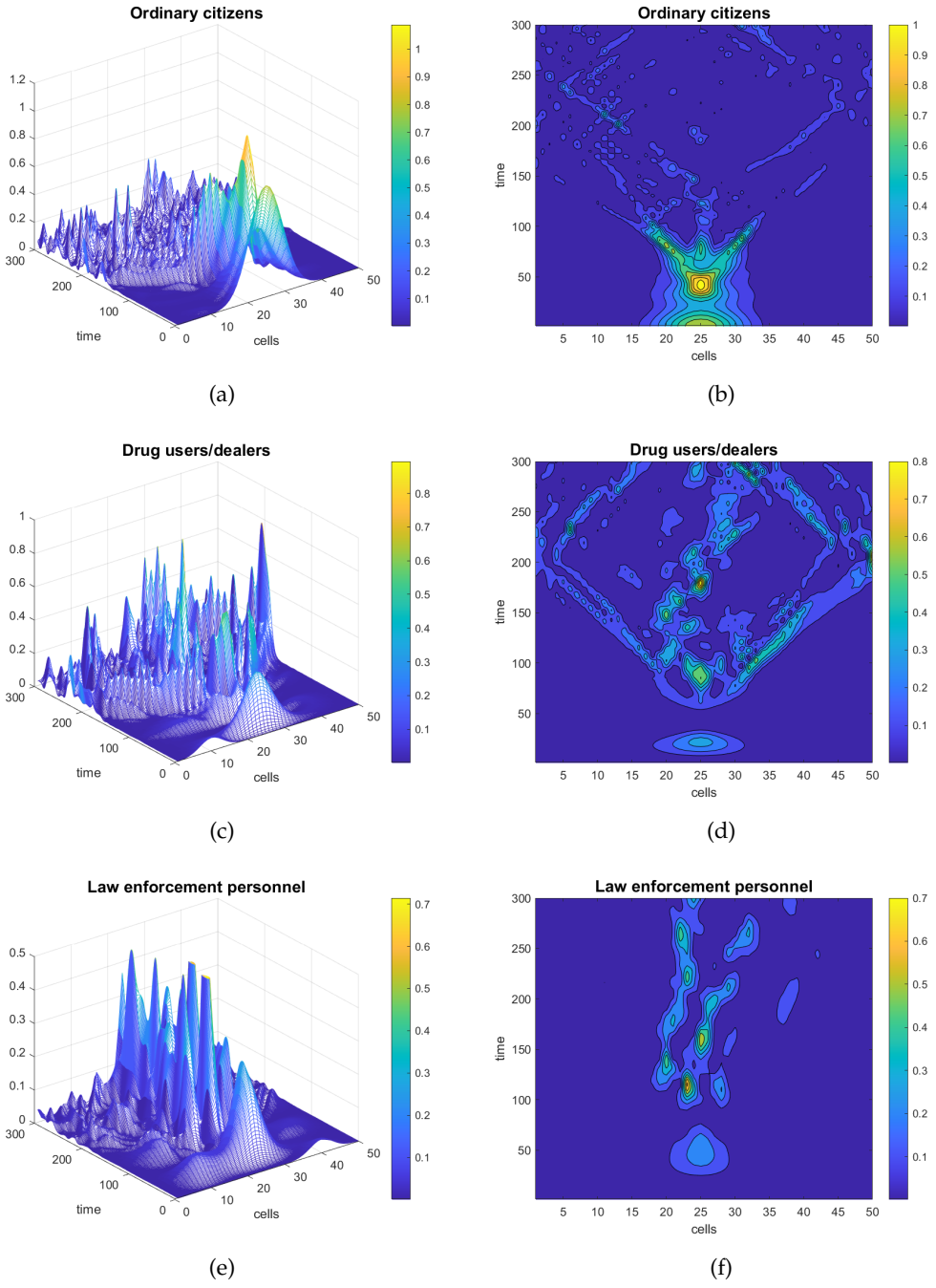

FIGURE 3.7: Time evolution (left) and contour plots (right) of the densities of the three subgroups in all the cells with $(\mathcal{H}, \rho)$–induced dynamics ($\tau = 2$): ordinary citizens ((a) and (b)), drug users/dealers ((c) and (d)) and law enforcement personnel ((e) and (f)). The values of the parameters are given in (3.12). The inertia parameters are: $\omega_1 = 0.5$, $\omega_2 = 0.3$, $\omega_3 = 0.2$ The initial conditions are given in (3.11).

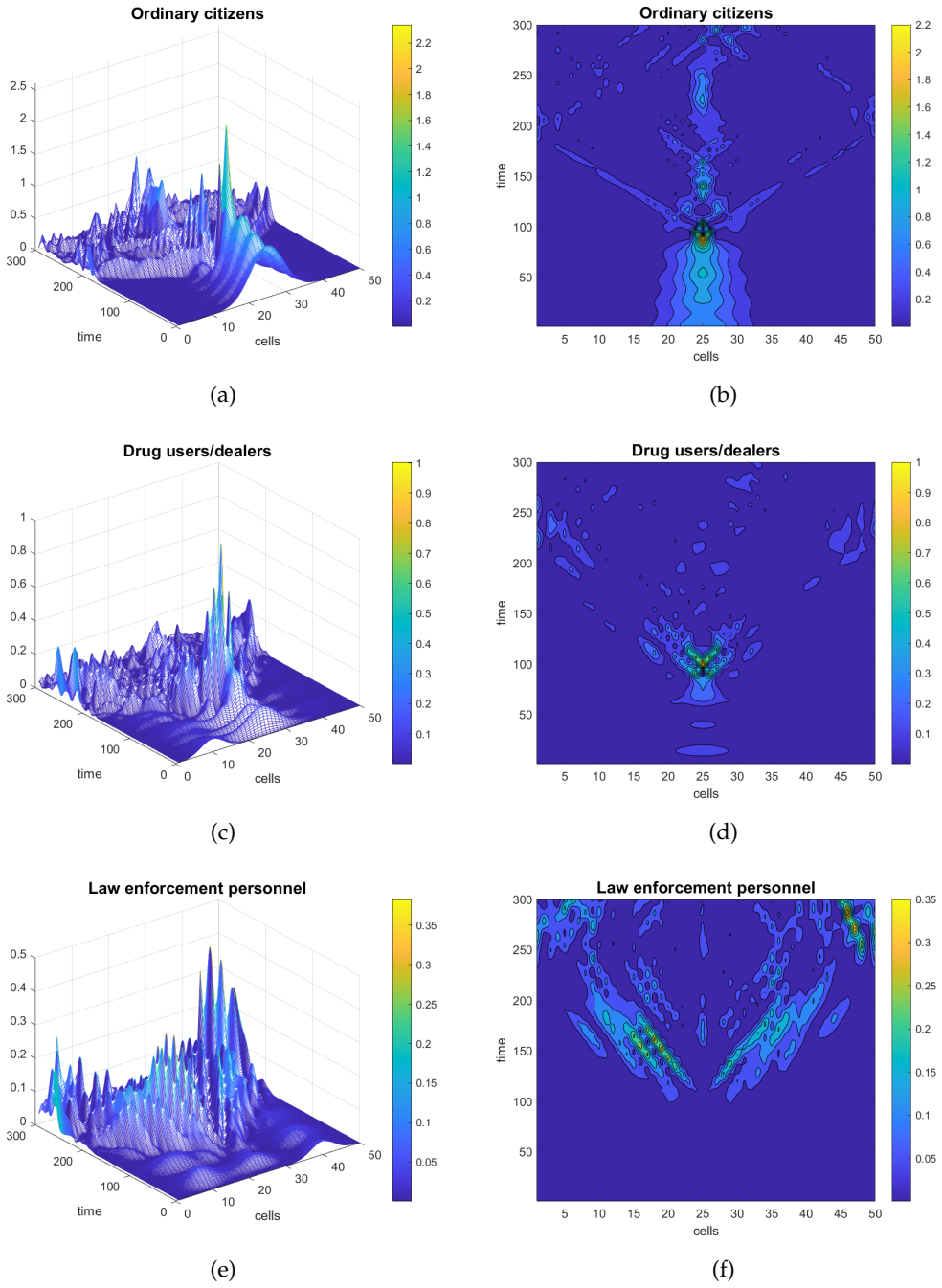

FIGURE 3.8: Time evolution (left) and contour plots (right) of the densities of the three subgroups in all the cells with $(\mathcal{H}, \rho)$–induced dynamics ($\tau = 2$): ordinary citizens ((a) and (b)), drug users/dealers ((c) and (d)) and law enforcement personnel ((e) and (f)). The values of the parameters are given in (3.12). The inertia parameters are: $\omega_1 = 0.5, \omega_2 = 0.2, \omega_3 = 0.2$ The initial conditions are given in (3.11).

Chapter 4

Operatorial Formulation of a Model of Spatially Distributed Competing Populations

The dynamics of different interacting species or populations occupying the same habitat is an important subject in theoretical biology. It is well known that Gause's law of competitive exclusion, stating that two identical species cannot coexist in the same ecological niche, can be violated in patchy environments where two like populations may coexist because of migration, so that the less fitted population may survive even in presence of a more competitive population provided that it is able to disperse more effectively into unoccupied patches so balancing local extinction in some patches (Slatkin, 1974; Hanski, 1981; Hanski, 1983; Ives and May, 1985; Hanski, 2008).

Standard models for the dynamics of spatially distributed interacting populations are written in terms of reaction-diffusion partial differential equations (Murray, 2003), or using the coupled map lattice formalism (Paparella and Oliveri, 2008). In both approaches various behaviors can be observed, such as the emergence of some persistent spatial patterns in the distributions of the competing species, or synchronization effects between the phases of nearby regions.

In this Chapter, we build and investigate an operatorial model (Inferrera and Oliveri, 2022). More in detail, we consider a system where two different populations in a patchy environment compete either locally (in the same cell) or nonlocally (in adjacent cells) and both are subject to migration phenomena. A similar model with local competition and migration has been investigated in Bagarello and Oliveri, 2013. Here, we include in the model also a nonlocal competition mechanism and consider, in addition to the standard Heisenberg view to dynamics, also the approach of $(\mathcal{H}, \rho)$–induced dynamics (Bagarello et al., 2018; Di Salvo, Gorgone, and Oliveri, 2020).

For the reasons explained in previous Chapters, we choose fermionic operators to model the actors of our system.

4.1 The operatorial model: Heisenberg dynamics and $(\mathcal{H}, \rho)$–induced dynamics

The system $\mathcal{S}$ we consider consists of two populations occupying a one-dimensional spatial region $\mathcal{C}$ composed by N cells; in each cell, two different populations, say $\mathcal{P}_1$ and $\mathcal{P}_2$, coexist and interact. Let $a_{1,\alpha}$ and $a_{2,\alpha}$ ($a^\dagger_{1,\alpha}$ and $a^\dagger_{2,\alpha}$, respectively) be the annihilation (creation, respectively) fermionic operators related to the two populations, where the subscript α is a label for the cells of the spatial region; moreover, let

$\widehat{n}_{j,\alpha} = a^\dagger_{j,\alpha} a_{j,\alpha}$ be the corresponding number operators. The mean values of number operators over a given initial conditions, say

$$n_{j,\alpha} = \langle \varphi_{n_1,n_2}, \widehat{n}_{j,\alpha} \varphi_{n_1,n_2} \rangle, \qquad j = 1,2,\ \alpha = 1,\dots,N \tag{4.1}$$

are interpreted as the local density of the population $\mathcal{P}_j$ in the cell α.

Let us assume the dynamics to be governed by a self-adjoint time-independent Hamiltonian operator $\mathcal{H}$, such that

$$\mathcal{H} = \mathcal{H}_0 + \mathcal{H}_I + \mathcal{H}_C + \mathcal{H}_M, \tag{4.2}$$

where

$$\begin{cases} \mathcal{H}_0 = \displaystyle\sum_{j=1}^{2} \sum_{\alpha=1}^{N} \omega_{j,\alpha} a^\dagger_{j,\alpha} a_{j,\alpha}, \\ \mathcal{H}_I = \displaystyle\sum_{\alpha=1}^{N} \lambda_\alpha (a_{1,\alpha} a^\dagger_{2,\alpha} + a_{2,\alpha} a^\dagger_{1,\alpha}), \\ \mathcal{H}_C = \displaystyle\sum_{\alpha=1}^{N} \left(\nu_\alpha \sum_{\beta=1}^{N} p_{\alpha,\beta} (a_{1,\alpha} a^\dagger_{2,\beta} + a_{2,\beta} a^\dagger_{1,\alpha}) \right), \\ \mathcal{H}_M = \displaystyle\sum_{j=1}^{2} \sum_{\alpha=1}^{N} \left(\mu_{j,\alpha} \sum_{\beta=1}^{N} p_{\alpha,\beta} (a_{j,\alpha} a^\dagger_{j,\beta} + a_{j,\beta} a^\dagger_{j,\alpha}) \right), \end{cases} \tag{4.3}$$

with $\omega_{j,\alpha}$, λ_α, $\mu_{j,\alpha}$, ν_α ($\alpha = 1,\dots,N$, $j = 1,2$) positive constants; moreover, the coefficients $p_{\alpha,\beta}$ ($\alpha,\beta = 1,\dots,N$), symmetric with respect to their indices, are equal to 1 if β denotes a cell in the Moore neighborhood M_α (the set of adjacent cells) and 0 elsewhere. Thus, the cells in the Moore neighborhood of the cell $\alpha \neq 1, N$ are labeled as $\alpha - 1$ and $\alpha + 1$, whereas the cells labeled with 1 and N have only one neighbor (labeled 2 and $N - 1$, respectively).

We repeat here some considerations about the various contributions in the Hamiltonian.

- $\mathcal{H}_0$ is the free part of the Hamiltonian, and $\omega_{j,\alpha}$ are parameters somehow related to the inertia of the operators associated to the agents of $\mathcal{S}$.
- $\mathcal{H}_I$ rules the local (i.e., in the same cell α) competitive interaction between the two populations; the coefficients λ_α give a measure of the strength of the interaction, and, when $\lambda_\alpha = 0$ for all α, there is no competition at all: the contribution $a_{1,\alpha} a^\dagger_{2,\alpha}$ is a competition term since the actor associated to $a_{1,\alpha}$ is *destroyed* and the actor associated to $a_{2,\alpha}$ is *created*; the adjoint term $a_{2,\alpha} a^\dagger_{1,\alpha}$ swaps the roles of the two actors.
- $\mathcal{H}_C$ takes into account a nonlocal competitive interaction between the two populations, and ν_α measure the strength of nonlocal interaction (absent if $\nu_\alpha = 0$, $\alpha = 1,\dots,N$): in fact the competition between the two populations occurs in adjacent cells.
- $\mathcal{H}_M$ is responsible for the diffusion of the two populations in the region, and $\mu_{j,\alpha}$ is the mobility coefficient of population $\mathcal{P}_j$ in the cell α: the contribution $a_{j,\alpha} a^\dagger_{j,\beta}$ is such that actor associated to $a_{j,\alpha}$ is *destroyed* and the actor associated to $a_{j,\beta}$ is *created*; once again, the adjoint term $a_{j,\beta} a^\dagger_{j,\alpha}$ swaps the roles of the two actors.

The choice (that could seem too much restrictive) of considering a one-dimensional spatial region where the two populations interact and — with different mobilities — migrate is not just (or only) a trick to simplify the analysis. In fact, migratory phenomena are often observed along well defined directions, *e.g.*, from south to north; in such circumstances a model where the two populations are assumed spatially distributed in a one–dimensional region can result appropriate.

Adopting the Heisenberg representation, the operators $a_{j,\alpha}$ evolve in time according to the differential equations

$$\frac{da_{j,\alpha}}{dt} = \mathrm{i}[\mathcal{H}, a_{j,\alpha}], \tag{4.4}$$

where $[\mathcal{H}, a_{j,\alpha}] = \mathcal{H}a_{j,\alpha} - a_{j,\alpha}\mathcal{H}$ is the commutator between $\mathcal{H}$ and $a_{j,\alpha}$. Using (4.4), we get the following linear system of ordinary differential equations:

$$\begin{aligned}
\frac{da_{1,1}}{dt} &= \mathrm{i}\left(-\omega_{1,1}a_{1,1} + \lambda_1 a_{2,1} + (\mu_{1,1}+\mu_{1,2})a_{1,2} + \nu_1 a_{2,2}\right),\\
\frac{da_{1,\alpha}}{dt} &= \mathrm{i}\left(-\omega_{1,\alpha}a_{1,\alpha} + \lambda_\alpha a_{2,\alpha} + (\mu_{1,\alpha}+\mu_{1,\alpha-1})a_{1,\alpha-1} + (\mu_{1,\alpha}+\mu_{1,\alpha+1})a_{1,\alpha+1}\right.\\
&\quad \left. +\nu_\alpha(a_{2,\alpha-1}+a_{2,\alpha+1})\right), \qquad \alpha = 2,\dots,N-1,\\
\frac{da_{1,N}}{dt} &= \mathrm{i}\left(-\omega_{1,N}a_{1,N} + \lambda_N a_{2,N} + (\mu_{1,N}+\mu_{1,N-1})a_{1,N-1} + \nu_N a_{2,N-1}\right),\\
\frac{da_{2,1}}{dt} &= \mathrm{i}\left(-\omega_{2,1}a_{2,1} + \lambda_1 a_{1,1} + (\mu_{2,1}+\mu_{2,2})a_{2,2} + \nu_2 a_{1,2}\right),\\
\frac{da_{2,\alpha}}{dt} &= \mathrm{i}\left(-\omega_{2,\alpha}a_{2,\alpha} + \lambda_\alpha a_{1,\alpha} + (\mu_{2,\alpha}+\mu_{2,\alpha-1})a_{2,\alpha-1} + (\mu_{2,\alpha}+\mu_{2,\alpha+1})a_{2,\alpha+1}\right.\\
&\quad \left. +\nu_{\alpha-1}a_{1,\alpha-1} + \nu_{\alpha+1}a_{1,\alpha+1}\right), \qquad \alpha = 2,\dots,N-1,\\
\frac{da_{2,N}}{dt} &= \mathrm{i}\left(-\omega_{2,N}a_{2,N} + \lambda_N a_{1,N} + (\mu_{2,N}+\mu_{2,N-1})a_{2,N-1} + \nu_{N-1}a_{1,N-1}\right).
\end{aligned} \tag{4.5}$$

As explained in the previous chapters, let us introduce the formal column vector

$$\mathbf{A} = [a_{1,1},\dots,a_{1,N},a_{2,1},\dots,a_{2,N}]^T,$$

(^{T} stands for the transposition operator) and a suitable $2N\times 2N$ real matrix Γ (whose entries, once we fix N, can be constructed from (4.5)), the evolution equations for the annihilation operators can be written in the compact form as

$$\frac{d\mathbf{A}}{dt} = \mathrm{i}\Gamma\mathbf{A}. \tag{4.6}$$

Let us now consider the compact version of the evolution equations for the creation operators, say

$$\frac{d\mathbf{A}^\dagger}{dt} = -\mathrm{i}\Gamma\mathbf{A}^\dagger; \tag{4.7}$$

coupling (4.6) and (4.7), we have the system

$$\frac{d}{dt}\begin{bmatrix}\mathbf{A}\\ \mathbf{A}^\dagger\end{bmatrix} = \begin{bmatrix}\mathrm{i}\Gamma & \mathbf{0}_{2N}\\ \mathbf{0}_{2N} & -\mathrm{i}\Gamma\end{bmatrix}\begin{bmatrix}\mathbf{A}\\ \mathbf{A}^\dagger\end{bmatrix}, \tag{4.8}$$

$\mathbf{0}_{2N}$ being a zero matrix of order $2N$; actually, we do not need to consider also the equations for the creation operators, but this simplifies the formulae for the mean values of the number operators (see below).

The formal solution to system (4.8) is

$$\begin{bmatrix} \mathbf{A}(t) \\ \mathbf{A}^\dagger(t) \end{bmatrix} = \exp\left(\begin{bmatrix} \mathrm{i}\Gamma t & \mathbf{0}_{2N} \\ \mathbf{0}_{2N} & -\mathrm{i}\Gamma t \end{bmatrix} \right) \begin{bmatrix} \mathbf{A}_0 \\ \mathbf{A}_0^\dagger \end{bmatrix} = \mathcal{B}(t) \begin{bmatrix} \mathbf{A}_0 \\ \mathbf{A}_0^\dagger \end{bmatrix}. \tag{4.9}$$

Let $n^0_{i,\alpha}$ $(i = 1, 2, \alpha = 1, \dots, N)$ be the initial density of population $\mathcal{P}_i$ in the cell α, and let $\mathbf{n}^0$ the vector with $2N$ components

$$\mathbf{n}^0 = \left(\sqrt{n^0_{1,1}}, \dots, \sqrt{n^0_{1,N}}, \sqrt{n^0_{2,1}}, \dots, \sqrt{n^0_{2,N}} \right);$$

denoting with $B_{j,k}$ the generic entry of the $4N \times 4N$ matrix $\mathcal{B}(t)$, it is easy to derive, by using the canonical anticommutation relations (2.5), the formula giving the mean values of the number operators (that is, the densities of the two populations in each cell) at time t:

$$\begin{aligned} n_{1,\alpha}(t) = {} & \sum_{i=1}^{2N} \left(n_i^0\right)^2 \sum_{\ell=1}^{2N} \left(B_{\alpha,f(\ell,i)} B_{\alpha+2N,g(\ell,i)} \right) \\ & + \sum_{i=1}^{2N-1} \sum_{j=i+1}^{2N} n_i^0 n_j^0 \left(B_{\alpha,i} B_{\alpha+2N,j+2N} + B_{\alpha,j} B_{\alpha+2N,i+2N} \right. \\ & \left. - B_{\alpha,i+2N} B_{\alpha+2N,j} - B_{\alpha,j+2N} B_{\alpha+2N,i} \right), \\ n_{2,\alpha}(t) = {} & \sum_{i=1}^{2N} \left(n_i^0\right)^2 \sum_{\ell=1}^{2N} \left(B_{\alpha+N,f(\ell,i)} B_{\alpha+3N,g(\ell,i)} \right) \\ & + \sum_{i=1}^{2N-1} \sum_{j=i+1}^{2N} n_i^0 n_j^0 \left(B_{\alpha+N,i} B_{\alpha+3N,j+2N} + B_{\alpha+N,j} B_{\alpha+3N,i+2N} \right. \\ & \left. - B_{\alpha+N,i+2N} B_{\alpha+3N,j} - B_{\alpha+N,j+2N} B_{\alpha+3N,i} \right), \end{aligned}$$

where

$$f(\ell,i) = \begin{cases} i & \text{if} \quad i = \ell, \\ i+2N & \text{if} \quad i \neq \ell, \end{cases} \qquad g(\ell,i) = \begin{cases} i+2N & \text{if} \quad i = \ell, \\ i & \text{if} \quad i \neq \ell. \end{cases}$$

Let us divide the region $\mathcal{C}$ in three different subregions: a left region ($\mathcal{C}_1$), a central region ($\mathcal{C}_2$), and a right region ($\mathcal{C}_3$); this distinction is because we assume that some of the parameters entering the Hamiltonian are somehow different in the three subregions. Moreover, we will distinguish two different cases in order to simulate two different realistic scenarios.

The quadratic form of the Hamiltonian has an immediate consequence: the dynamic behavior that we can obtain in each cell is at most quasiperiodic. Furthermore, due to the relation

$$\left[\mathcal{H}, \sum_{\alpha=1}^{N} \left(\widehat{n}_{1,\alpha} + \widehat{n}_{2,\alpha} \right) \right] = 0,$$

the Hamiltonian possesses a first integral, expressing the fact that the sum of the densities of the two populations in all the cells of the domain is constant in time.

More complex outcomes (not necessarily quasiperiodic) could be recovered including in the Hamiltonian terms more than quadratic. Nevertheless, in such a case

we would be forced to solve numerically a very huge number of differential equations. Another strategy to enrich the dynamics without rendering the problem computationally hard, if not impossible from a practical point of view, is the one introduced in a series of recent papers (Di Salvo and Oliveri, 2017; Di Salvo, Gorgone, and Oliveri, 2017b; Di Salvo, Gorgone, and Oliveri, 2017a; Bagarello et al., 2017; Bagarello et al., 2018) where it was shown how to obtain more interesting dynamics still retaining a quadratic and time-independent Hamiltonian.

4.1.1 $(\mathcal{H}, \rho)$–induced dynamics

We use three different rules that are detailed below. Fixing a value for τ (the choice of τ plays a role in the dynamics, as will be shown in the following), let us define

$$\delta_{j,\alpha} = n_{j,\alpha}(k\tau) - n_{j,\alpha}((k-1)\tau), \quad j = 1,2, \quad \alpha \in \mathcal{C},$$
$$\overline{\delta}_j^{(r)} = \text{mean}(\delta_{j,\alpha}), \qquad r = 1,2,3, \quad \alpha \in \mathcal{C}_r.$$

where r is the index of the three regions of the lattice. Let us consider three different set of rules by updating at fixed instants $k\tau$ ($k = 1,2,\ldots$) some of the parameters entering the Hamiltonian as follows:

Rule 1:

$$\omega_{j,\alpha} = \omega_{j,\alpha}(1 + \delta_{j,\alpha});$$

this means that the inertia parameter of the population $\mathcal{P}_j$ in the cell α increases (decreases) if the local density in the subinterval of length τ, increases (decreases); due to the meaning of the inertia parameters, this means that a population increasing its local density tends to lower its tendency to change. The rationale of the rule is that an increase of the local density of a population in the cell α has the effect of inducing a lower tendency to change, whereas a decrease induces the population to be less conservative.

Rule 2:

$$\omega_{j,\alpha} = \omega_{j,\alpha}(1 + \delta_{j,\alpha}), \qquad \mu_{j,\alpha} = \mu_{j,\alpha}(1 + \overline{\delta}_j^{(r)});$$

besides updating the inertia parameters like in Rule 1, we update the mobility parameters of the two population according to the mean value of the local densities in each subregion: in this way each population increases its mobility parameter if the mean variation of the densities in a subregion increases; essentially, the change of the mobility parameters accounts for a change in the attitude of the population so that an increase of the mobility parameters is a sort of reaction to over population in each subregion.

Rule 3:

$$\omega_{j,\alpha} = \omega_{j,\alpha}(1 + \delta_{j,\alpha}), \quad \mu_{1,\alpha} = \mu_{1,\alpha}(1 + \overline{\delta}_2^{(r)}), \quad \mu_{2,\alpha} = \mu_{2,\alpha}(1 + \overline{\delta}_1^{(r)});$$

also in this case, the inertia parameters are updated as in Rule 1; however, the mobility parameters of each population changes as a function of the mean variation of the densities in each subregion of the other population; this rule models a sort of escaping effect of a population when the local density of the other population increases.

4.2 Numerical simulations

In this Section, we present various numerical simulations by using two special sets of initial conditions with the aim of describing real situations.

Let $\mathcal{C}$ be a one-dimensional region made by $N = 50$ cells, and let $\mathcal{C}_1$ be the subregion made by the cells in the range 1–15, $\mathcal{C}_2$ be the subregion made by the cells in the range 16–35, and $\mathcal{C}_3$) be the subregion made by cells in the range 36–50. Two qualitatively different scenarios are considered. In both situations, we compare the numerical results obtained by the standard Heisenberg dynamics and those coming from the superposition of the Heisenberg dynamics with the rules above described.

4.2.1 First scenario

Let us assume that initially in the left region population $\mathcal{P}_1$ is much more abundant than population $\mathcal{P}_2$, in the central region both populations have comparable and very small local densities, whereas in the right region population $\mathcal{P}_2$ is much more abundant than population $\mathcal{P}_1$. This means that the central region is a sort of transit region from the subregion $\mathcal{C}_1$ to $\mathcal{C}_3$.

Let us choose the following initial local densities for the two populations:

$$\begin{array}{lll} n^0_{1,\alpha} = 0.9, & n^0_{2,\alpha} = 0.05, & \alpha \in \mathcal{C}_1, \\ n^0_{1,\alpha} = r_\alpha(0, 10^{-2}), & n^0_{2,\alpha} = r_\alpha(0, 10^{-2}) & \alpha \in \mathcal{C}_2, \\ n^0_{1,\alpha} = 0.05, & n^0_{2,\alpha} = 0.9, & \alpha \in \mathcal{C}_3, \end{array} \tag{4.10}$$

where $r_\alpha(a, b)$ denotes a random real number in the interval $[a, b]$. Thus, the initial distributions of each population is uniform in the first and third region, whereas in the central region both populations have very small random initial densities.

As far as the parameters are concerned, we make the following choices:

$$\begin{array}{llll} \omega_{1,\alpha} = 0.4, & \omega_{2,\alpha} = 0.7, & \alpha \in \mathcal{C}, \\ \lambda_\alpha = 0.05, & \nu_\alpha = 0.025, & \alpha \in \mathcal{C}_1, \\ \lambda_\alpha = 0.01, & \nu_\alpha = 0.005, & \alpha \in \mathcal{C}_2, \\ \lambda_\alpha = 0.1, & \nu_\alpha = 0.05, & \alpha \in \mathcal{C}_3, \\ \mu_{1,\alpha} = 0.2, & \mu_{2,\alpha} = 0.05, & \alpha \in \mathcal{C}. \end{array} \tag{4.11}$$

Each of the parameters entering the Hamiltonian is constant in each subregion; population P_1 possesses inertia parameters smaller than those of population $\mathcal{P}_2$, but greater mobility parameters μ's; the competitive interaction parameters in the first and third subregions are greater than those in the central subregion, and the nonlocal interaction is weaker than the local one. Moreover, the parameters responsible for competition (λ_α and ν_α) are very small in the central region, and have their maximum in the right region. The concrete situation we want to describe is the following one. The left subregion $\mathcal{C}_1$ could be thought of as a *poor region*, the right subregion $\mathcal{C}_3$ as a *rich region*, and the central subregion $\mathcal{C}_2$ as the region that the poorer population $\mathcal{P}_1$ needs to cross with the aim of going to the richest subregion and improving its wealth. Such a situation is somehow similar to the one considered in Bagarello and Oliveri, 2013 where a model including only local competition and migration (without any rule) has been investigated. As clearly shown in Figure 4.1 (subfigures (b), (d) and (f) for the rule 1), the dynamical outcome is rather different if we take into account the $(\mathcal{H}, \rho)$–induced dynamics approach.

Without the rules, the behavior of the local density in each cell is oscillatory, although the migration terms tend to make uniform the densities all over the three

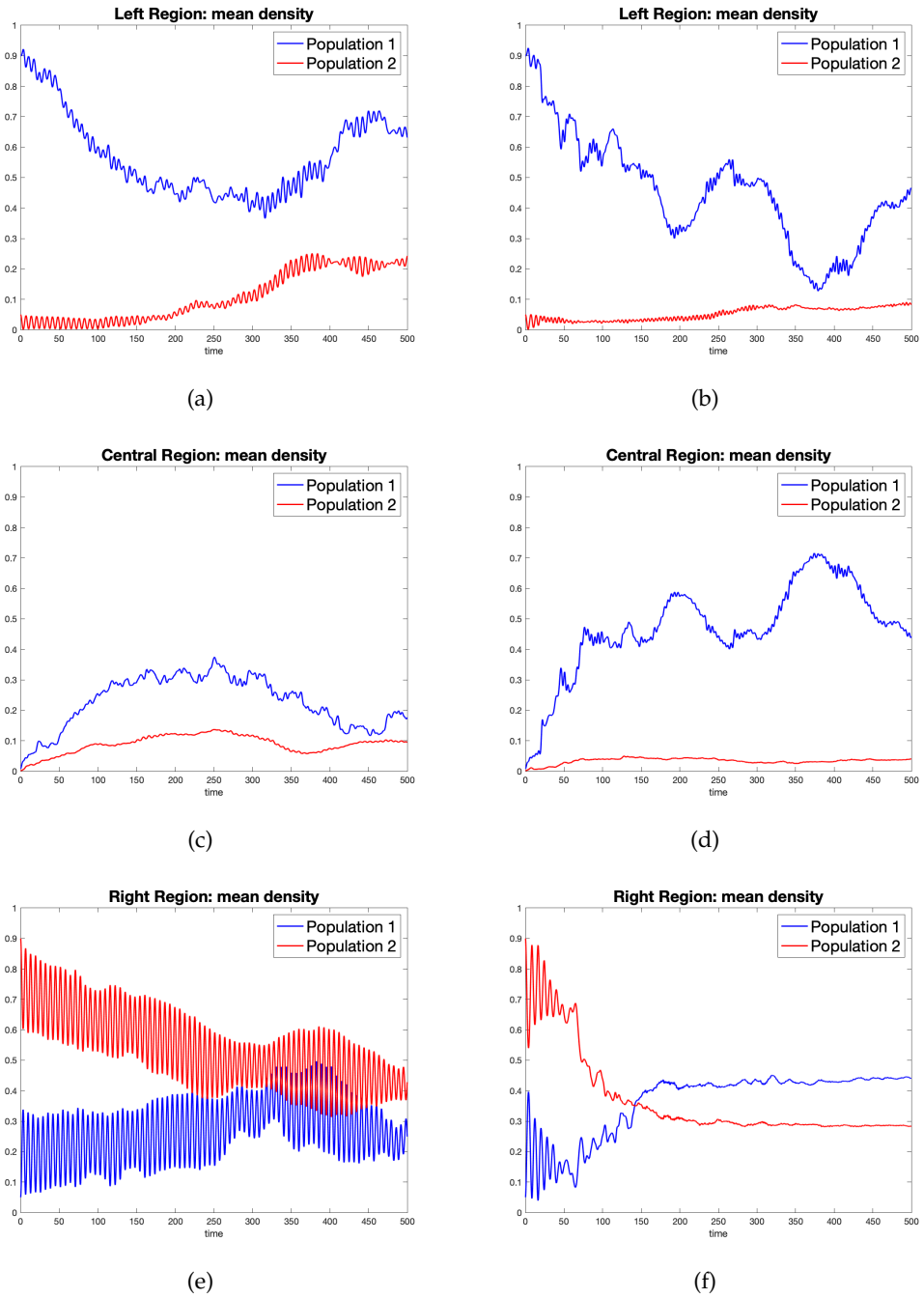

FIGURE 4.1: Time evolution (standard Heisenberg dynamics with no rule) of the mean local densities in subregion $\mathcal{C}_1$ (a), subregion $\mathcal{C}_2$ (c) and subregion $\mathcal{C}_3$ (e). The subfigures (b), d) and (f) display the time evolution in the framework of (H, ρ)–induced dynamics with rule 1 and $\tau = 1$.

subregions. It is observed that both populations move to the right cells, and this effect is more evident for population $\mathcal{P}_1$ (Figure 4.1, subfigures (a), (c) and (e)); also, due to the structure of the Hamiltonian (and, consequently, to the quasiperiodic regime), the local densities do not definitely increase moving from the left to the right. On the contrary, a clear movement from left to right emerges when the rules are considered (Figure 4.1, subfigures (b), (d) and (f) for the rule 1). In the classical Heisenberg dynamics (no rule at all), population $\mathcal{P}_1$ tends to move towards the subregion $\mathcal{C}_3$: at least in the time interval $[0, 200]$ the mean local density of $\mathcal{P}_1$ decreases in $\mathcal{C}_1$, and increases in $\mathcal{C}_2$ and $\mathcal{C}_3$. On the contrary, the mean local density of population $\mathcal{P}_2$ increases in $\mathcal{C}_1$, has a small variation in $\mathcal{C}_2$, and decreases in $\mathcal{C}_3$. Nevertheless, due to the quasiperiodic regime, this trend is not preserved for all times. Using rule 1 (Figure 4.1, subfigures (b), (d) and (f)), this movement of population $\mathcal{P}_1$ towards subregion $\mathcal{C}_3$ is much more evident than the movement of population $\mathcal{P}_2$, and this is resaonable because of the different mobility parameters. Here it is worth noting that, in the right region, the mean local densities of the two populations tend to approach a sort of equilibrium; moreover, there is also an inversion, in the sense that population $\mathcal{P}_2$ becomes more abundant than population $\mathcal{P}_1$ (this is due to the initial values of inertia parameters of the two populations: population $\mathcal{P}_1$ has a greater tendency to change with respect to population $\mathcal{P}_2$). The quasi periodic regime of the classical Heisenberg dynamics is modified by the effect of the rule that introduces a sort of irreversibility in the evolution, even if the sum of the local densities of the two populations in all cells remains constant, that is, the rule preserves the existence of the first integral.

The same general considerations, though the dynamical outcomes are somehow different, apply also when the rules 2 and 3 are used. In fact, the effects of the rules 2 and 3 (one again with the choice $\tau = 1$), that modify also the mobility parameters, are shown in Figure 4.2, where, the migration of both populations towards the right cells has a more definite trend; moreover, it is observed that the amplitude of the oscillations of the mean densities in the three subregions decreases with time.

4.2.2 Second scenario

Here, the only difference with respect to the previous case is that the central region is not sparsely inhabitated even if population $\mathcal{P}_1$ is more abundant than population $\mathcal{P}_2$; in some sense, the central subregion is not a transit area but a region with intermediate conditions of wealth.

We assume the following initial conditions:

$$\begin{array}{lll} n^0_{1,\alpha} = 0.9, & n^0_{2,\alpha} = 0.05 & \alpha \in \mathcal{C}_1, \\ n^0_{1,\alpha} = r_\alpha(0.3, 0.5), & n^0_{2,\alpha} = r_\alpha(0.15, 0.35) & \alpha \in \mathcal{C}_2, \\ n^0_{1,\alpha} = 0.05, & n^0_{2,\alpha} = 0.7 & \alpha \in \mathcal{C}_3. \end{array} \tag{4.12}$$

As far as the choice of parameters is concerned, we choose

$$\begin{aligned} &\omega_{1,\alpha} = 0.4, \qquad \omega_{2,\alpha} = 0.7, \quad \alpha \in \mathcal{C}, \\ &\lambda_\alpha = \begin{cases} 0.05, & \alpha \in \mathcal{C}_1, \\ 0.01, & \alpha \in \mathcal{C}_2, \\ 0.1, & \alpha \in \mathcal{C}_3, \end{cases} \qquad \nu_\alpha = \frac{\lambda_\alpha}{2}, \\ &\mu_{1,\alpha} = \begin{cases} (0.3\alpha + 1.1)/14, & \alpha \in \mathcal{C}_1, \\ 0.4, & \alpha \in \mathcal{C}_2, \\ (-0.3\alpha + 5.9)/14, & \alpha \in \mathcal{C}_3, \end{cases} \qquad \mu_{2,\alpha} = \frac{\mu_{1,\alpha}}{20}. \end{aligned} \tag{4.13}$$

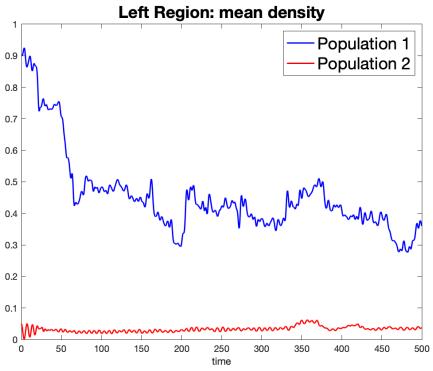

(a)

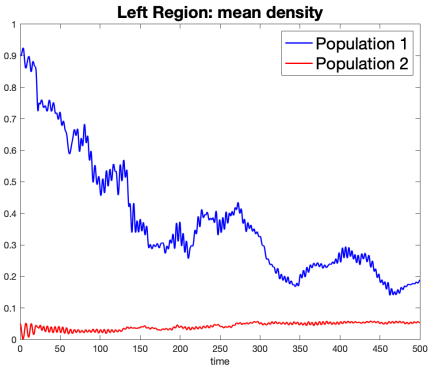

(b)

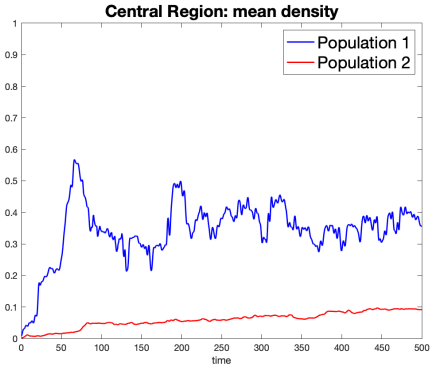

(c)

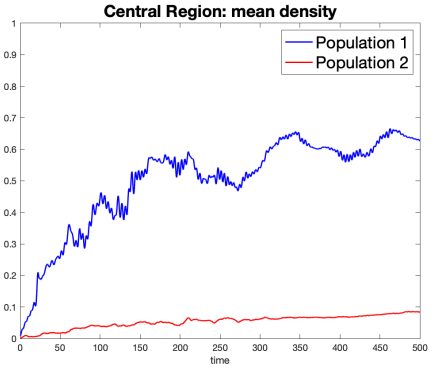

(d)

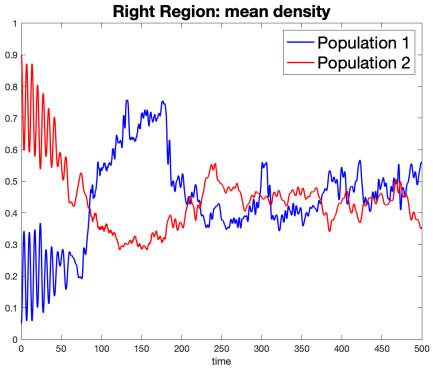

(e)

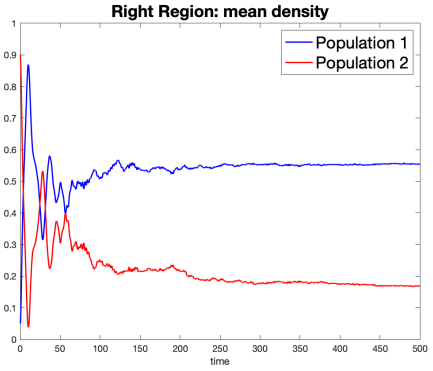

(f)

FIGURE 4.2: First scenario: time evolution of the mean of local densities in the three subregions; rule 2 (subfigures (a), (c) and (e)), and rule 3 (subfigures (b), (d) and (f)); $\tau = 1$.

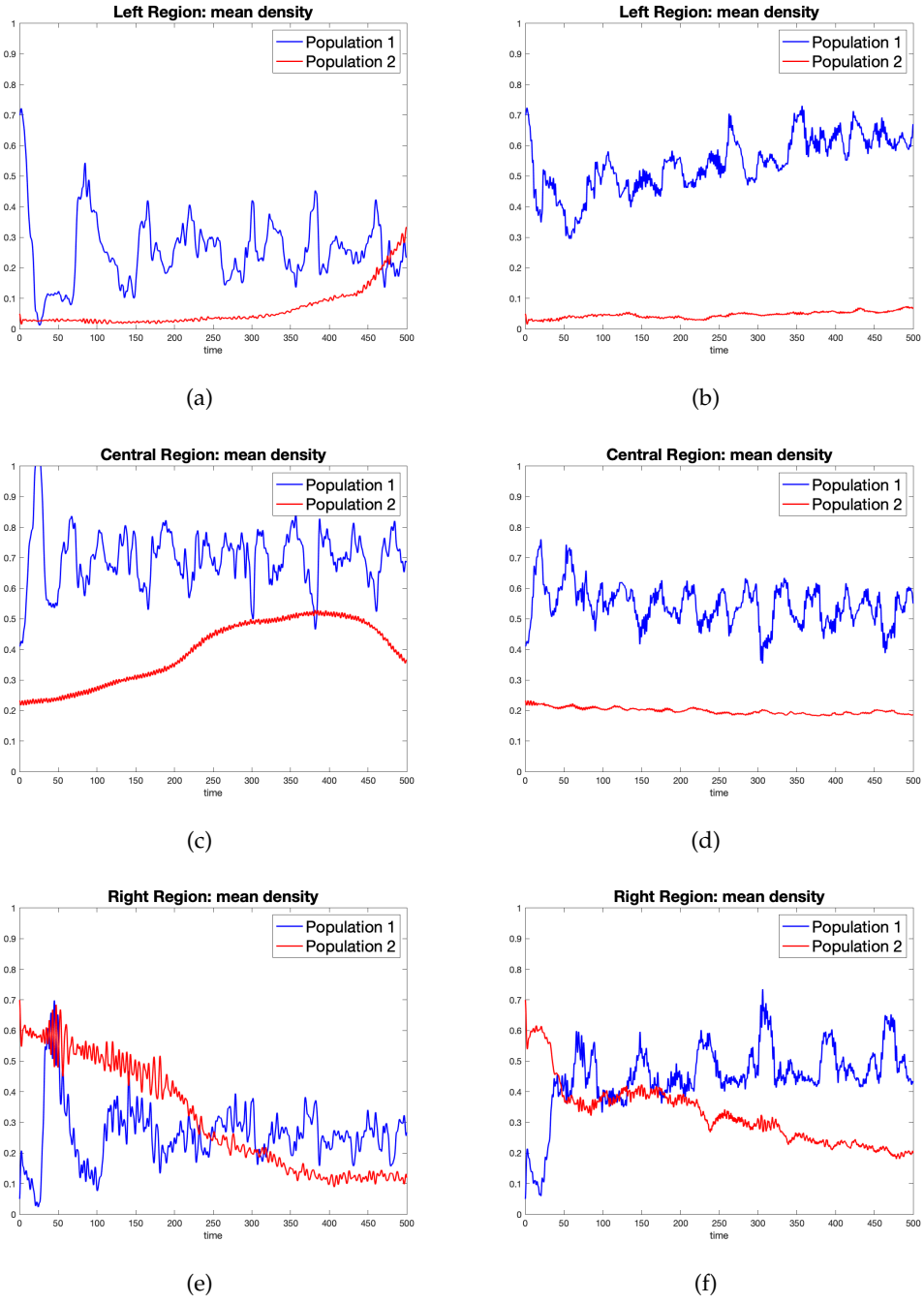

FIGURE 4.3: Second scenario: time evolution of the mean of local densities in the three subregions; classic Heisenberg dynamics (subfigures (a), (c) and (e)), and rule 1 with $\tau = 1$ (subfigures (b), (d) and (f)).

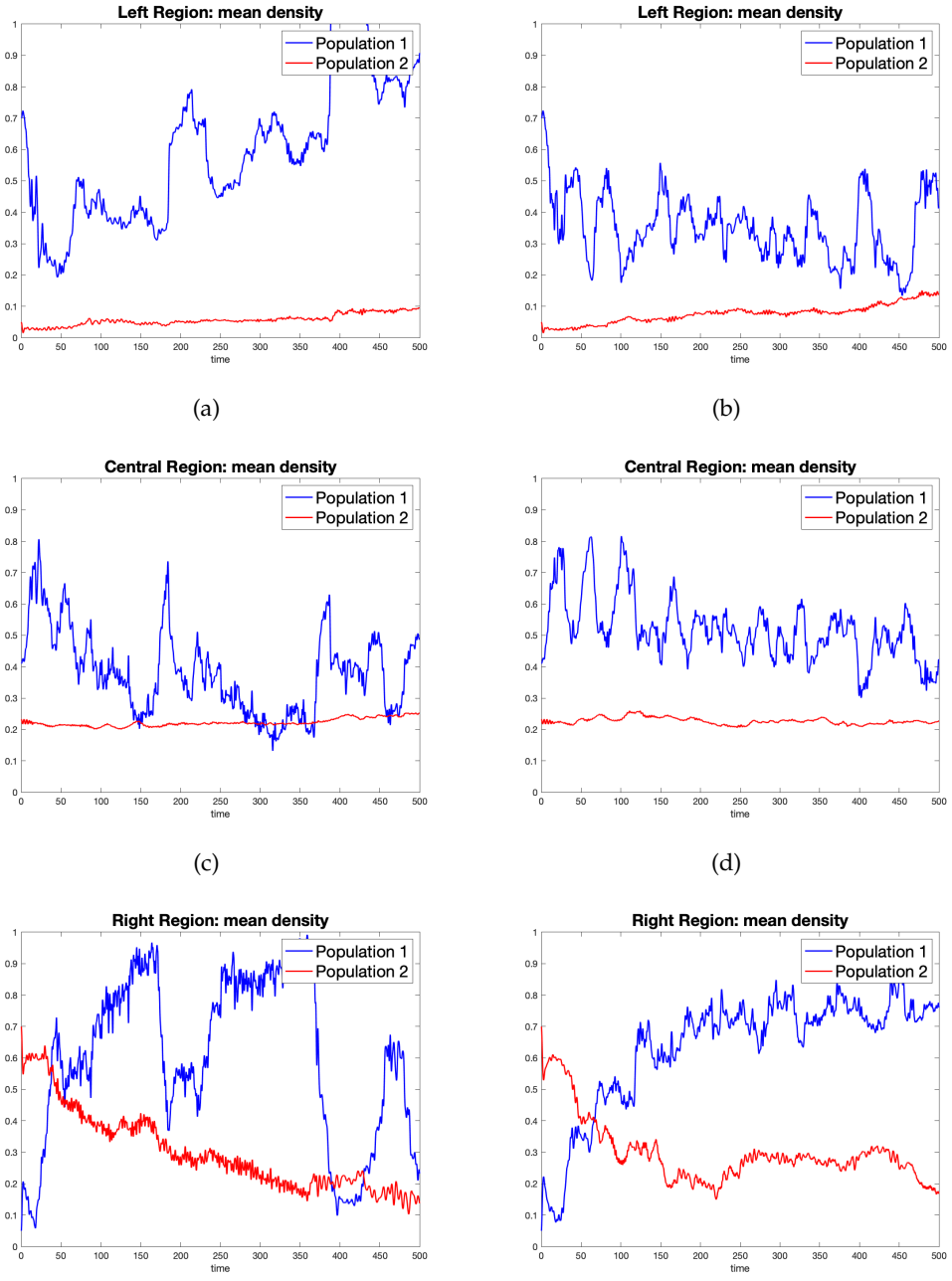

FIGURE 4.4: Second scenario: time evolution of the mean of local densities in the three subregions; rule 2 (subfigures (a), (c) and (e)) and rule 3 rule 1 with $\tau = 1$ (subfigures (b), (d) and (f)); the value $\tau = 1$ has been used.

Similar considerations as above can be made also in the second scenario, and the effect of the rules (Figure 4.3, subfigures (b), (d) and (f)), and Figure 4.4) is evident with respect to the outcomes of the classical Heisenberg dynamics. In the $(\mathcal{H}, \rho)$–induced dynamics approach, the choice of the value of τ, that is the length of the time interval after which some of the parameters entering the Hamiltonian are changed, has its influence on the time evolution. This is shown in Figures 4.5, 4.6 and 4.7 (for the first scenario), and Figures 4.8, 4.9 and 4.10 (for the second scenario).

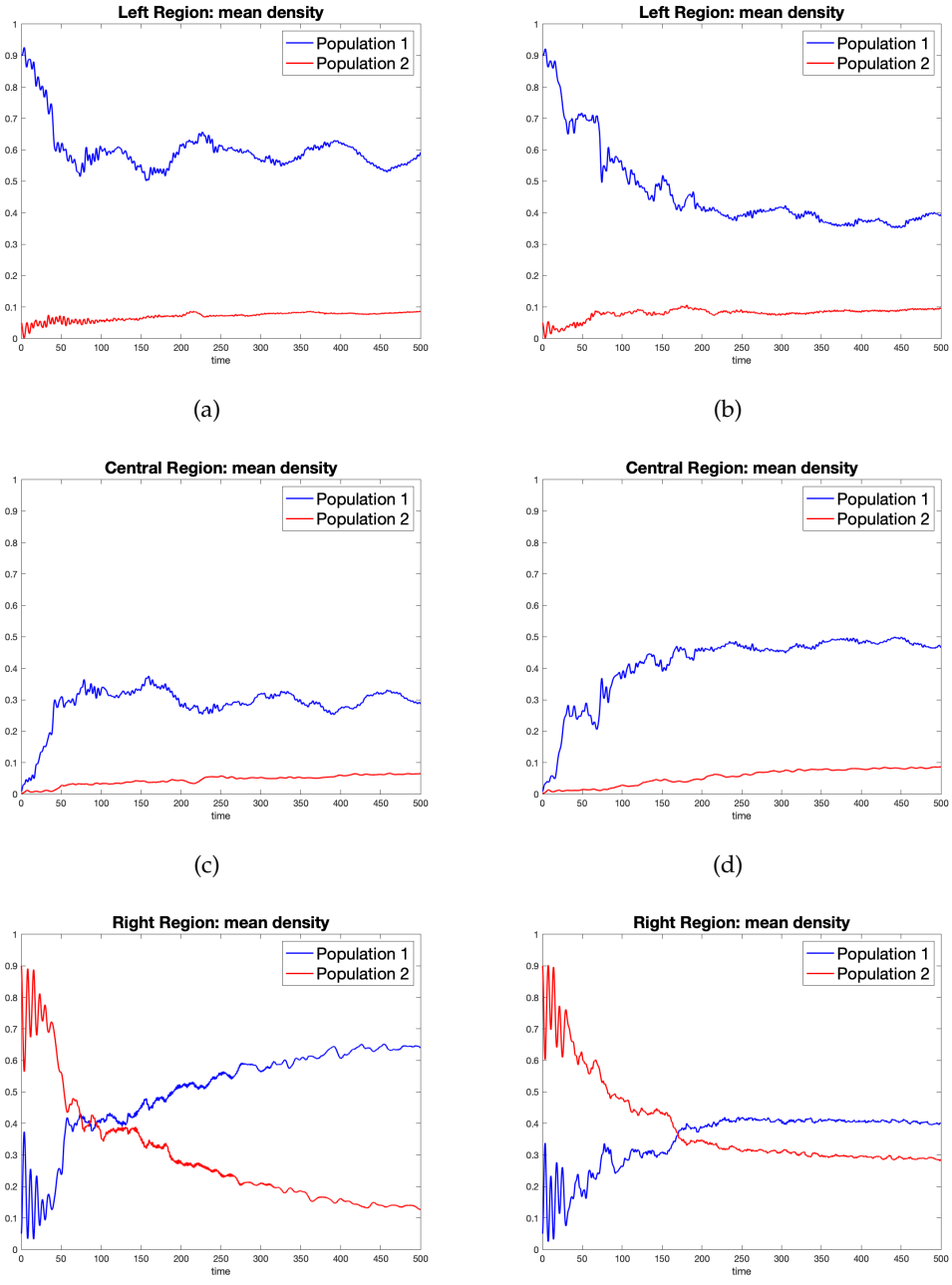

FIGURE 4.5: First scenario, $(\mathcal{H}, \rho)$–induced dynamics with rule 1: $\tau = 2$ (subfigures (a), (c) and (e)) and $\tau = 4$ (subfigures (b), (d) and (f)).

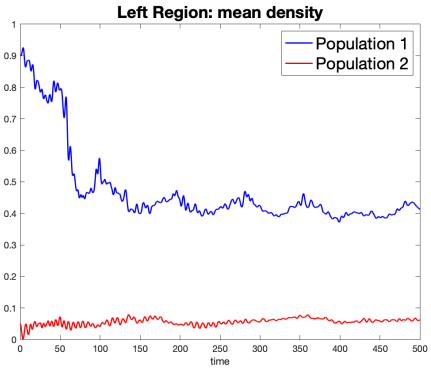

(a)

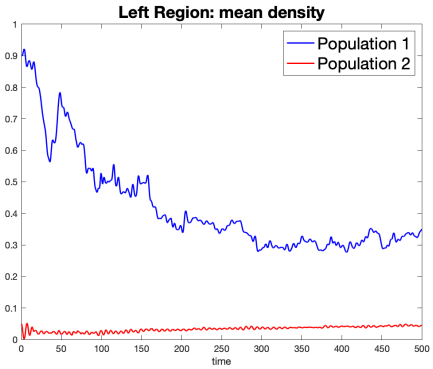

(b)

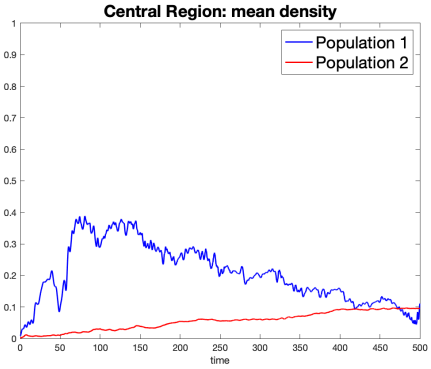

(c)

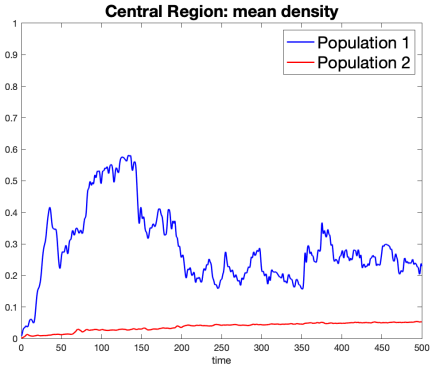

(d)

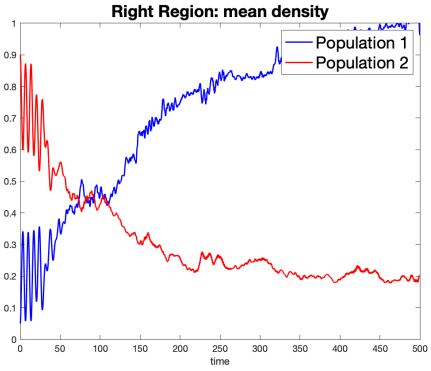

(e)

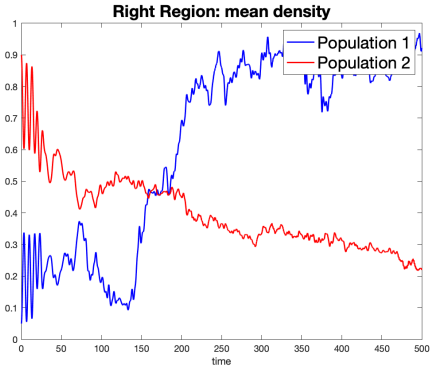

(f)

FIGURE 4.6: First scenario, $(\mathcal{H}, \rho)$–induced dynamics with rule 2: $\tau = 2$ (subfigures (a), (c) and (e)) and $\tau = 4$ (subfigures (b), (d) and (f)).

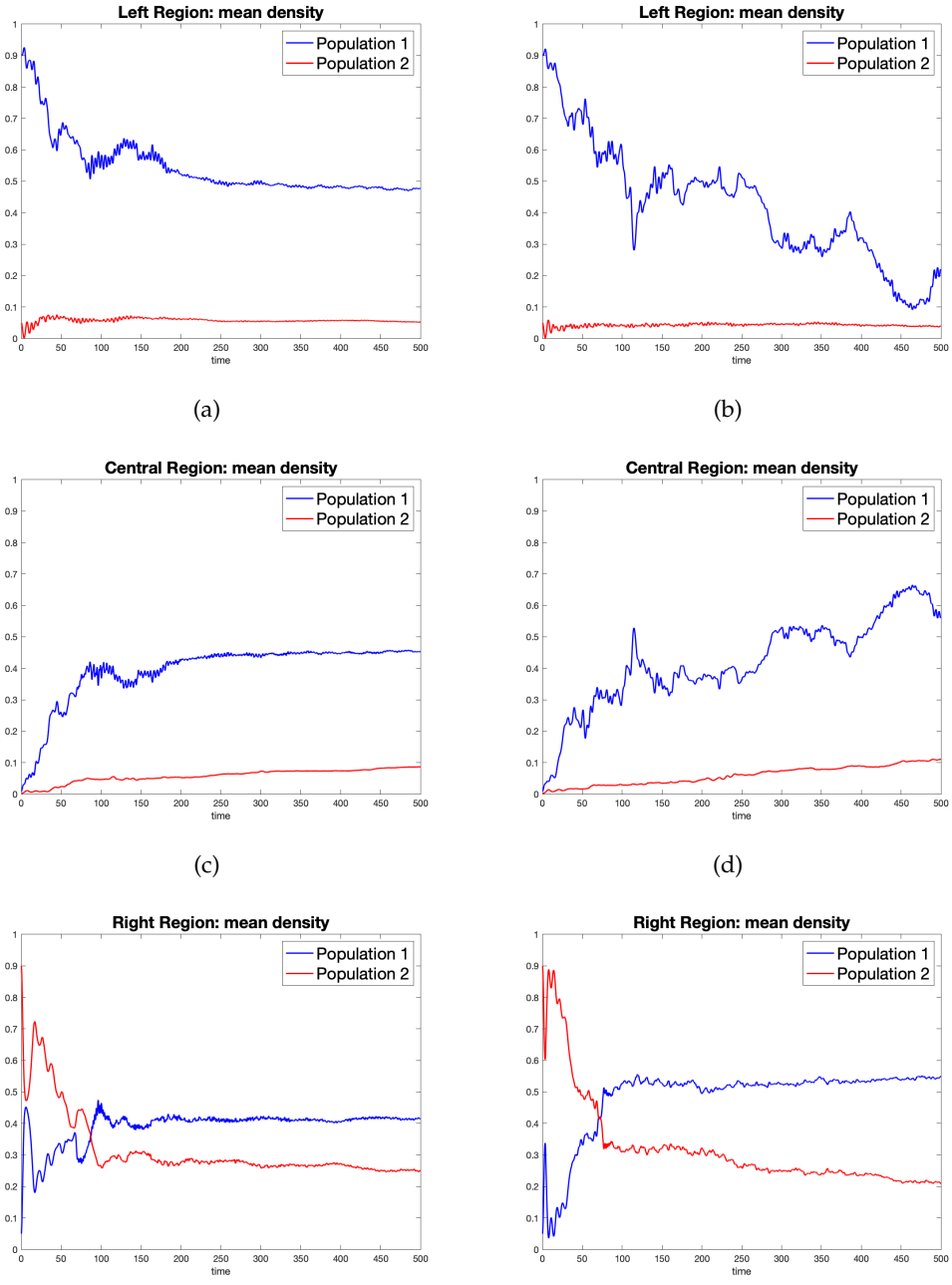

FIGURE 4.7: First scenario, $(\mathcal{H}, \rho)$–induced dynamics with rule 3: $\tau = 2$ (subfigures (a), (c) and (e)) and $\tau = 4$ (subfigures (b), (d) and (f)).

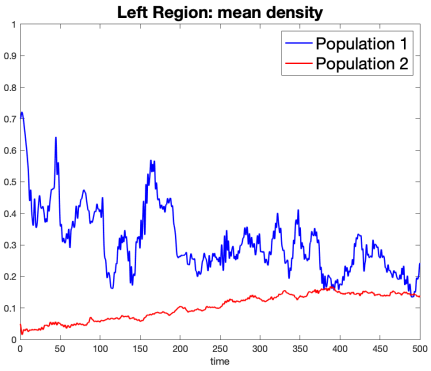

(a)

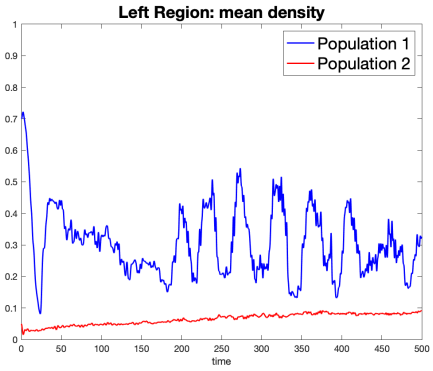

(b)

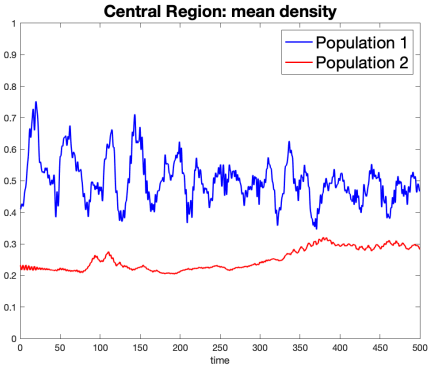

(c)

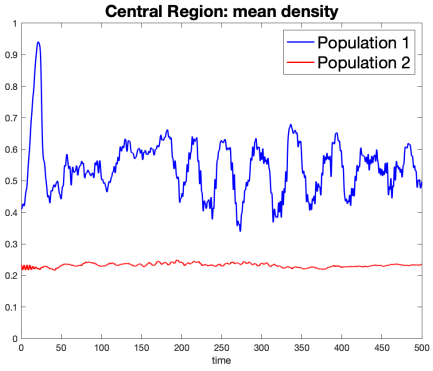

(d)

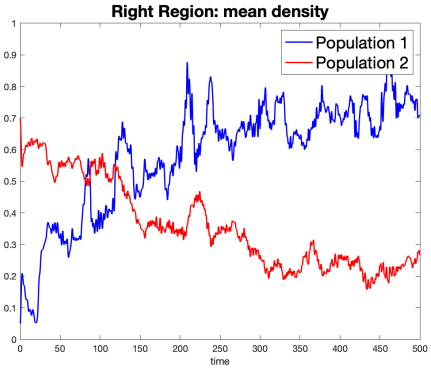

(e)

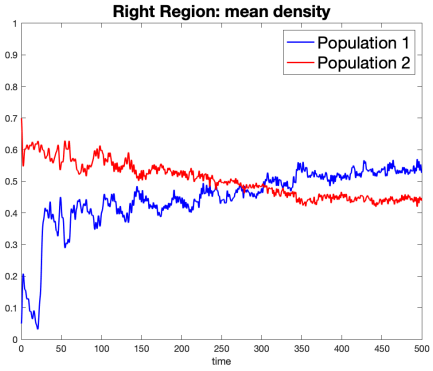

(f)

FIGURE 4.8: Second scenario, $(\mathcal{H}, \rho)$–induced dynamics with rule 1: $\tau = 2$ (subfigures (a), (c) and (e)) and $\tau = 4$ (subfigures (b), (d) and (f)).

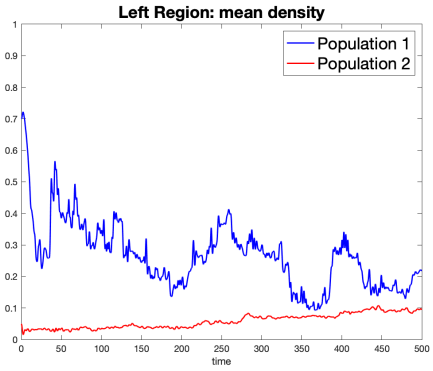

(a)

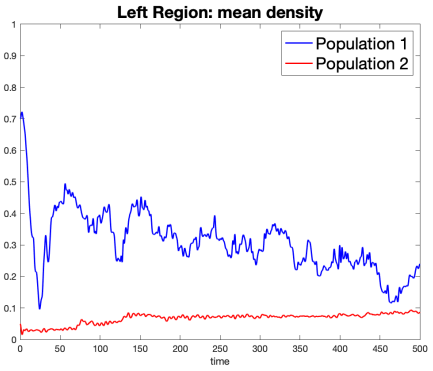

(b)

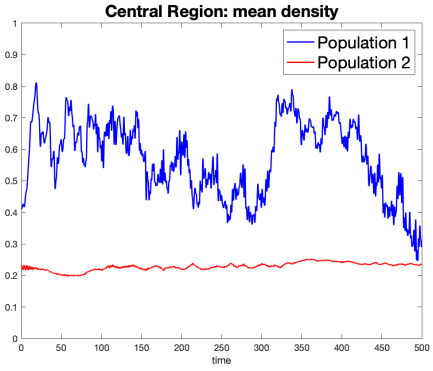

(c)

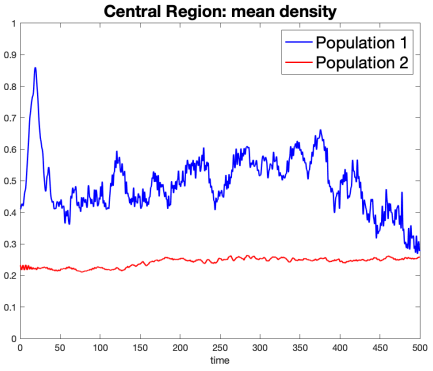

(d)

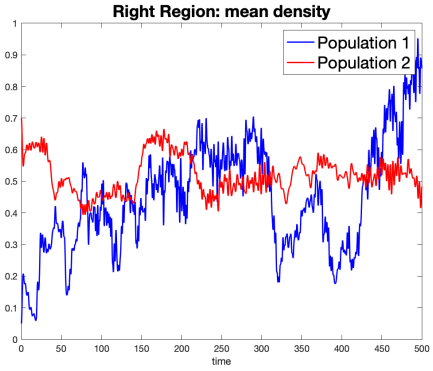

(e)

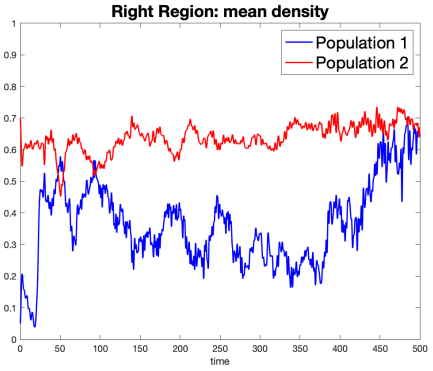

(f)

FIGURE 4.9: Second scenario, $(\mathcal{H}, \rho)$–induced dynamics with rule 2: $\tau = 2$ (subfigures (a), (c) and (e)) and $\tau = 4$ (subfigures (b), (d) and (f)).

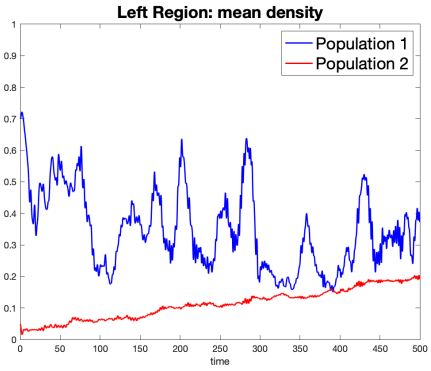

(a)

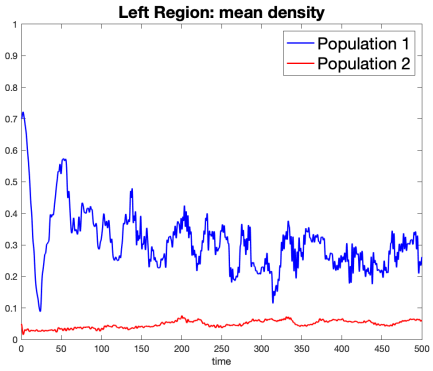

(b)

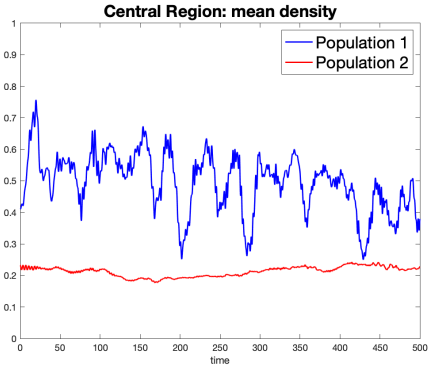

(c)

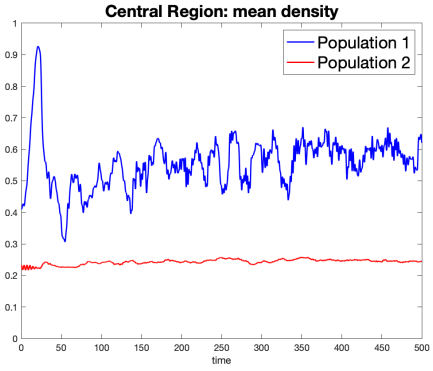

(d)

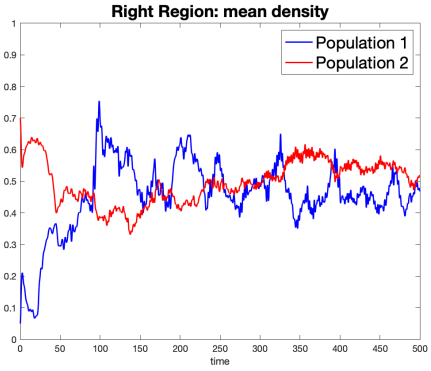

(e)

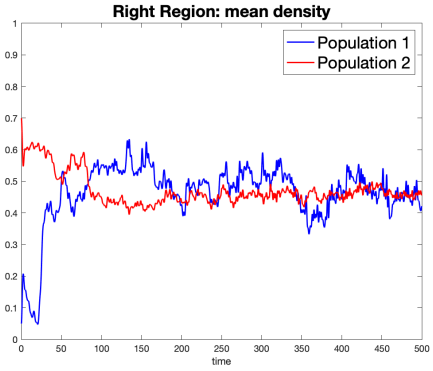

(f)

FIGURE 4.10: Second scenario, $(\mathcal{H}, \rho)$–induced dynamics with rule 3: $\tau = 2$ (subfigures (a), (c) and (e)) and $\tau = 4$ (subfigures (b), (d) and (f)).

Chapter 5

Fermionic operatorial model of a system with competitive and cooperative agents

In this Chapter, we implement a model made by a finite number of agents interacting each other with competitive as well as cooperative mechanisms (Gorgone, Inferrera, and Oliveri, 2022). The agents are described by fermionic annihilation and creation operators, and the mean values associated to the number operators are interpreted as a measure of their wealth. In particular, we consider a simple model made by seven agents divided in three subgroups (three agents with competitive interaction, three agents with cooperative interaction, and one opportunist agent with both types of interaction); by choosing suitable value to the interaction parameters, we present the results of some numerical simulations. The dynamical outcomes of classical Heisenberg dynamics, as well as that of $(\mathcal{H}, \rho)$–induced dynamics approach are given. Moreover, a similar model where the agents are spatially distributed in a one–dimensional torus, with interaction parameters depending on the distance between the agents, is considered.

5.1 The fermionic operatorial model

Let us consider a system $\mathcal{S}$ made by N interacting agents $A_1, \ldots, A_N$; an annihilation (a_j), a creation $(a_j^\dagger)$, and an occupation number $(\widehat{n}_j = a_j^\dagger a_j)$ fermionic operator is associated to each agent.

The Hilbert space $\mathbb{H}$ in which the fermionic operators are defined is constructed as the linear span of the orthonormal set of vectors

$$\varphi_{n_1,n_2\ldots,n_N} = (a_1^\dagger)^{n_1}(a_2^\dagger)^{n_2}\cdots(a_N^\dagger)^{n_N}\varphi_{0,0,\ldots,0}, \tag{5.1}$$

generated by acting on the *vacuum* $\varphi_{0,0,\ldots,0}$ (*i.e.*, an eigenvector of all the annihilation operators) with the operators $(a_\ell^\dagger)^{n_\ell}$, $n_\ell = 0, 1$ for $\ell = 1, \ldots, N$; therefore, it is $\dim(\mathbb{H}) = 2^N$. The vector $\varphi_{n_1,n_2,\ldots,n_N}$ means that to the k–th agent it is initially assigned a mean value equal to n_k $(k = 1, \ldots, N)$. We have

$$\widehat{n}_k\varphi_{n_1,n_2,\ldots,n_N} = n_k\varphi_{n_1,n_2,\ldots,n_N}, \qquad k = 1, \ldots, N. \tag{5.2}$$

The interpretation we give to the mean values n_k $(k = 1, \ldots, N)$ is that of a measure of the wealth of the k–th agent. The interactions we consider to occur among the agents in the system $\mathcal{S}$ fall in two different classes: competition and cooperation.

Let the dynamics of $\mathcal{S}$ be governed by the self–adjoint Hamiltonian

$$\mathcal{H} = \mathcal{H}_0 + \mathcal{H}_I, \tag{5.3}$$

where

$$\begin{cases} \mathcal{H}_0 = \sum_{k=1}^{N} \omega_k a_k^\dagger a_k, \\ \mathcal{H}_I = \sum_{1\le j<k\le N} \lambda_{j,k} \left(a_j\, a_k^\dagger + a_k\, a_j^\dagger \right) + \sum_{1\le j<k\le N} \mu_{j,k} \left(a_j^\dagger\, a_k^\dagger + a_k\, a_j \right), \end{cases} \tag{5.4}$$

where the constants ω_j, $\lambda_{j,k}$ and $\mu_{j,k}$ are real positive quantities; we remark that in concrete applications not all parameters $\lambda_{j,k}$ and $\mu_{j,k}$ have to be non–vanishing.

The contribution $\mathcal{H}_0$ is the standard free part of the Hamiltonian, and ω_k are parameters somehow related to the inertia of the operators associated to the agents of $\mathcal{S}$ (and so describe their attitude).

On the contrary, $\mathcal{H}_I$ rules the interactions among the agents. These interactions split in two contributions:

- the term $\lambda_{j,k} \left(a_j\, a_k^\dagger + a_k\, a_j^\dagger \right)$ can be interpreted as a competitive contribution, and the coefficient $\lambda_{j,k}$ gives a measure of the strength of the interaction between the agents A_j and A_k; more precisely, the contribution $a_j a_k^\dagger$ is a competition term since it destroys a *particle* for the agent associated to a_j and creates a *particle* for the agent associated to a_k; the adjoint term $a_k a_j^\dagger$ swaps the roles of the two agents; in other words, *the loss (gain) of an agent is the gain (loss) of the other agent*;

- the term $\mu_{j,k} \left(a_j^\dagger\, a_k^\dagger + a_k\, a_j \right)$ can be interpreted as a cooperative contribution, and $\mu_{j,k}$ is a measure of the strength of this cooperation; the term $a_j^\dagger a_k^\dagger$ creates a *particle* for both agents, and the adjoint part destroys a *particle* for both agents: in other words, *the gain (loss) of an agent is the gain (loss) of the other agent*.

Adopting the Heisenberg view for the dynamics, the time evolutions of the annihilation operators $a_j(t)$ is ruled by

$$\frac{da_j}{dt} = \mathrm{i} \left[\mathcal{H}, a_j \right], \qquad j = 1, \dots, N, \tag{5.5}$$

$[\mathcal{H}, a_j] = \mathcal{H} a_j - a_j \mathcal{H}$ being the commutator between $\mathcal{H}$ and a_j, whereupon we have the system of linear ordinary differential equations

$$\frac{da_j}{dt} = \mathrm{i} \left(-\omega_j a_j + \sum_{1\le \ell<j} \left(\lambda_{\ell,j} a_\ell + \mu_{\ell,j} a_\ell^\dagger \right) + \sum_{j<k\le N} \left(\lambda_{j,k} a_k - \mu_{j,k} a_k^\dagger \right) \right), \tag{5.6}$$

that have to be solved with suitable initial conditions $a_j(0) = a_j^0$, $j = 1, \dots, N$.

Also in this case, let us introduce a formal vector $\mathbf{A} \equiv \left(a_1, \dots, a_N, a_1^\dagger, \dots, a_N^\dagger \right)^T$ (the superscript ^{T} stands for transposition) and the square matrix of order $2N$

$$\Gamma = \begin{bmatrix} \Gamma_0 & \Gamma_1 \\ -\Gamma_1 & -\Gamma_0 \end{bmatrix},$$

where the $N \times N$ symmetric block Γ_0 and the antisymmetric block Γ_1 are

$$\Gamma_0 = \begin{bmatrix} -\omega_1 & \lambda_{1,2} & \cdots & \cdots & \lambda_{1,N} \\ \lambda_{1,2} & -\omega_2 & \lambda_{2,3} & \cdots & \lambda_{2,N} \\ \cdots & \cdots & \cdots & \cdots & \cdots \\ \cdots & \cdots & \cdots & \cdots & \cdots \\ \lambda_{1,N}, & \lambda_{2,N} & \cdots & \lambda_{N-1,N} & -\omega_N \end{bmatrix}$$

and

$$\Gamma_1 = \begin{bmatrix} 0 & -\mu_{1,2} & \cdots & \cdots & -\mu_{1,N} \\ \mu_{1,2} & 0 & -\mu_{2,3} & \cdots & -\mu_{2,N} \\ \cdots & \cdots & \cdots & \cdots & \cdots \\ \cdots & \cdots & \cdots & \cdots & \cdots \\ \mu_{1,N}, & \mu_{2,N} & \cdots & -\mu_{N-1,N} & 0 \end{bmatrix},$$

respectively.

With these positions, equations (5.6), together with their adjoint version, write in the compact form

$$\frac{d\mathbf{A}}{dt} = \mathrm{i}\Gamma\mathbf{A}, \qquad \mathbf{A}(0) = \mathbf{A}^0,$$

whose solution formally is

$$\mathbf{A}(t) = \mathcal{B}(t)\,\mathbf{A}^0, \qquad \mathcal{B}(t) = \exp\left(\mathrm{i}\Gamma t\right).$$

Now, let us define the vector

$$\Phi = \sqrt{n_1^0}\varphi_{1,0,\ldots,0} + \sqrt{n_2^0}\varphi_{0,1,\ldots,0} + \cdots + \sqrt{n_N^0}\varphi_{0,0,\ldots,1},$$

where $(n_1^0, n_2^0, \ldots, n_N^0)$ represent the initial values of the mean values of the number operators associated to the agents of the system.

If $B_{j,k}$ is the generic entry of matrix $\mathcal{B}(t)$, we have

$$\begin{aligned} a_k^\dagger(t) &= \sum_{j=1}^{N} \left(B_{k+N,j} a_j^0 + B_{k+N,j+N} a_j^{0\dagger} \right), \\ a_k(t) &= \sum_{j=1}^{N} \left(B_{k,j} a_j^0 + B_{k,j+N} a_j^{0\dagger} \right), \end{aligned} \tag{5.7}$$

whereupon the formula

$$n_k(t) = \left\langle \Phi, a_k^\dagger(t) a_k(t) \Phi \right\rangle, \tag{5.8}$$

using the canonical anticommutation relations (2.5), provides the mean values of the number operators at time t:

$$\begin{aligned} n_k(t) = &\sum_{i=1}^{N} \Phi_i^2 \sum_{\ell=1}^{N} B_{k,f(\ell,k)} B_{k+N,g(\ell,k)} \\ &+ \sum_{i=1}^{N-1} \sum_{j=i+1}^{N} \Phi_i \Phi_j \left(B_{k,i} B_{k+N,j+N} + B_{k,j} B_{k+N,i+N} \right. \\ &\left. - B_{k,i+N} B_{k+N,j} - B_{k,j+N} B_{k+N,i} \right), \end{aligned} \tag{5.9}$$

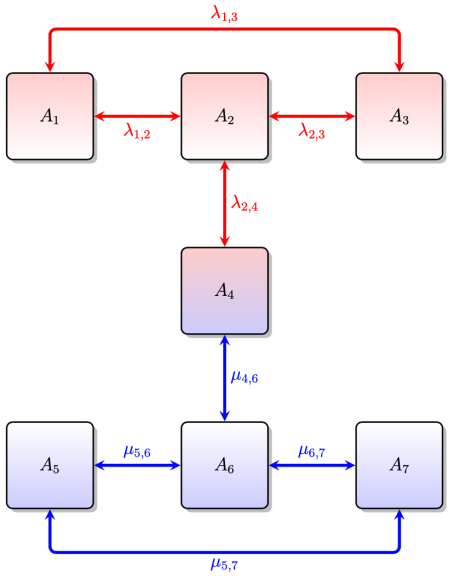

FIGURE 5.1: Schematic view of a system with seven agents.

where

$$f(\ell,i)=\begin{cases} i & \text{if} \quad i=\ell,\\ i+N & \text{if} \quad i\neq\ell,\end{cases} \qquad g(\ell,i)=\begin{cases} i+N & \text{if} \quad i=\ell,\\ i & \text{if} \quad i\neq\ell.\end{cases}$$

We interpret the real functions given by (5.8) as measures of the wealth of the agents of the system. Due to the quadratic form of the Hamiltonian H, the solution will exhibit a never ending oscillatory behavior.

5.2 A simple concrete model: numerical simulations

As a first simple example to illustrate the above considerations, let us consider a system $\mathcal{S}$ composed by seven agents interacting according to the scheme shown in Figure 5.1. In the system $\mathcal{S}$ we can recognize:

- a purely competitive subsystem $\mathcal{S}_1$, made by the agents A_1, A_2, A_3, interacting each other in a competitive way;
- an *opportunist* subsystem $\mathcal{S}_2$, made by the agent A_4, competing with A_2 and cooperating with A_6;
- a purely cooperative subsystem $\mathcal{S}_3$, made by the agents A_5, A_6, A_7, interacting each other in a cooperative way.

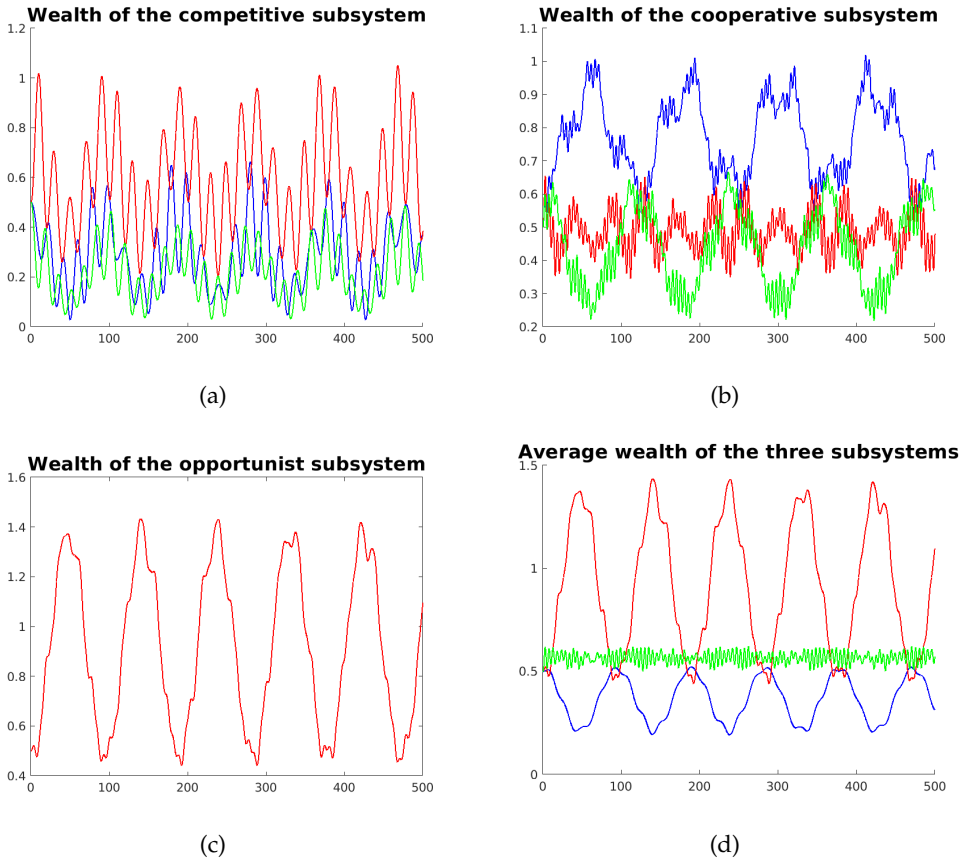

FIGURE 5.2: Time evolution of wealth of the agents as a function of time according to the classical Heisenberg dynamics: subfigure (a) is concerned with the competitive subsystem (blue for A_1, red for A_2 and green for A_3); subfigure (b) is concerned with the cooperative subsystem (blue for A_5, red for A_6 and green for A_7); subfigure (c) displays the wealth of the opportunist agent A_4; finally, subfigure (d) displays the average of the wealth of competitive subsystem (blue), cooperative subsystem (green), and opportunist subsystem (red).

For the considered model, the evolution equations read:

$$\begin{aligned}
\dot{a}_1 &= \mathrm{i}\left(-\omega_1 a_1 + \lambda_{1,2} a_2 + \lambda_{1,3} a_3\right), \\
\dot{a}_2 &= \mathrm{i}\left(-\omega_2 a_2 + \lambda_{1,2} a_1 + \lambda_{2,3} a_3 + \lambda_{2,4} a_4\right), \\
\dot{a}_3 &= \mathrm{i}\left(-\omega_3 a_3 + \lambda_{1,3} a_1 + \lambda_{2,3} a_2\right), \\
\dot{a}_4 &= \mathrm{i}\left(-\omega_4 a_4 + \lambda_{2,4} a_2 - \mu_{4,6} a_6^\dagger\right), \\
\dot{a}_5 &= \mathrm{i}\left(-\omega_5 a_5 - \mu_{5,6} a_6^\dagger - \mu_{5,7} a_7^\dagger\right), \\
\dot{a}_6 &= \mathrm{i}\left(-\omega_6 a_6 + \mu_{4,6} a_4^\dagger + \mu_{5,6} a_5^\dagger - \mu_{6,7} a_7^\dagger\right), \\
\dot{a}_7 &= \mathrm{i}\left(-\omega_7 a_7 + \mu_{5,7} a_5^\dagger + \mu_{6,7} a_6^\dagger\right),
\end{aligned}$$

to be considered together with their adjoints. Let us assign the following values to the parameters involved in the model:

$$\begin{aligned}
&\omega_1 = 0.5,\ \omega_2 = 0.45,\ \omega_3 = 0.55,\ \omega_4 = 0.3,\ \omega_5 = 0.65,\ \omega_6 = 0.5,\ \omega_7 = 0.7, \\
&\lambda_{1,2} = 0.1,\ \lambda_{1,3} = 0.1,\ \lambda_{2,3} = 0.1,\ \lambda_{2,4} = 0.05, \\
&\mu_{4,6} = 0.05,\ \mu_{5,6} = 0.1,\ \mu_{5,7} = 0.1,\ \mu_{6,7} = 0.1,
\end{aligned}$$

and let us assign at $t = 0$ to every agent the same amount of wealth (equal to 0.5).

Some comments about the choice of the values of the parameters are in order. The inertia parameters of the purely competitive agents are smaller than those of the purely cooperative agents, and the opportunist agent has the lower inertia parameter. Also, the parameter responsible for competition among the subsystem $\mathcal{S}_1$ is the same as the parameter responsible for cooperation among the subsystem $\mathcal{S}_3$; finally, the parameters entering in the competitive and cooperative interactions of the opportunist agent are taken smaller. Figure 5.2 displays the time evolution of the wealth of the agents, that, as one expects, is oscillatory. Figure 5.2(d) displays the average values of wealth of the three subsystems as a function of time: the amplitude of the oscillation is quite small for the cooperative subsystem, whereas the opportunist agent experiences the maximum amplitude of oscillations. Moreover, the maximum of wealth of the opportunist agent is higher than those of cooperative and competitive subsystems; finally, the minimum wealth of opportunist agent is close to the maximum wealth of the competitive subsystem and to the average wealth of cooperative system.

Situation drastically changes if we apply periodically a rule, that is, if the agents are able to change their attitudes according to the evolution of their wealth, as shown in the next subsection.

5.2.1 Numerical simulations with the $(\mathcal{H}, \rho)$–induced dynamics approach

We enrich the dynamics by introducing a *rule* able to include in the model some effects that can not be easily included in the definition of $\mathcal{H}$. The rule we use is detailed below.

Fixing a value for τ (the choice of τ plays a role in the dynamics, as will be shown in the following), let us define

$$\delta_j = n_j(k\tau) - n_j((k-1)\tau), \quad j = 1, \ldots, 7$$

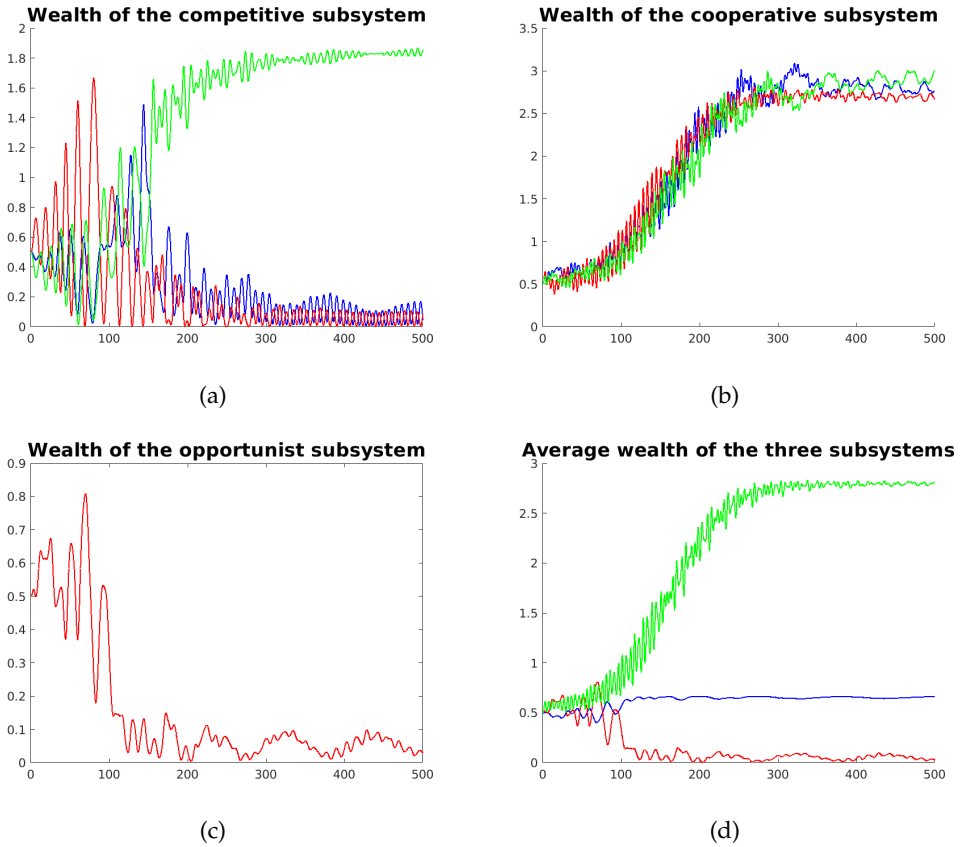

(a) (b)

(c) (d)

FIGURE 5.3: Time evolution of wealth of the agents as a function of time using the $(\mathcal{H}, \rho)$–induced dynamics approach with $\tau = 1$: subfigure (a) is concerned with the competitive subsystem (blue for A_1, red for A_2 and green for A_3); subfigure (b) is concerned with the cooperative subsystem (blue for A_5, red for A_6 and green for A_7); subfigure (c) displays the wealth of the opportunist agent A_4; finally, subfigure (d) displays the average of the wealth of competitive subsystem (blue), cooperative subsystem (green), and opportunist subsystem (red).

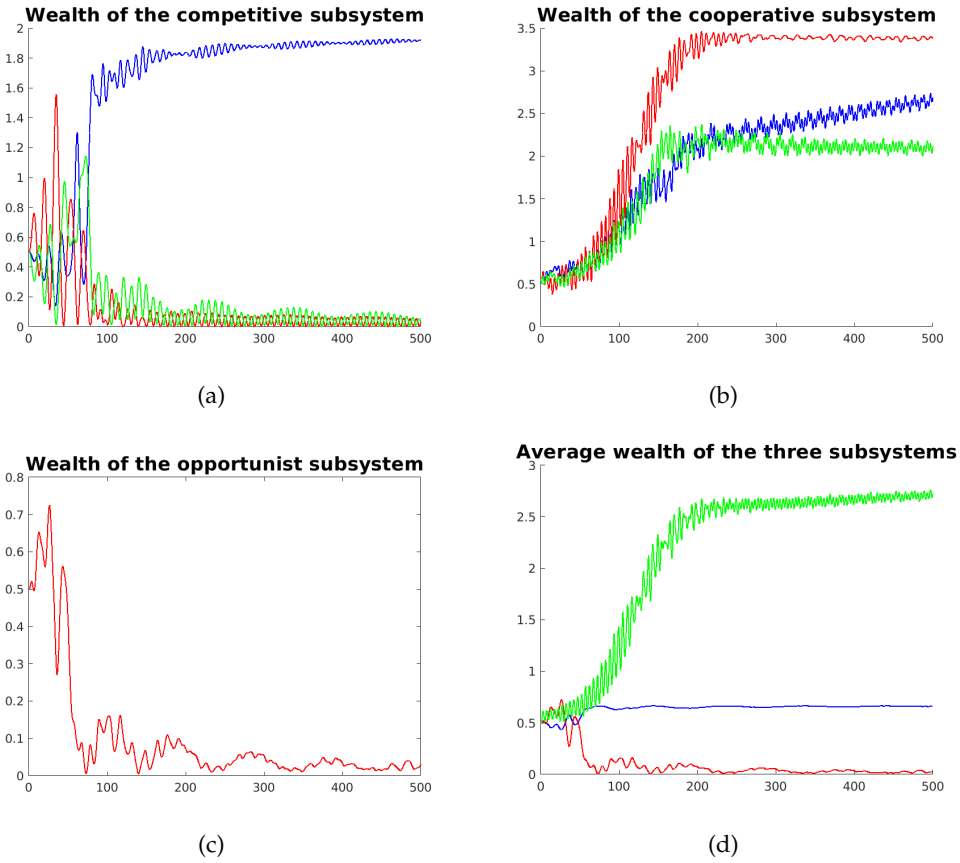

FIGURE 5.4: Time evolution of wealth of the agents as a function of time using the $(\mathcal{H}, \rho)$–induced dynamics approach with $\tau = 2$: subfigure (a) is concerned with the competitive subsystem (blue for A_1, red for A_2 and green for A_3); subfigure (b) is concerned with the cooperative subsystem (blue for A_5, red for A_6 and green for A_7); subfigure (c) displays the wealth of the opportunist agent A_4; finally, subfigure (d) displays the average of the wealth of competitive subsystem (blue), cooperative subsystem (green), and opportunist subsystem (red).

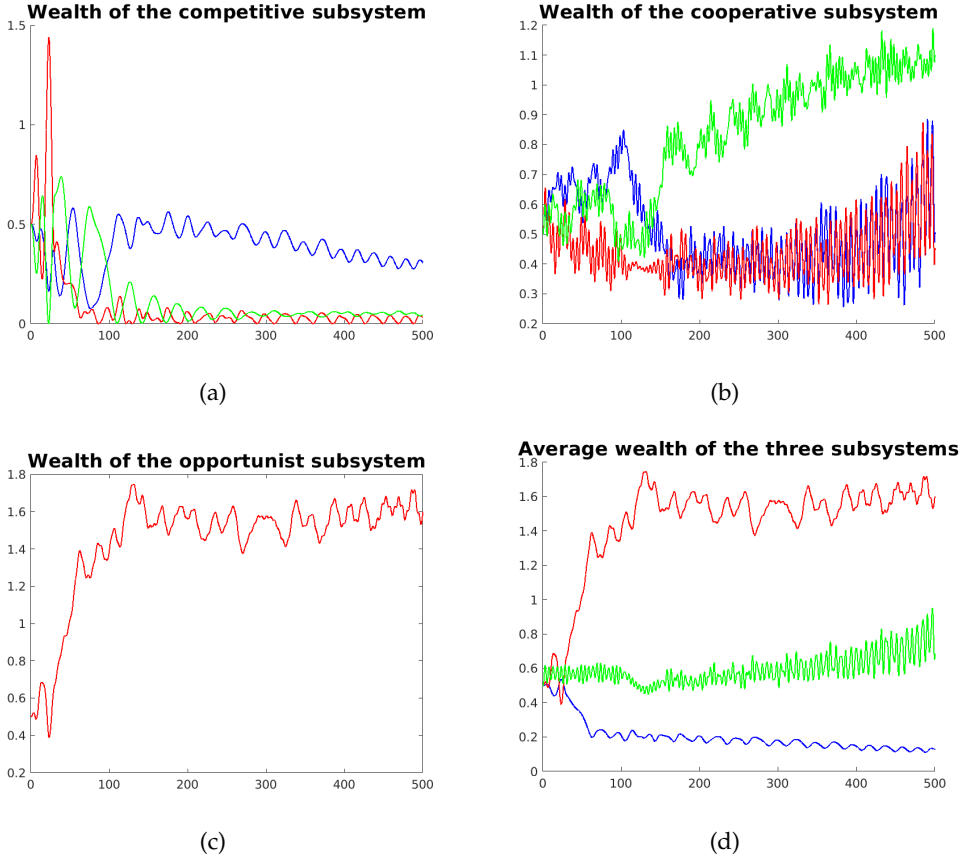

(a) (b)

(c) (d)

FIGURE 5.5: Time evolution of wealth of the agents as a function of time using the $(\mathcal{H}, \rho)$–induced dynamics approach with $\tau = 5$: subfigure (a) is concerned with the competitive subsystem (blue for A_1, red for A_2 and green for A_3); subfigure (b) is concerned with the cooperative subsystem (blue for A_5, red for A_6 and green for A_7); subfigure (c) displays the wealth of the opportunist agent A_4; finally, subfigure (d) displays the average of the wealth of competitive subsystem (blue), cooperative subsystem (green), and opportunist subsystem (red).

At the instants $k\tau$ ($k = 1, 2, \ldots$) we modify the inertia parameters as follows:

$$\omega_j = \omega_j(1 + \delta_j), \qquad j = 1, \ldots, 7;$$

therefore, the inertia parameter of the agent A_j increases (decreases) if its wealth state in the subinterval of length τ increases (decreases); due to the meaning of the inertia parameters, this means that an agent increasing its wealth lowers its tendency to change. On the contrary, an agent undergoing to a decrease of its wealth is induced to become less conservative.

Figures 5.3, 5.4 and 5.5 show the results when the $(\mathcal{H}, \rho)$–induced dynamics approach is used with $\tau = 1$, $\tau = 2$ and $\tau = 5$, respectively. We observe that the transient behavior of the time evolution changes with τ and there is a general damping of the amplitudes of the oscillations. Moreover, if we look at the subfigures (d), we observe that, for $\tau = 1$ and $\tau = 2$, as t increases, the cooperative subsystem gains the higher amount of wealth, whereas the wealth of the competitive subsystem is almost conserved, and the wealth of the opportunist subsystem experiences the greatest loss. The situation is a little bit different for $\tau = 5$ where the opportunist subsystem has the best performance.

5.3 An extended spatial model

Let us consider a more sophisticated system made by N agents; each agent is located in a cell of a one–dimensional torus partitioned in N cells, so that the cell 1 is adjacent to the cell N. Moreover, the distance between adjacent cells is assumed to be 1, whereupon the maximum distance between the cells is $\max = \lfloor N/2 \rfloor$.

Let us choose randomly:

- N_1 agents (the competitive subgroup) interacting each other with a competitive mechanism;
- N_2 agents (the cooperative subgroup) interacting each other with a cooperative mechanism;
- $N_3 = N - N_1 - N_2$ opportunist agents, *i.e.*, each opportunist agent has a competitive interaction with an agent of the competitive subgroup, and a cooperative interaction with an agent of the cooperative subgroup; moreover, the opportunist agents compete each other.

.

We assume that when two agents are interacting in some way, in the case of competition, the parameter $\lambda_{j,k}$ is not constant but decreases with the distance $d(j,k)$ between the cells j and k; on the contrary, in the case of cooperation, the parameter $\mu_{j,k}$ increases with $d(j,k)$. The values of these coefficients are given by the relations

$$\lambda_{j,k} = \lambda \left(1 - \tanh\left(d(j,k) - \max/2\right)\right),$$
$$\mu_{j,k} = \mu \left(1 + \tanh\left(d(j,k) - \max/2\right)\right),$$

where λ and μ are constant, that we choose both equal to 0.1.

Finally, as far as the inertia parameters are concerned, each agent has an inertia parameter randomly chosen in the range between 0.5 and 0.7.

The numerical integration of the dynamics equations, using the classical Heisenberg dynamics and the $(\mathcal{H}, \rho)$–induced dynamics approach provide some interesting results. In all the simulations all the agents start with the same initial amount of

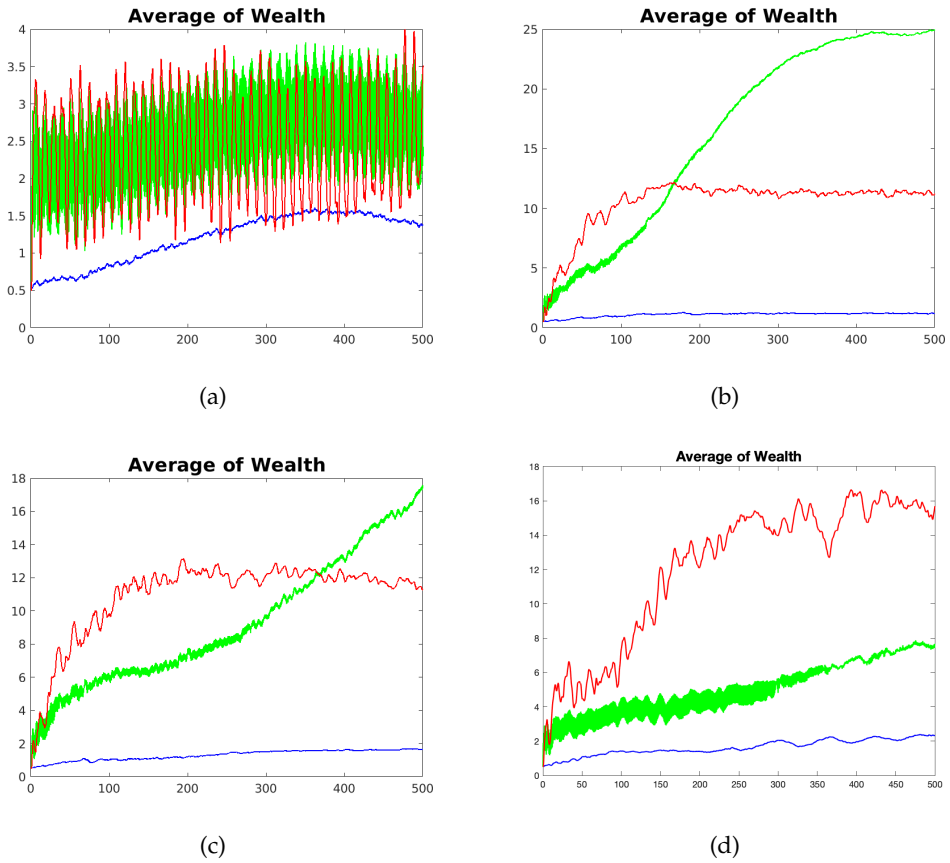

(a) (b)

(c) (d)

FIGURE 5.6: Time evolution of wealth of the system with 100 agents: the cooperative (green) and competitive (blue) subgroups contain 45 agents and the opportunist (red) subgroup 10 agents; subfigure (a) displays the results without using the rule, subfigures (b), (c) and (d) the results using the $(\mathcal{H}, \rho)$–induced dynamics approach with $\tau = 1$, $\tau = 2$ and $\tau = 5$, respectively.

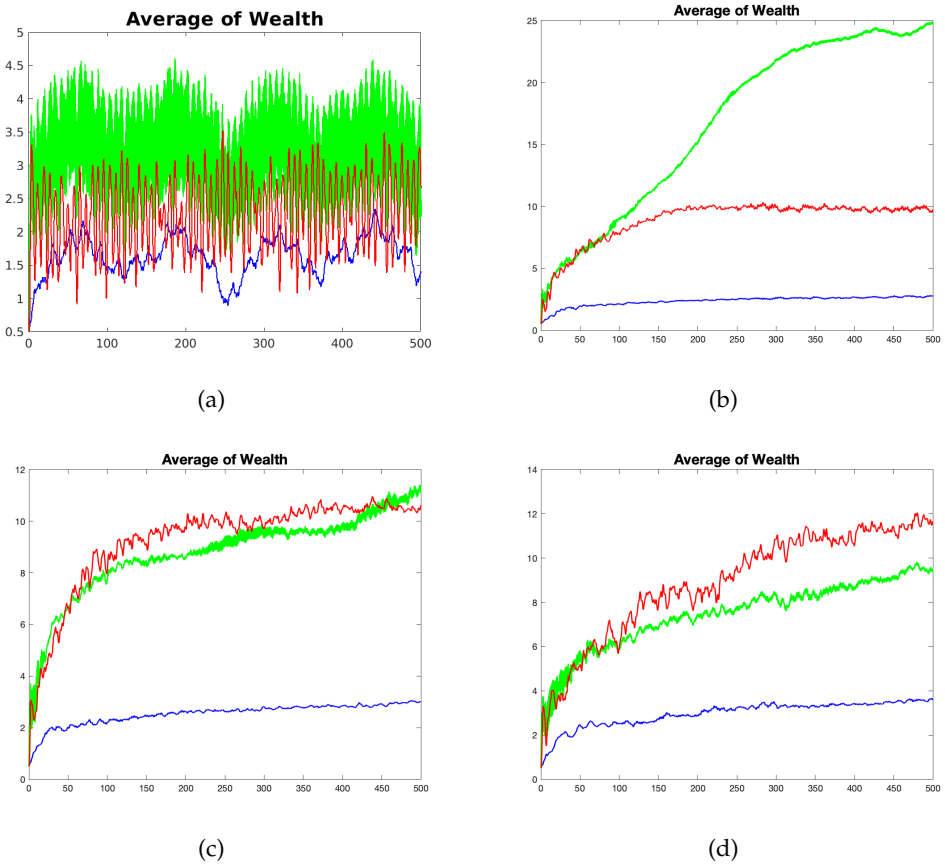

FIGURE 5.7: Time evolution of wealth of the system with 100 agents: the cooperative (green) and competitive (blue) subgroups contain 42 agents and the opportunist (red) subgroup 16 agents; subfigure (a) displays the results without using the rule, subfigures (b), (c) and (d) the results using the $(\mathcal{H}, \rho)$–induced dynamics approach with $\tau = 1$, $\tau = 2$ and $\tau = 5$, respectively.

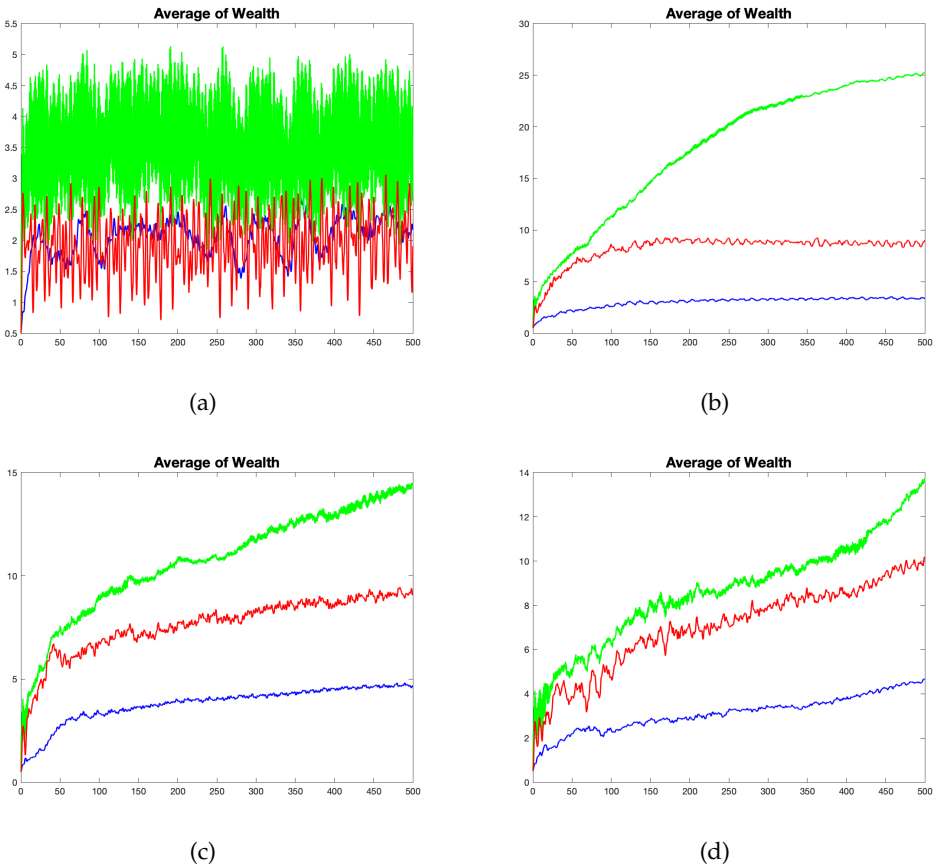

(a) (b)

(c) (d)

FIGURE 5.8: Time evolution of wealth of the system with 100 agents: the cooperative (green) and competitive (blue) subgroups contain 40 agents and the opportunist (red) subgroup 20 agents; subfigure (a) displays the results without using the rule, subfigures (b), (c) and (d) the results using the $(\mathcal{H}, \rho)$–induced dynamics approach with $\tau = 1$, $\tau = 2$ and $\tau = 5$, respectively.

wealth, say 0.5; moreover, the number of the purely competitive agents (N_1) is equal to the number of the purely cooperative agents (N_2); three different values of N_3 (the number of opportunist agents) are considered. To fix the rule, let us define

$$\delta_j = n_j(k\tau) - n_j((k-1)\tau), \qquad j = 1, \dots, N, \quad k \in \mathbb{N},$$
$$\delta = \max\{|\delta_j| \, : \, j = 1, \dots, N\};$$

then, at times $k\tau$ the inertia parameters change according to the law:

$$\omega_j = \omega_j \left(1 + \frac{\delta_j}{\delta}\right).$$

Figures 5.6 (the opportunist subsystem made by 10 agents), 5.7 (the opportunist subsystem made by 16 agents) and 5.8 (the opportunist subsystem made by 20 agents) show the average wealth of the three subgroups of agents in the various cases, that is, using the classical Heisenberg dynamics, or using the $(\mathcal{H}, \rho)$–induced dynamics approach with $\tau = 1, 2, 5$. We can observe that, in general, using the $(\mathcal{H}, \rho)$–induced dynamics approach, cooperation gives better results in terms of wealth; cooperative subgroup, as time increases, obtains an amount of wealth always higher than that of the purely competitive subgroup and often than that of the opportunist subgroup. Moreover, the results seem to suggest that the opportunist subsystem has better performances as τ increases. We are conscious that these results are only preliminary and that a deeper investigation with systems involving a large number of agents in different scenarios is needed, at least if we want to compare the performances of the behaviors of the agents (cooperative, competitive or opportunist).

Chapter 6

Conclusions

This final Chapter contains some comments and remarks, as well as future possible research lines.

The analysis carried out in this thesis started within the well established and classical framework where the models write in terms of partial differential equations (in particular, parabolic reaction-diffusion equations) and then moved to alternative formulations of macroscopic models using the operator algebra of quantum mechanics. In the latter approach, unknowns are not real-valued functions but annihilation, creation and number operators of a complex Hilbert space, and the dynamics is assumed to be ruled by a Hamiltonian operator. The computation of the mean values of the number operators, over an assigned initial condition, enables to obtain real-valued functions that can be phenomenologically interpreted.

Classical models written as differential equations, whose unknowns are real-valued functions directly linked to the observables of the system we have in mind, possess a well defined basis, and allow for many degrees of freedom in the choice of the form of interactions among the actors (or the compartments) of the system. A lot of theoretical results and technical tools are available; for instance, it is possible to consider the (linear or nonlinear) stability of the equilibrium configurations, the existence and uniqueness of solutions, the explicit determination of exact or approximate solutions (*e.g.*, travelling or self-similar solutions); in addition, we can resort to numerical methods by means of well defined algorithm able to give estimates about the order of magnitude of the errors. For reaction-diffusion equations the analysis first introduced by Turing in 1952, where stable homogeneous equilibrium configurations may lose their stability so leading to the emergence of some characteristic patterns, has been successfully used in many contexts; it explains many important features experimentally observed in bio-ecological and social phenomena.

On the contrary, the construction of operatorial models, and in particular those in the spirit of the formalism of second quantization, poses some restrictions; most of these models involve a Hermitian Hamiltonian operator, and this often leads to periodic or quasi periodic dynamical outcomes. Considering operators of fermionic type we can work in a finite–dimensional Hilbert spaces; however, the dimension of the Hilbert space grows exponentially as the number of the actors of the system increases, whence it follows that realistic problems become very hard from a computational viewpoint. This can be avoided if the self–adjoint Hamiltonian is taken time independent and quadratic. In such a case, the Heisenberg equations ruling the dynamics turn out to be linear. Nevertheless, using linear models is not always adequate.

A step forward has been made with the introduction of the approach of $(\mathcal{H}, \rho)$–induced dynamics, superposing to the classical Heisenberg dynamics the effect of some *rules* ρ acting periodically on the system. The action of the rules is not merely a

mathematical expedient but in a very simple and natural way allows to take into account some effects that are not easy to introduce in a purely Hamiltonian description; remarkably, $(\mathcal{H}, \rho)$–induced dynamics does not introduce technical and/or computational difficulties, and it is often able to produce time evolutions approaching asymptotic equilibrium states. Moreover, a sort of *irreversible* effects are observed.

The use of time independent quadratic Hermitian Hamiltonians, even when the $(\mathcal{H}, \rho)$–induced dynamics approach is used, requires to solve large systems of linear ordinary differential equations with constant coefficients; anyway, existence and uniqueness of the solutions is trivially granted. In the Hamiltonian we can embed terms that can be interpreted as competitive or cooperative (both local and nonlocal), as well as migration–like terms. With a suitable rewriting, as shown in Chapter 2, we may see the ordinary differential equations as the discretized version of a reaction–diffusion system. The computational complexity of the numerical integration of these operatorial models is of the same order as that of numerically solving the reaction-diffusion systems adopting a finite difference method.

As far as we know, the crimo-taxis model, analyzed in its classical formulation in Chapter 1, is the first example where an operatorial version has been implemented (Chapter 3). A comparison between the outcomes of these two different formulations could open new perspectives and justify the operatorial approach in the description of macroscopic systems.

A lot of things are worth of being investigated, so this is not really a conclusion.

Bibliography

Arlotti, L., N. Bellomo, and M. Lachowicz (2000). "Kinetic equations modelling population dynamics". In: *Transport Theory and Statistical Physics* 29, pp. 125–139.

Aymard, B. (2022). "On Pattern Formation in Reaction–Diffusion Systems Containing Self- and Cross-Diffusion". In: *Communications in Nonlinear Science and Numerical Simulations* 105, p. 106090.

Bagarello, F. (2006). "An operatorial approach to stock markets". In: *Journal of Physics A: Mathematical and General* 39 (22), pp. 6823–6840.

— (2012). *Quantum dynamics for classical systems: with applications of the number operator*. New York: John Wiley and Sons.

— (2019). *Quantum concepts in the social, ecological and biological sciences*. Cambridge: Cambridge University Press.

Bagarello, F., A. M. Cherubini, and F. Oliveri (2016). "An Operatorial Description of Desertification". In: *SIAM Journal on Applied Mathematics* 76 (2), pp. 479–499.

Bagarello, F., F. Gargano, and F. Oliveri (2015). "A phenomenological operator description of dynamics of crowds: Escape strategies". In: *Applied Mathematical Modelling* 39 (8), pp. 2276–2294.

— (2020). "Spreading of Competing Information in a Network". In: *Entropy* 22, p. 1169.

Bagarello, F. and E. Haven (2016). "First results on applying a non-linear effect formalism to alliances between political parties and buy and sell dynamics". In: *Physica A: Statistical Mechanics and its Applications* 444, pp. 403–414.

Bagarello, F. and F. Oliveri (2013). "An operator description of interactions between populations with applications to migration". In: *Mathematical Models and Methods in Applied Sciences* 23, pp. 471–492.

— (2014). "Dynamics of closed ecosystems described by operators". In: *Ecological Modelling* 275, pp. 89–99.

Bagarello, F. et al. (2017). "(H, ρ)-induced dynamics and the quantum game of life". In: *Applied Mathematical Modelling* 43, pp. 15–32.

— (2018). "(H, ρ)-induced dynamics and large time behaviors". In: *Physica A: Statistical Mechanics and its Applications* 505, pp. 355–373.

Bianca, C. and M. Menale (2021). "Existence and uniqueness of the weak solution for a space–velocity thermostatted kinetic theory framework". In: *The European Physical Journal Plus* 136, pp. 1–18.

Chakraborty, B., H. Baek, and N. Bairagi (2021). "Diffusion-induced regular and chaotic patterns in a ratio-dependent predator-prey model with fear factor and prey refuge". In: *Chaos* 31, p. 033128.

DellaMarca, R. et al. (2022). "Mathematical Modelling of Oscillating Patterns for Chronic Autoimmune Diseases". In: *Mathematical Methods in the Applied Sciences* 45, pp. 7144–7161.

Di Salvo, R., M. Gorgone, and F. Oliveri (2017a). "(H, ρ)-induced political dynamics: facets of the disloyal attitudes into the public opinion". In: *International Journal of Theoretical Physics* 56, pp. 3912–3922.

— (2017b). "Political Dynamics Affected by Turncoats". In: *International Journal of Theoretical Physics* 56, pp. 3604–3614.

Di Salvo, R., M. Gorgone, and F. Oliveri (2020). "Generalized Hamiltonian for a two-mode fermionic model and asymptotic equilibria". In: *Physica A: Statistical Mechanics and its Applications* 540, p. 123032.

Di Salvo, R. and F. Oliveri (2016a). "An operatorial model for long-term survival of bacterial populations". In: *Ricerche di Matematica* 65 (2), pp. 435–447.

— (2016b). "On fermionic models of a closed ecosystem with application to bacterial populations". In: *Atti Accademia Peloritana dei Pericolanti* 94, A5.

— (2017). "An operatorial model for complex political system dynamics". In: *Mathematical Methods in the Applied Sciences* 40, pp. 3912–3922.

Epstein, J. M. (1997). *Nonlinear Dynamics, Mathematical Biology, and Social Science*. Reading, MA: Addison-Wesley.

Gargano, F. (2014). "Dynamics of Confined Crowd Modelled Using Fermionic Operators". In: *International Journal of Theoretical Physics* 53 (8), pp. 2727–738.

Giunta, V., M. C. Lombardo, and M. Sammartino (2021). "Pattern formation and transition to chaos in a chemotaxis model of acute inflammation". In: *SIAM Journal on Applied Dynamical Systems* 20, pp. 1844–1881.

Gorgone, M., G. Inferrera, and F. Oliveri (2022). "Fermionic operatorial model of a system with competitive and cooperative interactions". Submitted.

Hanski, I. (1981). "Coexistence of competitors in patchy environment with and without predation". In: *Oikos* 37 (3), pp. 306–312.

— (1983). "Coexistence of competitors in patchy environment". In: *Ecology* 64 (3), pp. 493–500.

— (2008). "Spatial patterns of coexistence of competing species in patchy habitat". In: *Theoretical Ecology* 1 (1), pp. 29–43.

Hao, W. and C. Xue (2020). "Spatial pattern formation in reaction–diffusion models: a computational approach". In: *Journal of Mathematical Biology* 80, pp. 521–543.

Inferrera, G. and F. Oliveri (2022). "Operatorial Formulation of a Model of Spatially Distributed Competing Populations". In: *Dynamics* 2, pp. 414–433.

Inferrera, G. et al. (2022). "A reaction-diffusion model of crimo–taxis in a street". Submitted.

Ives, A. R. and R. M. May (1985). "Competition within and between species in a patchy environment: Relations between microscopic and macroscopic models". In: *Journal of Theoretical Biology* 115 (1), pp. 65–92.

Lam, K .Y. and Y. Lou (2022). *Introduction to Reaction-Diffusion Equations: Theory and Applications to Spatial Ecology and Evolutionary Biology*. Lecture Notes on Mathematical Modelling in the Life Sciences. New York: Springer.

Mitchell, A. R. and D. F. Griffiths (1980). *The finite difference method in partial differential equations*. New York: John Wiley & Sons.

Murray, J. D. (2002). *Mathematical Biology I: An introduction*. New York: Springer.

— (2003). *Mathematical Biology II: Spatial models and biomedical applications*. New York: Springer.

Paar, H. (2010). *An introduction to advanced quantum physics*. New York: John Wiley and Sons.

Paparella, F. and F. Oliveri (2008). "A particle-mesh numerical method for advection reaction diffusion equations with applications to plankton modelling". In: *Wascom 07, Proceedings International Conference on Waves and Stability in Continuous Media*. Singapore: World Scientific, pp. 469–474.

Planck, M. (1900). "Über die Elementar quanta der Materie und der Elektrizitaet". In: *Aus den Verhaudlungen der Deutschen Physikalischen Gesellschaft* 2, pp. 244–246.

Roman, P. (1965). *Advanced Quantum Mechanics*. New York: Addison-Wesley.

Short, M. B., A. L. Bertozzi, and P. J. Brantingham (2010). "Nonlinear patterns in urban crime: Hotspots, bifurcations, and suppression". In: *SIAM Journal on Applied Dynamical Systems* 9, pp. 462–483.

Short, M. B. et al. (2008). "A statistical model of criminal behavior". In: *Mathematical Models and Methods in Applied Sciences* 18, pp. 1249–1267.

Slatkin, M. (1974). "Competition and regional coexistence". In: *Ecology* 55 (1), pp. 128–134.

Smoller, J. (1983). *Shock Waves and Reaction-Diffusion Equations*. New York: Springer.

Turing, A. M. (1952). "The Chemical Basis of Morphogenesis". In: *Philosophical Transactions of the Royal Society of London. Series B, Biological Sciences* 237, pp. 37–72.

Vanag, V. K. and I. R. Epstein (2009). "Cross-diffusion and pattern formation in reaction-diffusion systems". In: *Physical Chemistry Chemical Physics* 11, pp. 897–912.

Wolpert, L. (1969). "Positional information and the spatial pattern of cellular differentiation". In: *Journal of Theoretical Biology* 25, pp. 1–47.

— (1981). "Positional information and pattern formation". In: *Philosophical Transactions of the Royal Society of London. Series B, Biological sciences* 295, pp. 441–450.

Xie, Z. (2012). "Cross-diffusion induced Turing instability for a three species food chain model". In: *Journal of Mathematical Analysis and Applications* 388, pp. 539–547.

Zincenko, A. et al. (2021). "Turing instability in an economic–demographic dynamical system may lead to pattern formation on a geographical scale". In: *Journal of the Royal Society Interface* 18, p. 20210034.